STOCHASTIC MODELING OF SPATIAL AND TEMPORAL WATER QUALITY VARIATIONS IN GROUNDWATER

by

Christopher J. Duffy

Submitted in Partial Fulfillment
of the Requirements for the Degree of
Doctor of Philosophy

NEW MEXICO INSTITUTE OF MINING AND TECHNOLOGY

Socorro, New Mexico

November 1981

ACKNOWLEDGMENTS

I would like to express my appreciation to the members of my dissertation committee for their support, suggestions and encouragement throughout this study. Professor Lynn W. Gelhar, who served as dissertation advisor, deserves special mention, since his perception of the transport problem largely influenced my efforts. Working for Peter J. Wierenga, Department of Agronomy, New Mexico State University, not only gave me the opportunity to continue my graduate training, but valuable field experience as well. Critical reviews by Professor Allen L. Gutjahr, Professor GerardoW. Gross, both of New Mexico Institute of Mining and Technology, and Dr. Leonard Konikow of the USGS Water Resources Division in Reston, greatly improved the final version of this manuscript.

Lastly, I would like to thank my wife Sue, and the boys Jamie and Colin, for their patience, especially during the final stages of this work.

ABSTRACT

The current controversy over problems of contamination of our groundwater environment has led to the development of new techniques for aquifer analysis and pollution control. The difficulty encountered in most studies of solute transport involve the complex spatial and temporal variations of field measured hydrogeologic and hydrochemical variables. Spectral analysis and stochastic differential equations has recently been shown to be a useful approach to problems of spatial and temporal variability. This research is concerned with (1) the analysis of continuous water quality time series of groundwater contamination or tracers subject to a time varying source, and (2) the analysis of spatial variations in water quality produced by a stochastic, nonuniform flow field. In the first case of water quality time series, solutions are found for three widely applied transport models subject to a stochastic source of contamination or tracer: (1) the lumped parameter or linear reservoir model, (2) a convection model applied to a curvilinear flow field and (3) a one-dimensional convection-dispersion model in a uniform flow field. Application of the stochastic theory is illustrated with an example for each model. The results of the time series analysis demonstrate the utility of spectral analysis and stochastic differential equations for evaluating stationary time series of water quality via the frequency domain approach. The method also indicates that the unique frequency characteristics of water quality time series may be used as a diagnostic tool for determining the appropriate transport model to apply in each case (ie. curvilinear flow, uniform flow, dispersive effects, etc.).

The effects of a nonuniform flow field on the depth-averaged equation of solute transport is evaluated for the case of a spatially variable and stochastic velocity field. The velocity field is shown to produce spatial variations in the solute concentration as well. A perturbation technique divides the transport process into a mean and fluctuating condition. Stochastic theory and spectral analysis is used to evaluate the significance of additional convective and dispersive flux terms in the mean equation. The analysis indicates that an overall reduction in the convective velocity of a solute, relative to the mean fluid velocity, may result when flow nonuniformity is significant. A corresponding increase in the effective dispersion coefficient is also observed. The stochastic theory provides a means of estimating the concentration variance due to a nonuniform flow field.

TABLE OF CONTENTS

TABLE OF CONTENTS (Continued)

LIST OF FIGURES

LIST OF FIGURES (Continued)

LIST OF FIGURES (Continued)

LIST OF TABLES

LIST OF SYMBOLS

Symbol	Description
a	linear reservoir outflow parameter (1/T)
a_∞	a symptotic dispersivity length (L)
a_T, a_L	transverse and longitudinal local dispersivities (L)
$b(x)$	aquifer thickness (L)
c	aquifer solute concentration (M/L^3)
c_i	input solute concentration (M/L^3)
c^*	dimensionless solute concentration
dZ_c	Fourier amplitude for c (M/L^3)
dZ_{c_i}	Fourier amplitude for c_i (M/L^3)
dZ_u	Fourier amplitude for u (L/T)
dZ_x, dZ_y	Fourier amplitudes for x and y
D	dispersion coefficient (L^2/T)
D_{ij}	dispersion tensor, i, j = 1,2,3 (L^2/T)
D_L	longitudinal disersion coefficient (L^2/T)
$h(x,t)$	impulse response function
$\bar{h}(t)$	spatial average water level (L)
$h(x)$, h_o	saturated thickness above a given reference (L)
$H(\omega)$	frequency response function
i	$\sqrt{-1}$
$J(x)$	hydraulic gradient (L/L)
J_x, J_z	horizontal and vertical dispersive flux terms (M/L^2T)

LIST OF SYMBOLS (Continued)

Symbol	Description
k	wave number, (1/L)
K	hydraulic conductivity, (L/T)
K_e	effective rate constant (1/T)
K_{yx}	coherency spectrum for x-y
K_z	vertical hydraulic conductivity (L/T)
l_x	horizontal correlation scale for u'(x) (L)
l_z	vertical correlation scale for u'(z) (L)
L	aquifer length dimension (L)
L_{yx}	cospectrum (see specific case for unit)
m_i, m_o, m_r	the mass flux terms for input, output and regional groundwater flows per unit aquifer area (M/L^2T)
M	total mass of solute c in the aquifer (M)
n	effective porosity (L^3/L^3)
$\tilde{n}$	unit normal vector
q, q_i, q_r	specific discharge per unit aquifer area for the outflow, inflow and regional groundwater (L/T)
q_x, q_y, q_s	components of the specific discharge vector along the x, y and s (curvilinear) coordinates (L/T)
Q	volumetric discharge rate (L^3/T)
Q_L	volumetric lateral inflow rate (L^3/T)

LIST OF SYMBOLS (Continued)

Symbol	Description
$Q_{yx}(\omega)$	quadrature spectrum (see specific case for units)
$R_{xx}(\tau)$	autocovariance of x(t) (units^2)
$R_{uu}(\xi)$	autocovariance of u(x) (L^2/T^2)
s	curvilinear space coordinate (L)
S	specific yield (L/L)
T	Transmissivity (L^2/T)
T_c	response time or residence time of solute c (T)
T_m	response time for mass flux (T)
T_o	parameter of convective transport example (T)
T_τ	dimensionless travel-time parameter (T/T)
u, v	vertical and horizontal components of the velocity (L/T)
α	effective dispersivity length (L)
β	amplitude factor (L/L)
$\delta(x)$	delta function (1/L)
ζ	dimensionless stream function, and dimensionless dispersivity length
η	dimensionless potential function
$\Theta(\omega)$	phase spectrum (radians)
κ	dimensionless rate constant
λ	correlation length or time scale (L,T)

LIST OF SYMBOLS (Continued)

Symbol	Description
λ_m	correlation time scale for the mass flux input (T)
μ_x	mean of variable x
ξ	lag number (L)
$\sigma_c, c_i, k, c^*, m_o, m_i, u$	standard deviation of c, c_i, k, c^*, m_o, m_i, and u
τ	travel time (T)
τ_ω	travel time from the river to the pumping well (T)
$\phi_{xx}(\omega)$	spectrum for x(t) (x-units^2)
$\phi_{cc}(\omega), \phi_{c_ic_i}(\omega)$	concentration spectra over frequency ω for c and c_i $(M/L^3)^2$
$\phi_{m_om_o}(\omega), \phi_{m_im_i}(\omega)$	mass flux spectra for m_o and m_i $(M/L^2T)^2$
$\phi_{uu}(k)$	velocity spectrum over wave number k $(L/T)^2$
$\phi_{uc}(k)$	cross-spectrum for velocity and concentration over wave number k (ML/L^2T)
$\phi_{yx}(\omega)$	cross-spectrum for x and y over frequency ω (units x · y)
ψ	stream function (L^2/T)

GENERAL INTRODUCTION

Objectives and scope of the research

In recent years the public has become increasingly aware of the susceptibility of groundwater to contamination from domestic, agricultural and industrial sources. As a result, a more realistic priority has been given to groundwater protection, and how groundwater fits into the overall strategy of environmental management. Concern over potential and existing contamination has stimulated researchers to develop a variety of new techniques and models to analyze and predict the transport of contaminants in groundwater systems. A fundamental difficulty encountered in these studies is how to incorporate within the methodology, the complex natural variations in the porous medium, as well as the time variable nature of the source of contaminant.

Recent developments in stochastic hydrology (Gelhar et al., 1979; Kisiel, 1969; Freeze, 1980; Gelhar, 1974) have demonstrated the merits of a stochastic approach for characterizing the random element of natural processes. The use of stochastic methods implies an element of uncertainty, in that variability is only distinguished in a probabilistic sense. If we view this variability as providing real information about the system, as opposed to 'noise', then the stochastic method (in this case stochastic differential equations) can provide an interpretive analytical tool.

In this research a variety of relatively simple models of mass transport are solved via stochastic differential equations and the theory of linear filters. The equations to be examined are deemed stochastic as a result of a time variable source of contamination (or

tracer), or as a result of a spatially variable velocity field effecting the average solute concentration. The procedure will point out that a random process need not have a complete probability definition (i.e. joint probability density function is not required), and that statistically stationary (in time) and homogeneous (in space) processes are adequately represented by the first two probability moments, the mean and the variance. Besides the mean and the variance it will be necessary to define an additional statistical measure - the correlation scale. The correlation scale is shown to be an especially important consideration for describing spatial and temporal variability in groundwater quality studies.

Application of the spectral theory is attempted for each case under investigation in order to demonstrate the suitability of the stochastic method to a variety of field problems, and to illustrate the diagnostic capability of the spectral analysis method in frequency response studies of water quality.

Review of literature

In the last two decades stochastic hydrology has been widely exploited for the study of random or partially random processes in hydrology and hydrogeology. It is not difficult to understand why stochastic methods have been accepted by earth scientists and engineers, since almost all natural processes contain some element of random behavior. However it is interesting that so many different methodologies for stochastic analysis have been adopted by hydrological scientists. In general these methodologies range from the purely descriptive aspects of random variables, to complex mathematical models of physical processes with multidimensional random components.

This review of literature is intended as a partial account of the significant developments in stochastic hydrology as it pertains to both theory and data analysis for the following topics:

(1) temporal variability of water quality (time series),

(2) spatial variability of the hydrogeologic media and its effect on water quality,

(3) a review of some water quality studies displaying spatially or temporally variable data.

As is the case in any scientific endeavor, research in stochastic hydrology has proceeded along two fronts. The first stage is the descriptive approach where data is simply evaluated without regard for the physical nature of the system, say for the purpose of detecting the maximum or minimum. The second stage might be called the interpretive approach which would include some form of physical model. Although this research is primarily concerned with the interpretive or modeling aspect, the former is of course essential to determining the problem itself, and will be included in this brief review. Since stochastic methods have evolved from a variety of scientific fields it will be necessary to survey developments from an interdisciplinary range of literature for pertinent material.

Time series: With the recent emphasis on pollution detection by regulatory agencies has come the need for efficient design of continuous monitoring networks. Gunnerson (1975) has demonstrated the use of stochastic methods for design of these networks for the purpose of pollution detection. The probabilistic-stochastic methods which he uses include empirical frequency distributions, range analysis, covariance-spectral techniques and regression methods for bivariate data

sets. Wastler (1969) also illustrates the use of spectral-covariance analysis for rivers and esturaries as a descriptive tool. In terms of groundwater quality, Gelhar et al., (1980) have used spectral-covariance techniques to describe the stochastic element of groundwater salinity time series. The report also points out how highly variable time series may display little visual similarity but are comparable in their probability moments and correlation scales.

The interpretation of water quality time series is generally viewed in a systems context. Researchers in watershed hydrology and river hydraulics have made extensive use of the input-output or systems method for both stochastic and deterministic problems. Dooge (1973) presents a general treatment of linear systems as applied to autocorrelated and cross-correlated hydrologic time series. Thomman (1974) uses a systems approach to examine a variety of deterministic surface water quality systems. Both Thomman and Dooge make use of the transfer function and phase as the principal tools of frequency response studies. Texts by Jenkins and Watts (1967) and Koopmans (1974) provide the detailed mathematical background necessary for linear filter theory and spectral analysis applications. Yevjevich (1972) treats a wide range of stochastic methods in hydrology including covariance-spectral analysis, surplus-deficit-range, the theory of runs, as well as applications of these methods.

A concise treatment of "Time Series Analysis of Hydrologic Data" is given by Kisiel (1969). The manuscript outlines many practical features of covariance-spectral analysis as well as how these relate to linear systems in hydrology. A series of papers from Colorado State University have dealt extensively with stochastic methods in hydrology (Jeng and

Yevjevich, 1966); Rodriguez-Iturbe, 1967; and Hendrick, 1973). Although stochastic methods have been applied to the hydraulics of groundwater flow, little has been done with regard to water quality time series in groundwater. Erikson (1970) has presented two papers on the spectral and cross-spectral analysis of groundwater levels when the variable is treated as an auto-regressive process. Solutions to stochastic differential equations describing phreatic aquifer flow were first developed in a paper by Gelhar (1974). This research utilizes frequency domain solutions to several aquifer flow equations in terms of the input-output spectral densities. This paper can be considered the basic reference for the time series methods to be presented in Chapter 1. Evaluation and interpretation of recharge mechanisms using the spectral method has been demonstrated and applied to the Roswell Basin, New Mexico by Duffy et al. (1978) and Gelhar et al (1979). Geldner (1981) has applied the spectral approach to a stream-aquifer situation in the Rhine River Valley between France and Germany.

Spatial Variability: In most applications of water quality modeling it is assumed that the general theory for mass transport in groundwater (as developed by Bachmat and Bear, 1964 for example) will apply, and can simply be 'taken off the shelf' in each case. In a mathematical sense this may of course be true, however, as has been pointed out by Anderson (1978), the parameters of the macro-dispersion process (the dispersivity or dispersion coefficient) do not have a precise physical meaning. Efforts to remedy this gap in our knowledge are currently being made. It is worthwhile then to review the progress which has been made towards the development of an encompassing theory of mass transport, as well as some problems facing those who wish to apply the

theory to field problems. Comprehensive reviews on parts of this topic can be found elsewhere (Bear, 1972; Anderson, 1979; Naff 1978) and thus only the highlights are discussed here.

In terms of porous media flow, Taylor (1954) and Aris (1956) have provided a quantitative description of the dispersion process in small pores using capillary tubes. In each case they were able to devise an exact mathematical formulation to describe the dispersion coefficient in terms of the geometrical and hydraulic properties of the tube or tubes. Statistical methods have been more commonly used for studying dispersion in porous media, largely due to the complexity of the local pore structure and the larger scale heterogeneities of the aquifer itself. Randomly oriented tube models have provided a basis for physical interpretation of dispersion and diffusion on a local scale (or REV scale). Proponents of the statistical approach suggest that it is not possible to give a precise mathematical description for the particle (tracer) path or velocity and thus its location can only be determined in a probabilistic sense. The work of Scheidegger (1954), de Josselin de Jong (1958) and Saffman (1960) are the most notable in this area of research.

In order to describe the larger scale heterogeneities of aquifer variability, Monte Carlo techniques have been employed. Warren and Skiba (1964) use a Monte Carlo scheme to study the macroscopic (large scale) dispersion which results from three-dimensional permeability variations of a porous medium. The effect of porosity variations on dispersion was considered and found to be a second order influence. Their study indicates that the scale of heterogeneity usually examined in the laboratory is not the same as the reservoir scale. Heller (1972) uses a Monte Carlo scheme to arrive at an effective dispersion co-

efficient which is the result of two-dimensional random permeability variations. His conclusions point to the significance of both local and global (large scale) heterogeneity as influencing the dispersion process. More recently Schwartz (1977) and Smith and Schwartz (1980) have used a Monte Carlo approach for simulation of macro-dispersion. The latter report includes the influence of autocorrelated permeability fields using a 'nearest-neighbor' stochastic process. The use of Monte Carlo methods appear to be a very powerful tool for studying random fields in groundwater simulation, and the applications thus far have been far from exhaustive.

Analytical methods have been especially useful for studying the problem of macrodispersion in stationary, or more correctly, homogeneous random fields. For example Mercado (1967) demonstrates the role of a horizontally stratified permeability field on the magnitude of the dispersion coefficient. His model clearly demonstrates the effect of convection during the early stages of the dispersion process. Local dispersion was not considered in his work. Marle et al. (1967) make use of an analytical procedure advanced by Aris (1956), called the method of moments. Marle's contribution was in deriving an expression for the longitudinal dispersion coefficient. Their results also suggest that after large time or displacement the macrodispersion process is Fickian. Buyevich et al. (1969) have examined both the large and small scale heterogeneity of porosity in a porous medium and their influence on the dispersion process. The authors obtain correlation expressions between the flow and transport variables which are given in terms of an effective coefficient of diffusion and porosity fluctuations. This method is particularly interesting to the present study since it makes

use of stochastic differential equations solved via the spectral method.

Stochastic methods have also been applied to the solution of groundwater flow problems (Freeze, 1975; Gelhar, 1976; Bakr et al., 1978; Gutjahr et al., 1978 and Mizell, 1980). The emphasis of these studies has been to devise expressions relating the variance of hydraulic head in one, two or three-dimensions to the length scales and variance of lnK or lnT (K = hydraulic conductivity, T = transmissivity). Naff (1978) has examined the nature of the dispersion coefficient produced by one and three-dimensional variations in permeability. In this work solutions to stochastic differential equations are used to express the relation between permeability variations, local dispersivities, the length scales of the medium, and concentration. His analysis also demonstrates that porosity variations tend to have a second-order effect on the magnitude of the dispersion coefficient. Subsequently Gelhar et al. (1979) have furthered the work of Naff by describing the transient development of the dispersion process, which takes into account the non-Fickian behavior observed in field experiments such as those performed by Sudicky and Cherry (1979) and Pickens et al. (1978).

Water Quality Data: The purpose of this segment of the Literature Review is to survey a limited number of field studies where water quality data have been compiled and evaluated. In most cases the water quality variable constitutes a pollution hazard or potential hazard. The similarity among the water quality data examined in the following reports is that each display significant variability in space and/or time, and that interpretation of this variability may be important for understanding the mechanisms of transport in groundwater and soils. The

emphasis of the present research is to suggest a method for interpreting this variability.

The leaching of pollutants through the soil zone has received considerable attention in recent years. Biggar and Nielson (1976) examined the spatial distribution of chlorides and nitrates at twenty sites within a 150 hectare field. The pore water velocities and dispersion coefficients were found using chloride ion concentration, and both were determined to be approximated by a log-normal distribution. Toler et al. (1974) examined the distribution of chloride from highway deicing salts in the unsaturated zone. A percentage of the annual amount of infiltrated salts was retained in the soil zone, and this retention was found to be correlated with grain size distribution, depth to water table and precipitation. Childs et al. (1974) examined the infiltration of septic tank wastes to the groundwater. Their results indicate that both spatial and temporal distribution of the contamination are necessary to describe the pollution problem. Feedlot operations and their pollution potential were studied by Crosby et al. (1971) in Washington state, where nitrate and chloride concentrations were determined for the soil zone and the groundwater beneath them. Although extensive contamination was evident in the upper soil layers, little evidence of contamination was found in the groundwater.

Subsurface discharge to stream or drains from agricultural watersheds can be a source of contamination to surface supplies. Devitt et al. (1976) have examined the contribution of agricultural practices to pollution of ground and surface waters at several sites in southern California. An attempt was made to correlate fertilizer input, soil concentration and drainage effluent. However no explicit accounting

of the groundwater flow system was made. Four watersheds in Iowa were the subject of a study by Burwell et al. (1976), which was conducted to determine the impact of fertilizers. They found that over application of nitrate fertilizers were a significant source of pollution of surface water leaving the area. Large temporal variability of nitrates was observed in the watershed output.

Regional groundwater studies have recently been performed to assess the impact of diverse land use practices on groundwater quality, as well as to determine the natural or geochemical characteristics of regional aquifers. The natural spatial and temporal variations in water quality of an aquifer in Saskatchewan, Canada were studied by Davison and Vonhof (1978). Spatial changes in major ion concentration were correlated with geologic-geochemical properties of the aquifer. Temporal variation of selected ions indicate that large variations were corrolated with rainfall and recharge, while the smaller scale time variations were explained in light of geochemical reactions. Rozkowski (1967) investigated the chemical groundwater quality of a hummocky moraine in southern Saskatchewan. Spatial groundwater quality patterns were explained based on chemical reactions which occur in the unsaturated and saturated zones. Perlemutter and Koch (1972) studied nitrate pollution from fertilizers and septic tank sewage in Nassau County, Long Island. More than 3000 chemical analyses were performed on wells ranging in depth from 20-1000 feet. Typical vertical and horizontal distributions of nitrate were given in several figures.

The regional distribution of chloride, nitrate and electrical conductivity is examined over a 27 county area in west Texas in a report by Reeves and Miller (1978). The regional water quality patterns are

suggested to be partially the result of long term migration of groundwater in the Ogallala aquifer, but local vertical migration at the chemical parameters is also suggested. Nearly 1600 samples distributed on an approximate three mile grid were analyzed in this unique study.

Young et al. (1976) examined the twenty-two sites in the United Kingdom for the presence of nitrate in the soil zone and groundwater. The sites were representative of three typical land use patterns: (1) fertilized arable (2) unfertilized grassland and (3) fertilized grassland. Land use patterns were shown to have a significant impact on nitrate levels in the unsaturated-saturated zone. The spatial distribution of nitrate in several deep soil profiles (25-70 meters) was given in the report, illustrating significant vertical variation. Nightingale (1970) compared the time trends of groundwater salinity and nitrate concentration in an urban zone and adjacent irrigated area in Fresno, California. A strong time trend in nitrate was evident in the urban area, while no trends and large variations in nitrate were found beneath the agricultrual area, during the 17 year sampling program.

Schmidt (1977) analyzed the short term and long term fluctuations of water quality from a pumping well. Considerable differences between ambient water quality (unpumped) and the quality of a pumping well were observed. Permeability and water quality stratification were suggested to influence the long and short term quality in a pumped well. A study of the impact of irrigated agriculture on water quality in the Rio Grande was carried out by Wierenga et al. (1979). The study included an extensive monitoring network for flow and chemical quality of the irrigation diversion, groundwater and drain flow or irrigation return flow.

Large variations in the salinity of irrigation return flow were associated with the seasonal application of irrigation water. However a significant fraction of the total dissolved solids in the outflow were actually derived from the regional groundwater system. The spatial variability of E.C., chloride and nitrate was examined by sampling along a transect at 25 foot intervals (100 sample points). A later report for this same study area (Gelhar et al., 1980) demonstrates the use of the spectral technique for characterising spatial and temporal variability in this irrigated field site.

1. ANALYSIS OF CONTINUOUS WATER QUALITY TIME SERIES

Introduction

This first chapter is devoted to the development of a series of water quality models using the theory of linear filters and spectral analysis of time series. The method provides a theory and technique for frequency domain analysis of stationary water quality time series in groundwater. Three types of solute transport models are examined: (1) the lumped parameter or linear reservoir model, (2) a convection or advection model and (3) a one-dimensional convection-dispersion model. Solutions to stochastic differential equations are given which describe the filtering or amplitude characteristic as well as the phase characteristic of each groundwater system. Dimensionless graphs illustrate how the theory can be used to determine the important parameters of mass transport for individual groundwater systems when suitable water quality records are available.

The theory presented here is intended to provide a physical interpretation of the random component of groundwater quality records and to illustrate the distinction between the frequency response of solutes in different groundwater flow systems.

Linear filters in time series analysis

Before examining particular models of mass transport in groundwater it will be useful to review the basic properties of linear filters and their general application to frequency response studies. We assume that the physical system of interest is described by a linear differential equation where the variables are random functions of time. The analysis

will make use of a frequency domain version of the convolution integral which converts stationary input time series into stationary output. The term stationary in time means that a particular process is adequately characterized by its first two probability moments, the mean and the variance or covariance. This kind of stationarity is also referred to as second-order stationary or weakly stationary. In addition, we also make the assumption that the mean, variance and covariance of a single realization of the process (a single time series) are reasonable estimates for the underlying stochastic process. This is known as the ergodic hypothesis.

An arbitrary input $X(t)$ operated on by a linear system to yield an output $Y(t)$ can be written in terms of the convolution filter

$$Y(t) = \int_{-\infty}^{\infty} h(t-\tau)\, X(\tau)\, d\tau \qquad (1.1)$$

where $h(t-\tau)$ is the impulse response function of the system. When the input to the filter is an impulse given by the Dirac delta function, $X(t) = \delta(t)$ then

$$h(t) = \int_{-\infty}^{\infty} h(t-\tau)\cdot\delta(\tau)\, d\tau \qquad (1.2)$$

and we see that $h(t)$ itself is a solution to the convolution equation. The properties of (1.1) are the usual ones for a time invariant linear transformation (Koopmans, p.81, 1974), (i) scale preservation, (ii) superposition and (iii) time invariance. The result in (1.1) can be extended to the frequency domain by making use of the Fourier transform of $h(t)$

$$H(\omega) = \int_{-\infty}^{\infty} h(\tau)\, e^{-i\omega t}\, dt \tag{1.3}$$

where $H(\omega)$ is the complex frequency response function. The real counterpart of $H(\omega)$ is the transfer function given by $|H(\omega)|^2$.

For a second order stationary process, the only condition necessary for (1.3) to exist is (Koopmans, 1974)

$$\int_{-\infty}^{\infty} h^2(\tau)\, d\tau < \infty \tag{1.4}$$

and

$$\int_{-\infty}^{\infty} |H(\omega)|^2\, d\omega < \infty \tag{1.5}$$

Except for (1.4) and (1.5) we have so far done nothing that is peculiar to a stochastic process, since (1.1) and (1.3) would apply equally well to periodic or aperiodic functions. When we define $X(t)$ as a stationary stochastic process we must introduce another complex stochastic process $Z(\omega)$ such that

$$X(t) = \int_{-\infty}^{\infty} e^{i\omega t}\, dZ_X(\omega) \tag{1.6}$$

where the $dZ(\omega)$'s are complex Fourier amplitudes of the process (Lumley and Panofsky, 1964). Equation (1.6) is the generalized Fourier-Stieltjes representation for any second-order stationary stochastic process. Substitution of this representation for X and Y into the convolution yields

$$Y(t) = \int_{-\infty}^{\infty} e^{i\omega t} dZ_y = \int_{-\infty}^{\infty} h(t-\tau) \left\{ \int_{-\infty}^{\infty} e^{i\omega t} dZ_x \right\} d\tau. \tag{1.7}$$

Rearranging the order of integration and simplifying will produce the frequency domain version of the convolution

$$dZ_y(\omega) = H(\omega)\, dZ_x(\omega) \tag{1.8}$$

which illustrates that in the frequency domain the convolution is simplified to a multiplication. An additional property of the $dZ(\omega)$'s is

$$E\left[dZ_x(\omega_1) \cdot dZ_x^*(\omega_2) \right] = \begin{cases} 0, & \omega_1 \neq \omega_2 \\ \phi_{xx} d\omega, & \omega_1 = \omega_2 \end{cases} \tag{1.9}$$

where E(dZ dZ*)) indicates expected value, the * is the complex conjugate, and $\phi_{xx}(\omega)$ is the spectral density or simply the spectrum of X(t). The spectrum describes how variations (variance) in the series are distributed over frequency. The spectrum is a property of the autocovariance of the series given by

$$R_{xx}(\tau) = E\left[(X(t)-\mu)(X(t-\tau)-\mu) \right] \tag{1.10}$$

where μ is the mean of X and τ is the lag. The spectrum-covariance relation is uniquely determined by the following Fourier transform pair

$$\phi_{xx}(\omega) = \frac{1}{2\pi} \int_{-\infty}^{\infty} e^{-i\omega\tau} R_{xx}(\tau) d\tau \tag{1.11}$$

$$R_{xx}(\tau) = \int_{-\infty}^{\infty} e^{i\omega\tau} \phi_{xx}(\omega) d\omega. \tag{1.12}$$

From (1.9) and (1.8) we can write an expression for the transfer function in terms of the input-output spectral density functions

$$\frac{\phi_{yy}(\omega)}{\phi_{xx}(\omega)} = |H(\omega)|^2 \tag{1.13}$$

which describes the amplitude filtering characteristics of the system as a function of frequency. Since we are concerned here with differential equations which have impulse response functions h(t), (1.3) and (1.13) tell us that as long as the Fourier transform of h(t) can be found, a spectral form of the solution can be found as well. Although we may not always use the convolution as a means of determining the frequency response function, the result does generalize the procedure to a wide class of time-variable problems.

So far we have limited our discussion to the autocorrelated properties of the bivariate process, X(t) and Y(t). It is also useful to consider the cross-correlated aspects of X and Y. We begin the development with a definition for the Fourier amplitudes of cross-correlated series (Lumley and Panofsky, 1964)

$$E\left[dZ_y(\omega_1) \cdot dZ_x^*(\omega_2) \right] = \begin{cases} 0, & \omega_1 \neq \omega_2 \\ \phi_{yx} d\omega, & \omega_1 = \omega_2 \end{cases} \tag{1.14}$$

which is similar to the case for a single variable (1.9). The function $\phi_{yx}(\omega)$ is the cross-spectrum. Making use of this result and (1.8) we get

$$E\left[dZ_y(\omega) \cdot d_x^*(\omega)\right] = E\left[dZ_x(\omega) \cdot dZ_x^*(\omega)\right] \cdot H(\omega) \tag{1.15}$$

which yields the cross-spectral form of the convolution filter

$$\phi_{yx}(\omega) = \phi_{xx}(\omega) \cdot H(\omega) = L_{yx} - iQ_{yx} \tag{1.16}$$

where $L_{yx}(\omega)$ and $Q_{yx}(\omega)$ are the real and imaginary parts of $\phi_{yx}(\omega)$, and are known as the co-spectrum and quadrature spectrum respectively. The phase is determined from $L_{yx}(\omega)$ and $Q_{yx}(\omega)$ according to

$$\Theta_{yx}(\omega) = - \text{Tan}^{-1} \left(\frac{Q_{yx}}{L_{yx}} \right) \tag{1.17}$$

where $\Theta_{yx}(\omega)$ is the phase spectrum or simply the phase. The phase, as described by Jenkins and Watts (1968), shows whether frequency components in the X series lead or lag the components at the same frequency in the Y series.

An important consideration in current modeling efforts involves the estimation of probability moments for sampled water quality variables. Estimates of the first two moments (the mean and the variance) are particularly important when designing site-specific water quality sampling networks, or evaluating the sensitivity of a particular model to variations in the source strength or hydrologic parameters.

A natural result of the linear filter-spectral analysis technique is that the theoretical output variance of a particular hydrologic system can be determined as a function of the source (input) variance and the transfer function. A basic property of a stationary time series is that the variance can be decomposed into contributions from a continuous range of frequencies

$$\sigma^2 = \int_{-\infty}^{\infty} \phi(\omega) \, d\omega. \tag{1.18}$$

We can use this result to determine the output variance of the convolution filter (1.13) simply by integrating over frequency

$$\sigma_y^2 = \int_{-\infty}^{\infty} \phi_{yy}(\omega)d\omega = \int_{-\infty}^{\infty} \phi_{xx}|H(\omega)|^2 d\omega. \tag{1.19}$$

After the transfer function is determined the only thing that remains is to specify the functional form of the input spectrum. A convenient form for $\phi_{xx}(\omega)$ which will be used extensively (but not exclusively) in this research is

$$\phi_{xx}(\omega) = \frac{\lambda\ \sigma_x^2}{\pi(1+\lambda^2\omega^2)} \quad . \tag{1.20}$$

This input spectrum assumes that the autocovariance for the input process is given by

$$R_{xx}(\tau) = \sigma_x^2\ e^{-\tau/\lambda} \tag{1.21}$$

which supposes an exponential reduction in correlation as the interval between samples is increased. A limiting case is the continuous time white noise process for the input series X(t). The autocovariance is given by

$$R_{xx}(\tau) = \begin{cases} \sigma_x^2\ \delta\ (\tau) > 0, \tau=0 \\ 0\ ,\ \tau \neq 0 \end{cases} \tag{1.22}$$

and the spectrum is

$$\phi_{xx}(\omega) = \frac{\sigma_x^2}{2\pi} \cdot \tag{1.23}$$

Substitution of (1.20) or (1.23) into (1.19) and performing the integration will provide the theoretical output variance for the frequency response functions to be developed next.

The Linear Reservoir

A functional approach to distributed sources of groundwater contamination makes use of the completely mixed assumption of the linear reservoir model. Applications of the linear reservoir to groundwater pollution problems has received some attention in recent years (Orlob et al., 1967; Gelhar and Wilson, 1974; McLin, 1981) and would seem to be especially useful in cases where only limited data and/or economic resources are available. Because of the limited requirements of the 'lumped parameter' technique, its use is also suitable for order of magnitude surveys, preliminary to detailed investigations. Whatever the situation, the model requires that the input and output characteristics of the groundwater reservoir be known, and that the outflow be linearly related to the average or well mixed behavior of the groundwater system.

When we view the hydrologic setting as a system which does not have a complete spatial description, but has a well defined input and output, we can propose a simple water balance of the form

$$S \frac{d\bar{h}}{dt} = - q + q_i + \text{other sources} \tag{1.24}$$

where $\bar{h}(t)$ = the average saturated thickness

S = specific yield

q = natural discharge/unit area

q_i = recharge rate/unit area

The field setting is illustrated in Figure 1.1. Outflow from a linear reservoir is approximated by (Gelhar, 1974)

$$q = a(\bar{h}-h_o) \tag{1.25}$$

Figure 1.1. The linear reservoir: $\bar{h}$ is the average water level, c is the 'well-mixed' concentration of solute in the aquifer and the outflow. q_i and c_i are the recharge rate and its concentration respectively.

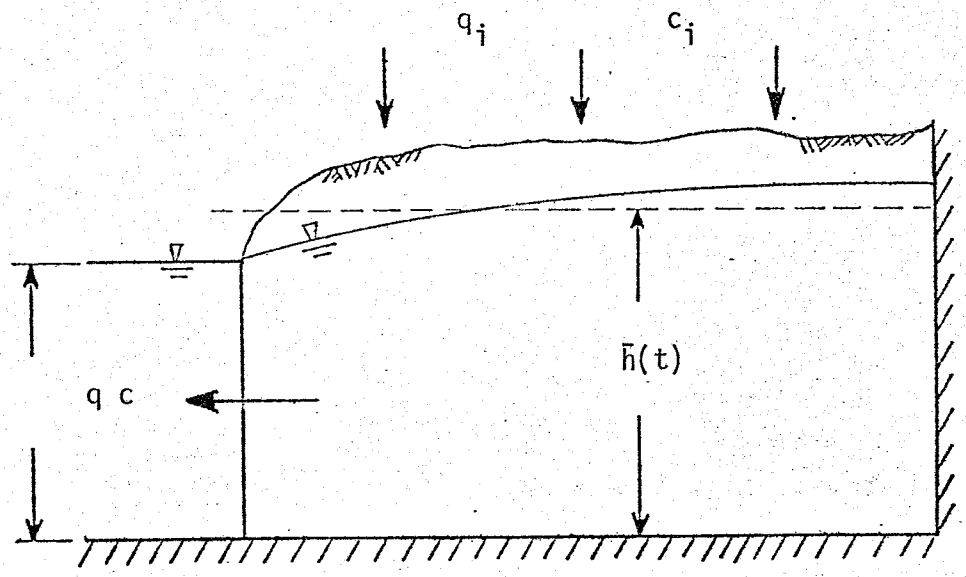
q_i
c_i
$\bar{h}(t)$
q c

where a is the outflow constant and h_o is the elevation at the stream or drain.

The mass balance for a conservative contaminant of solute concentration c(t) is

$$dM/dt = m_i - m_o + \text{other sources} \tag{1.26}$$

where

$M = \bar{n}\bar{h}c$ = average mass of solute c per unit aquifer area

$m_i = q_i c_i$ = input mass flux per unit area

$m_o = qc$ = outflow mass flux per unit area

n = effective porosity

For the case of steady-state groundwater flow $q = q_i$ and (1.26) is written

$$dc/dt + c/Tc = c_i/T_c \tag{1.27}$$

where $T_c = \bar{n}\bar{h}/q$ is the average residence time or solute response time of the system. Since the coefficients of (1.27) are constant a solution for an arbitrary input is given by the convolution integral

$$c(t) = \int_{-\infty}^{\infty} h(t-\tau)\, c_i(\tau)\, d\tau. \tag{1.28}$$

It was shown earlier that a unit impulse input $c_i = \delta(t)$ produces the following impulse response function

$$h(t) = (1/Tc) \exp(-t/Tc) \tag{1.29}$$

which provides a basic solution or kernel to any particular input concentration c_i.

We would now like to construct a frequency domain solution to (1.27) when $c_i(t)$ and $c(t)$ are stationary stochastic processes. A decomposition of the variables in time, separates each into a mean and a fluctuation about the mean given by

$$c(t) = E(c) + c'(t) \tag{1.30}$$

$$c_i(t) = E(c_i) + c_i'(t) \tag{1.31}$$

Substitution of (1.30) and (1.31) into equation (1.27) and subtracting the mean part gives the zero mean equation

$$dc'/dt + c'/Tc = c_i'/Tc \tag{1.32}$$

which has the frequency domain solution

$$\frac{dZ_c(\omega)}{dZ_{c_i}(\omega)} = 1/(1+i\omega t_c) = H(\omega) \tag{1.33}$$

where $H(\omega)$ is the frequency response function. As pointed out earlier $H(\omega)$ can also be found by taking the Fourier transform of $h(t)$

$$H(\omega) = \int_{-\infty}^{\infty} e^{i\omega t}\, h(t)dt = \int_{-\infty}^{\infty} e^{i\omega t}\, e^{-t/T_c}\, dt = 1/(1+i\omega t_c). \tag{1.34}$$

The spectral form of (1.33) is found by applying the properties of the dZ process given in (1.9), which yields the amplitude characteristic of the model, the transfer function

$$\frac{\phi_{cc}(\omega)}{\phi_{c_i c_i}(\omega)} = 1/(1+\omega^2 T_c^2). \tag{1.35}$$

The next step is to determine the phase behavior of the linear reservoir, which is a property of the cross-spectrum of input to output given by

Figure 1.2. The theoretical transfer function and phase (radians) for the linear reservoir model, plotted versus dimensionless frequency $\omega T_c = \Omega$.

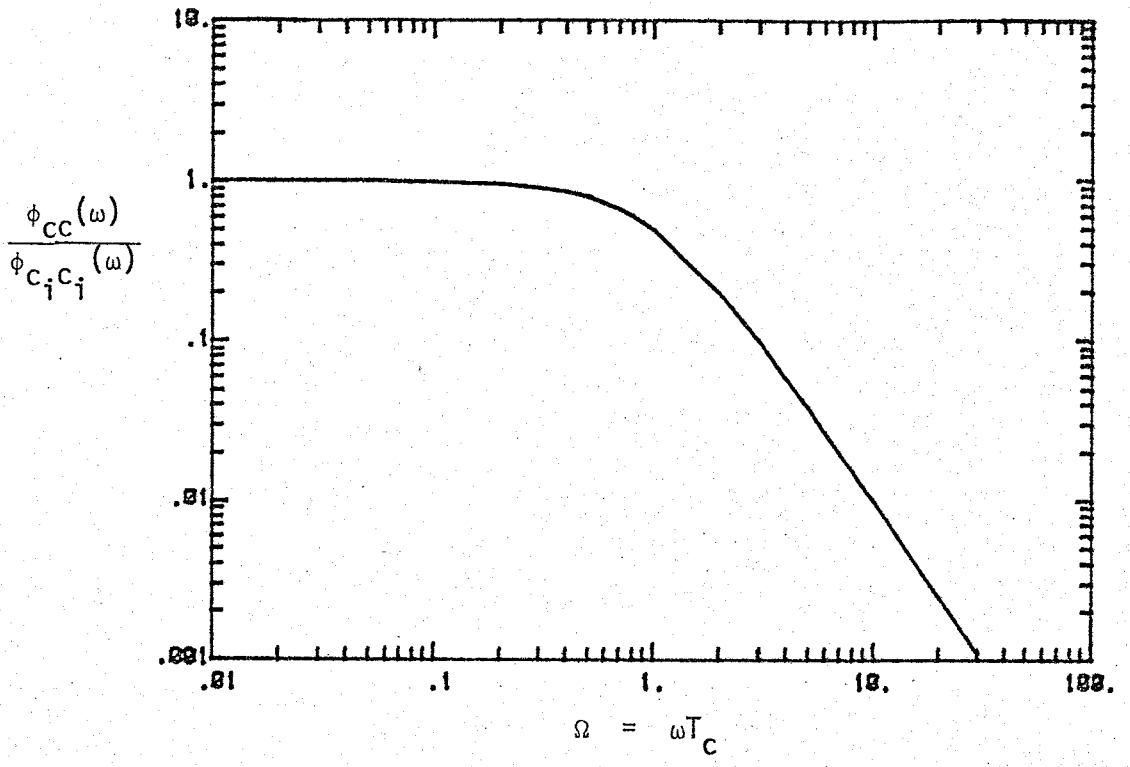
10.
1.
.1
.01
.001
.01
.1
1.
10.
100.
$\frac{\phi_{cc}(\omega)}{\phi_{c_i c_i}(\omega)}$
$\Omega = \omega T_c$

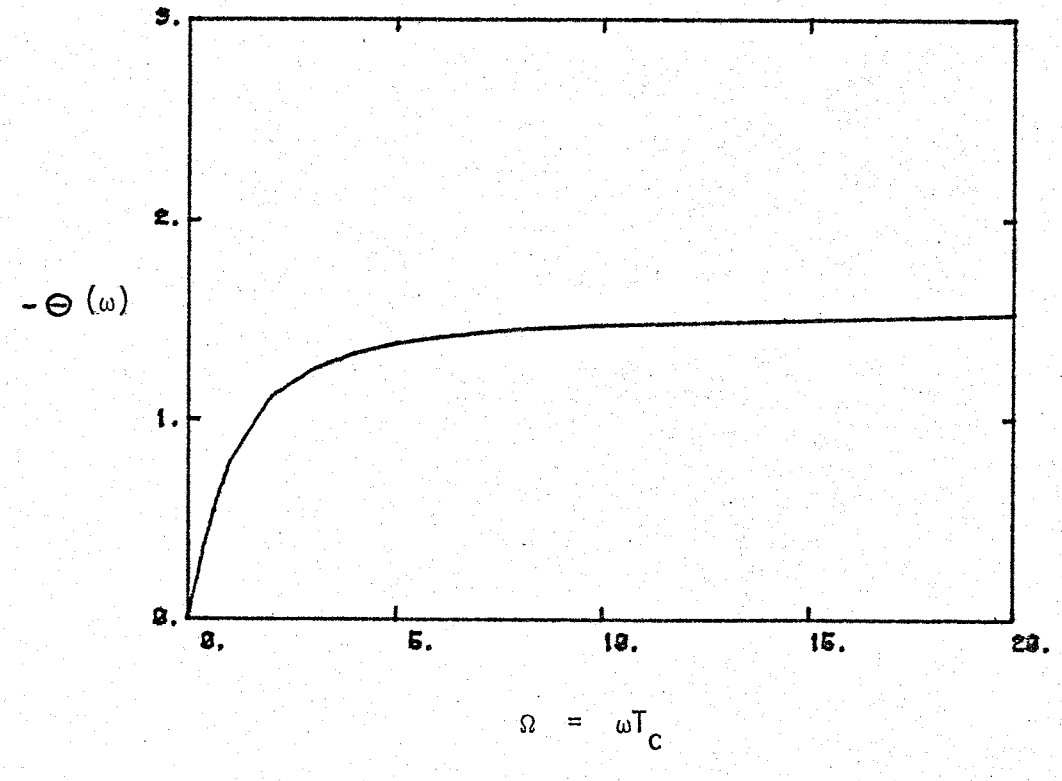
3.
2.
1.
0.
0.
5.
10.
15.
20.
$-\Theta(\omega)$
$\Omega = \omega T_c$

$$\phi_{cc_i}(\omega) = \frac{\phi_{c_i c_i}(\omega)}{(1+i\omega T_c)} = \frac{1}{(1+\omega^2 T_c^2)} \cdot e^{-i\theta_{cc_i}(\omega)} \qquad (1.36)$$

where $\phi_{cc_i}(\omega)$ is the cross-spectrum for $c(t)$ and $c_i(t)$, and the argument of the complex exponential is the phase spectrum, or simply the phase

$$\theta(\omega) = - \text{Tan}^{-1}(\omega T_c). \qquad (1.37)$$

Equations (1.35) and (1.37) describe the amplitude and phase properties of a simple linear reservior subject to a stochastic, distributed source of contaminant or tracer. The transfer function and phase are plotted against dimensionless frequency $\Omega = \omega T_c$ in Figure 1.2. The linear reservoir transfer function is typical of a 'low pass' filter, where high frequencies in the input time series are attenuated and low frequencies pass through the filter unaltered. The negative phase spectrum increases with frequency up to a maximum of $\pi/2$ radians.

Using (1.20) along with the transfer function given by (1.35) we can write down an expression for the output variance

$$\sigma_c^2 = \int_{-\infty}^{\infty} \frac{\lambda \sigma_{c_i}^2}{\pi(1+\lambda^2\omega^2)(1+\omega^2 T_c^2)} d\omega \qquad (1.38)$$

where λ is the correlation scale of the input process $c_i(t)$. Performing the integration yields

$$\sigma_c^2 / \sigma_{c_i}^2 = 1/(1+T_c/\lambda) \qquad (1.39)$$

The variance ratio shown in (1.39) and illustrated in Figure 1.3 indicates how input variations in water quality are attenuated by the natural filtering properties of the groundwater system. It is perhaps useful to comment on the significance of the input-output variance ratio with

Figure 1.3. The variance ratio of output to input concentration.

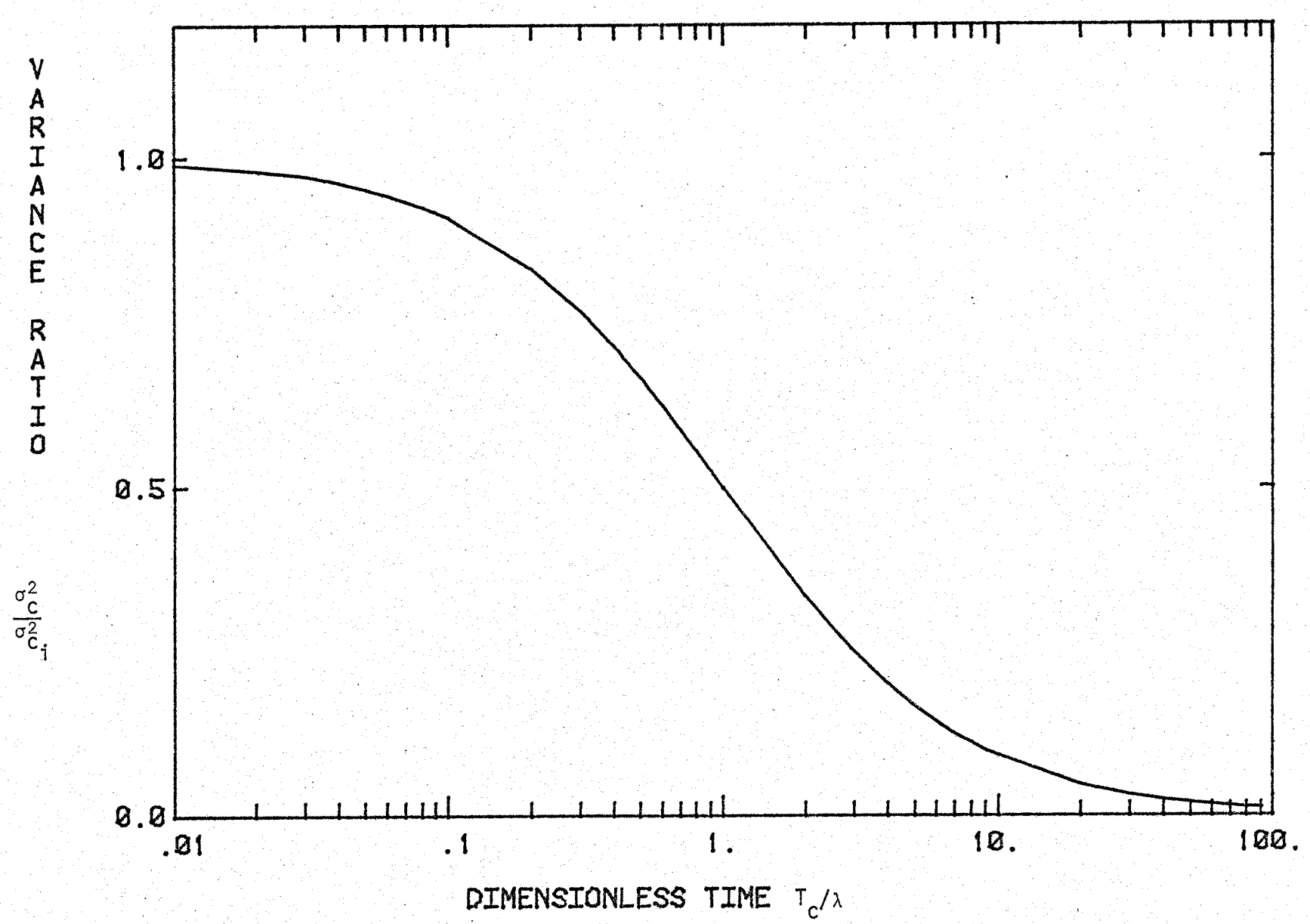
VARIANCE RATIO
$\frac{\sigma_c^2}{\sigma_{c_i}^2}$
1.0
0.5
0.0
.01
.1
1.
10.
100.
DIMENSIONLESS TIME T_c/λ

respect to analysis of field data. It is readily apparent in Figure 1.3 that, for systems with large residence times T_c and/or small input correlation scales λ, continuous solute inputs will produce little variance in the outflow quality. This fact might have a considerable impact on how one would sample this system under field conditions.

Transport by Convection

The contamination of groundwater from point and distributed sources has recently been examined by the use of travel-time calculations based on the velocity field (eg. Jury, 1975; Nelson, 1978). The approach considers the effect of dispersion and diffusion to be second order and can thus be neglected, while the solute is assumed to move along the streamline in a piston flow. If the contaminant is examined at a point of discharge, say a pumping well or river, the concentration at the discharge point would exhibit a mixing of the individual stream tubes displaying an 'apparent' dispersion of the solute which is actually due to the arrival of different travel paths. In the following analysis a general solution for convective transport in a curvilinear flow will be developed. The approach will transform the continuous time process effecting water quality into the frequency domain making use of the spectral representation theorem given earlier.

If we consider an arbitrary streamline in a steady, nonuniform flow field with velocity U(S) the equation for convection only can be written (Hoopes and Harleman, 1967)

$$\partial c/\partial t + u(s)\ \partial c/\partial s = - Kc \qquad (1.40)$$

where s is distance along the streamline and dispersive transport has been neglected. The coefficient K is a rate constant describing simple

first order decay (i.e. radioactive decay). The aquifer is assumed to be homogeneous and isotropic with regard to all material properties. Thus variations in the solute are entirely due to variations in the source strength. Equation (1.40) can be expressed in another form, where we make use of a travel-time coordinate

$$\partial c/\partial t + \partial c/\tau = - Kc \tag{1.41}$$

with the new coordinate system defined as

$$\tau = \int_{s_o}^{s} \frac{ds}{u(s)}. \tag{1.42}$$

The continuous time input enters the groundwater system as a point source boundary condition

$$s = o \ (\tau=o) \ , \ c(o,t) = c_i(t) \tag{1.43}$$

providing a complete description of the problem. The impulse response function for (1.41) is given by (Thomann, 1972)

$$h(\tau,t) = e^{-K\tau}\,\delta(t-\tau) \tag{1.44}$$

where the Dirac delta function $\delta(t-\tau)$ implies a unit source strength at $s=0$ ($\tau=0$). To construct the frequency domain solution we again write the water quality variables in terms of a mean and perturbation

$$c(s,t) = \bar{c}(s) + c'(s,t) \tag{1.45}$$

$$c_i(t) = \bar{c}_i + c_i'(t) \tag{1.46}$$

Substituting the perturbations into the convection equation we get

$$\frac{\partial}{\partial t}(\bar{c}+c') + \frac{\partial}{\partial \tau}(\bar{c}+c') = -K(\bar{c}+c') \tag{1.47}$$

with the boundary condition

$$\tau=0 \ (s=0) \ , \ \bar{c}+c' = \bar{c}_i+c'_i \tag{1.48}$$

Subtracting the mean equation from (1.47) and (1.48) we arrive at the equation for the fluctuations

$$\partial c'/\partial t + \partial c'/\tau = -Kc' \ , \ c'(t) = c_i(t), \ \tau=0 \tag{1.49}$$

The spectral representation theorem allows us to write the input and output perturbations in the following way

$$c'(\tau,t) = \int_{-\infty}^{\infty} e^{i\omega t} \, dZ_c(\tau,\omega) \tag{1.50}$$

$$c'_i(t) = \int_{-\infty}^{\infty} e^{i\omega t} \, dZ_{c_i}(\omega) \tag{1.51}$$

Substituting (1.50) and (1.51) into the convection equation yields

$$\frac{d}{d\tau} (dZ_c) + (i\omega+K) \, dZ_c = 0 \tag{1.52}$$

with the boundary condition

$$dZ_c(o,\omega) = dZ_{c_i}(\omega), \ \tau=0 \tag{1.53}$$

The solution to (1.52) is

$$\frac{dZ_c(\tau,\omega)}{dZ_{c_i}(\omega)} = e^{-(i\omega+K)\tau} = H(\tau,\omega) \tag{1.54}$$

where $H(\tau,\omega)$ is the frequency response function for the convection equation. An alternative way to arrive at $H(\tau,\omega)$ is simply to take the Fourier transform of $h(t)$ in (1.44)

$$H(\tau,\omega) = \int_{-\infty}^{\infty} e^{-i\omega t} \ e^{-K\tau} \delta(t-\tau) \, dt = e^{-(i\omega+K)\tau}$$

which provides a check on (1.54). Having determined the frequency response of the system we can now apply the properties of the dZ's (1.9) to arrive at the spectral form of the solution

$$\phi_{cc}(\tau,\omega) = \phi_{c_i c_i}(\omega)|H(\tau,\omega)|^2 \tag{1.55}$$

where τ is given by (1.42) and

$$|H(\tau,\omega)|^2 = e^{-2K\tau} \ . \tag{1.56}$$

It is immediately apparent that the transfer function does not depend on frequency ω. This is due to the fact that input variations are simply displaced along a streamline unaltered, except for the factor $e^{-2K\tau}$, which is characteristic of piston flow. In communications theory, (1.55) is known as an 'ideal' filter, where the signal is either amplified or attenuated by a constant factor. The phase for (1.54) is given by

$$\theta(\omega) = -\omega\tau = -\omega \int \frac{ds}{u(s)} \tag{1.57}$$

The negative phase spectrum, which does not depend on the rate constant K, increases linearly with frequency and distance along the streamline.

Another aspect of interest is the output variance σ_c^2 . Using (1.19) and (1.20) the output variance is determined to be

$$\sigma_c^2 = \sigma_{c_i}^2 \quad |H(\tau,\omega)|^2 \tag{1.58}$$

If we assume for the moment that the tracer is conservative then there is no variance reduction as the solute moves through the aquifer and $\sigma_c^2 / \sigma_{c_i}^2 = 1$, which is the expected result for piston displacement.

Because (1.55) lacks the filtering characteristics normally observed in solute experiments in porous materials we might draw the conclusion that the convection only approach is of limited interest. However in many field situations it has been shown that the convective mode of transport overwhelms the influence of dispersion. For example Hoopes and Harleman (1967) show that the effect of dispersion and diffusion play a relatively minor role in the case of artificial waste disposal using recharge-discharge wells. Eldor and Dagan (1972) have shown that, for a two-dimensional steady flow to a drain or ditch with uniform recharge, dispersion has little effect at the point of discharge. They conclude that since the flow is two-dimensional, as much solute is displaced ahead of the front as behind it, and thus at the discharge point, where contributions from all stream tubes are mixed, the dispersion effect is canceled.

A specific example of convective transport in a curvilinear flow field was examined by Kirkham and Affleck (1977). The flow system they considered, which is shown in Figure 1.4 assumes a homogeneous, isotopic aquifer in hydraulic connection with an adjacent river. The steady plane flow is developed between the constant head boundary at the river and the constant discharge well located a distance L from the river. The hydraulic situation is identical to the pumping well fed by a line drive shown by Muskat (1937). The velocity and potential field are determined by superimposing the effect of an imaginary injection well located a distance -L from the axis of the constant head boundary. The Kirkham and Affleck paper goes on to develop an analytical expression for the travel time of a conservative solute entering the aquifer at the river

Figure 1.4. A. Aquifer-river cross-section. B. A pumping well adjacent to a river. C. Streamlines and equipotential lines for B.

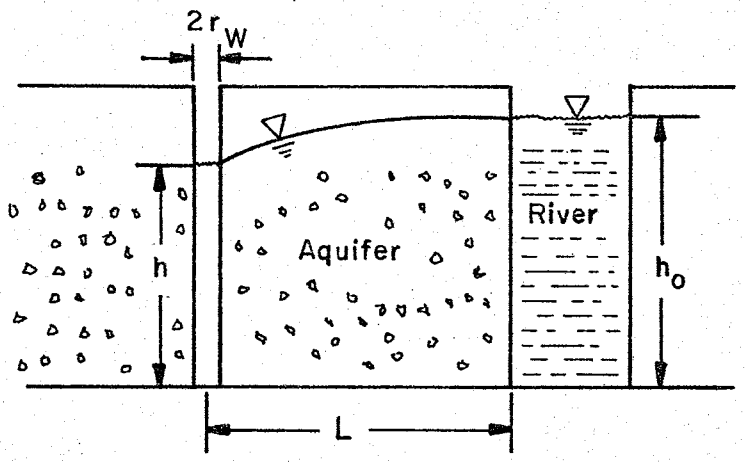
2r
W
River
Aquifer
h
h
o
L

A.

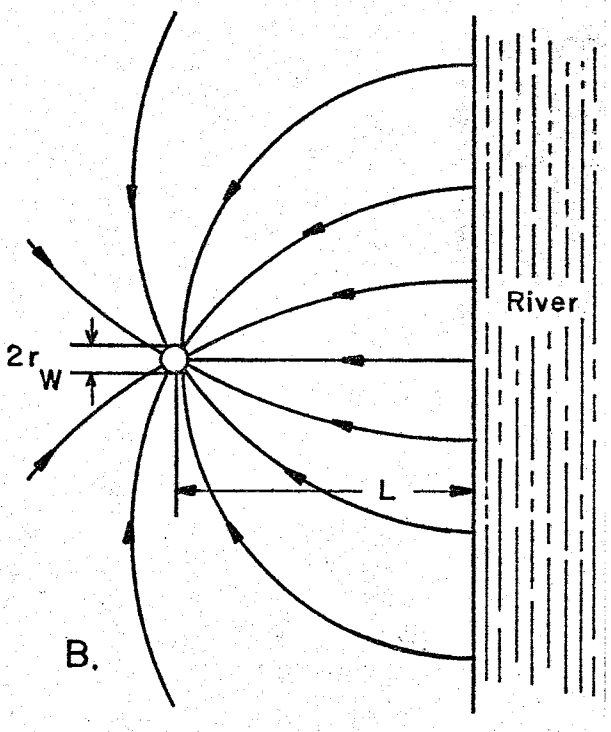
River
2r
W
L

B.

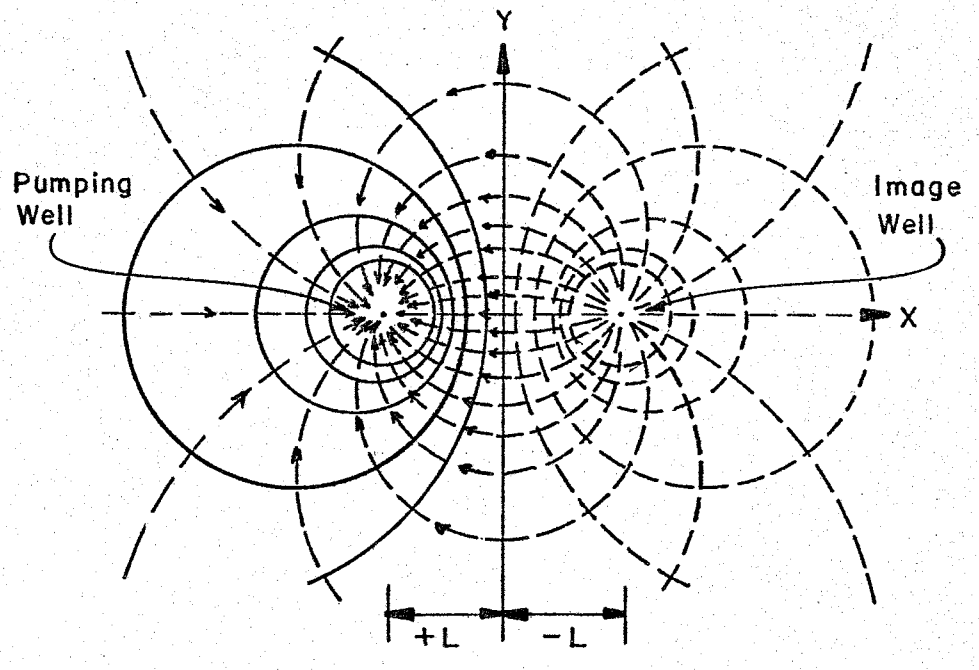
Y
Pumping
Well
Image
Well
X
+L
-L

C.

$$h-h_o = \frac{Q}{4\pi T} \text{Ln} \left[\frac{(X-L)^2+Y^2}{(X+L)^2+Y^2} \right] \tag{1.61}$$

The travel time in a curvilinear flow field is

$$\tau = \int_{s1}^{s2} \frac{ds}{q_s/n} \tag{1.42a}$$

Since on a particular streamline it takes a particle the same time to move the distance dx as it takes to move the distance dy (1.42) can also be written

$$\tau = \int_{x1}^{x2} \frac{dx}{q_x/n} = \int_{y1}^{y2} \frac{dy}{q_y/n} \tag{1.62}$$

The x component of the seepage velocity is determined from Darcy's law

$$q_x = - \frac{K}{n} \frac{\partial h}{\partial x} \tag{1.63}$$

or

$$q_x = - \frac{Q}{2\pi n h_o} \left[\frac{Y}{y^2+(x-L)^2} - \frac{Y}{y^2+(x+L)^2} \right] \tag{1.64}$$

The travel time to the well is determined by integration of (1.62) and evaluation of τ at the well (x=L, y=0)

$$\tau_\omega = \frac{T_o}{\text{SIN}^2\zeta} \left[1 - \zeta \text{ COT } \zeta \right] \tag{1.65}$$

where

$$T_o = \frac{nL^2}{Q/2\pi h_o} \tag{1.66}$$

As shown by Kirkham and Affleck, and in a slightly different form by Hoopes and Harleman, (1.65) describes the time for the solute to travel from a point on the river (X=0, Y) to the well. The shortest time for the solute to reach the well is along the streamline which passes through Y=0. The minimum time can be expressed as $\tau_\omega = T_o/3$.

To obtain the frequency response function at the well ($\tau=\tau_\omega(\zeta)$) it is necessary to integrate the result in (1.54) around the point of discharge ($-\pi<\zeta<\pi$)

$$dZ_{c_\omega}(\omega)=\frac{1}{2\pi}\int_{-\pi}^{\pi} dZ_{c_\omega}(\omega,\tau_\omega(\zeta))d\zeta = \frac{dZ_{c_i}(\omega)}{\pi}\int_{o}^{\pi} e^{-i\omega\tau_\omega(\zeta)}d\zeta \qquad (1.66)$$

where the first order rate constant K is taken to be zero, $dZ_{c_\omega}(\omega)$ is the Fourier amplitude for concentration c_ω at the well and $dZ_c(\omega,\tau_\omega(\zeta))$ is the Fourier amplitude for concentration along any streamline near the well. The transfer function is then found to be

$$\frac{\phi_{c_\omega c_\omega}(\omega)}{\phi_{c_i c_i}(\omega)} = \frac{1}{\pi^2}\left|\int_{o}^{\pi}\exp(-i\omega\tau_\omega(\zeta))\,d\zeta\right|^2 \qquad (1.67)$$

where $\phi_{c_\omega c_\omega}(\omega)$ is the spectrum for the solute time series at the well, and $\phi_{c_i c_i}(\omega)$ is the spectrum for the river concentration (x=0). Likewise the phase function is found to be

$$\theta(\omega) = -\,\mathrm{Tan}^{-1}\left[\frac{\int_o^\pi \mathrm{SIN}(\omega\tau_\omega(\zeta))d\zeta}{\int_o^\pi \mathrm{COS}(\omega\tau_\omega(\zeta))d\zeta}\right]. \qquad (1.68)$$

The integral expressions in (1.67) and (1.68) were evaluated numerically and the results are shown in Figure (1.5) plotted against dimensionless frequency $\Omega = \omega T_o$. The frequency characteristics of this model behave

Figure 1.5. Theoretical transfer function $\phi_{C_\omega C_\omega}(\omega)/\phi_{C_i C_i}(\omega)$ and phase $\theta(\omega)$ (radians) for the convective transport model of a pumping well adjacent to a river.

$$\frac{\phi_{c_\omega c_\omega}(\omega)}{\phi_{c_i c_i}(\omega)}$$

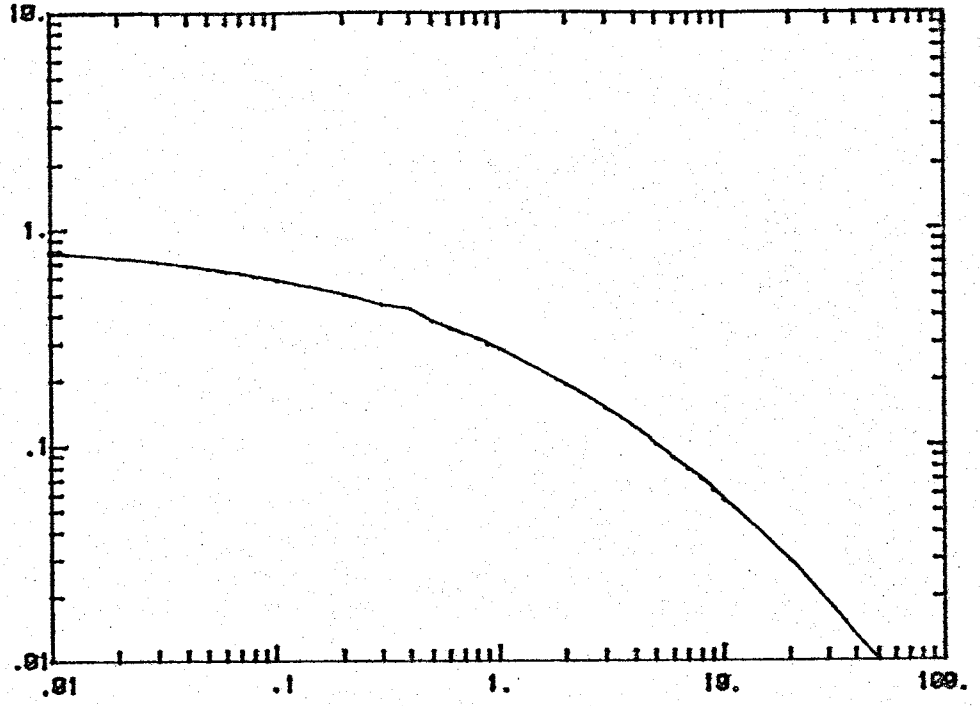

$\Omega = \omega T_0$

$-\Theta(\omega)$

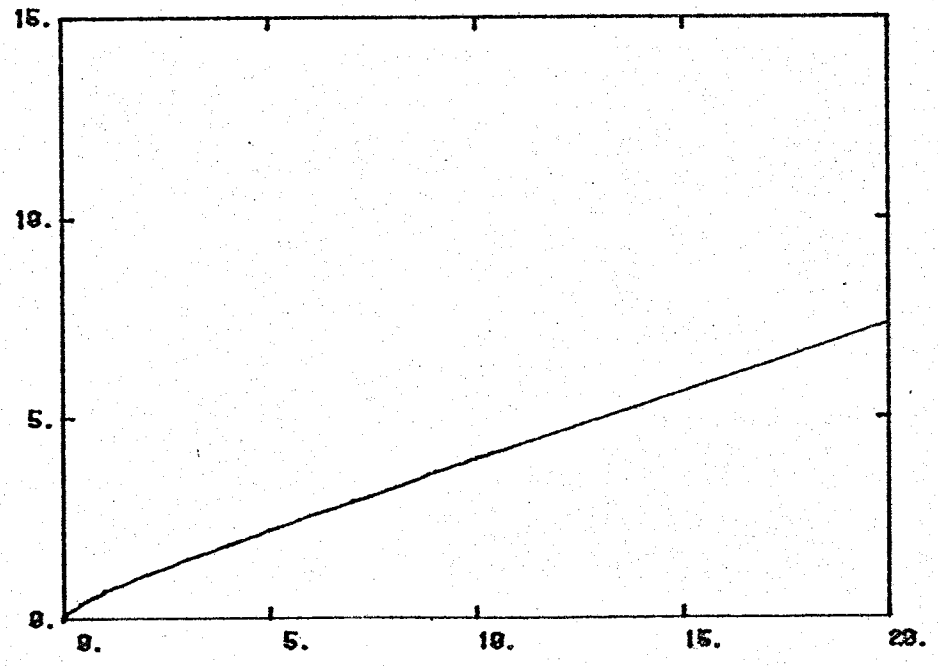

$\Omega = \omega T_0$

much differently than the linear reservoir case. The transfer function indicates significant amplitude filtering in the low frequency range ($\Omega<1.0$) while over the rest of the range ($\Omega>1.0$) there is proportionally less amplitude filtering. The phase for this model increases linearly beyond $\Omega=1$, while demonstrating some curuature near the origin. We can say then that water quality variations in a curvilinear groundwater flow display distintive behavior when compared to either the linear reservoir, or for convection in the uniform flow case given earlier. An application of this method will be examined in a later section.

Convective-Dispersive Transport

Recalling that the primary objective of the models in this section is to characterize time variability in groundwater quality observations which are affected by a continuous and stochastic source of solute, the analysis now turns to the case of solute transport in a dispersive flow field. The linear filter theory and spectral representation theorem are again used to evaluate the frequency response characteristics of the dispersive system. Dimensionless plots are constructed for the transfer function, phase and variance ratio, each versus dimensionless frequency. The limiting case of pure convection ($\alpha=0$) is compared with the dispersion result for a wide range of parameters. The influence of radioactive decay is also examined.

The basic equation describing one-dimensional convective-dispersive transport in a curvilinear steady flow is given by Gelhar and Collins (1971)

$$\frac{\partial c}{\partial t} + u(s)\frac{\partial c}{\partial s} \quad \alpha \cdot u(s)\,\frac{\partial^2 c}{\partial s^2} - Kc \tag{1.69}$$

where K is a first order rate constant which could include the effect of radioactive decay or other first order reactions. The longitudinal dispersion coefficient is assumed to vary linearly with the seepage velocity u along the coordinate s and is expressed as

$$D = \alpha \cdot u \tag{1.70}$$

where α is the dispersivity length. A complete description of the dispersion process would include the effects of molecular diffusion and transverse dispersion. However based on both theoretical (de Josselin de Jong, 1958) and experimental evidence (Harleman and Rumer, 1963) the magnitude of diffusive transport is small relative to longitudinal dispersion, and all transverse components are assumed to be lost in the vertical averaging process implied by (1.69). Another useful form of (1.69) can be obtained by substitution of the travel time coordinate (Gelhar and Collins 1971)

$$\tau(s) = \int_{s_o}^{s} \frac{ds}{u(s)} \tag{1.71}$$

which transforms (1.69) into the following form

$$\frac{\partial c}{\partial t} + \frac{\partial c}{\partial \tau} = \frac{\alpha}{u} \left(\frac{\partial^2 c}{\partial \tau^2} - \frac{\partial u}{\partial s} \frac{\partial c}{\partial \tau}\right) - Kc \tag{1.72}$$

where τ is a moving coordinate representing the time of travel for a particle to move from s_o to s at a velocity u(s).

The most elementary application of (1.72) assumes a uniform flow field or s=x and u=constant. It is assumed that the influence of non-parallel boundaries on dispersive mixing can be neglected, and that

local perturbations in the velocity derived from medium variability are represented by a statistical average u, and thus $D=\alpha \cdot u=$constant. The case of uniform flow will be developed in this section, however, the result could be extended to particular situations of nonuniform flow as well. Figure 1.6 illustrates a field setting where environmental tracers might be used in conjunction with a regional groundwater flow field.

The source of solute enters the groundwater system at the boundary x=0, by the application of a concentration type boundary condition

$$c(o,t) = c_i(t) \tag{1.73}$$

or a flux type condition

$$\left(-D\frac{\partial c}{\partial x} + uc\right)\Bigg|_{x=o+} = uc_i(t). \tag{1.74}$$

A second necessary condition is $c=0$, $x\to\infty$. The impulse response function for (1.69) is given by

$$h(x,t) = \frac{c_1}{\sqrt{4\pi t^3}}\left[\exp\left(-\frac{(x-ut)^2}{4Dt} - Kt\right)\right] \tag{1.75}$$

with the condition $c_i(t) = c_1\int\delta dt = c_1$. Other time domain solutions can be constructed from (1.75). To determine the frequency domain solution we write $c(x,t)$ and $c_i(t)$ as a mean and perturbation as before

$$c(x,t) = \bar{c}(x) + c'(x,t) \tag{1.76}$$

$$c_i(t) = \bar{c}_i + c_i'(t) \tag{1.77}$$

Substitution of (1.76) and (1.77) into (1.72) and then subtracting the steady-state result produces the zero-mean equation

Figure 1.6. Illustration of regional transport of environmental tracers in a uniform flow.

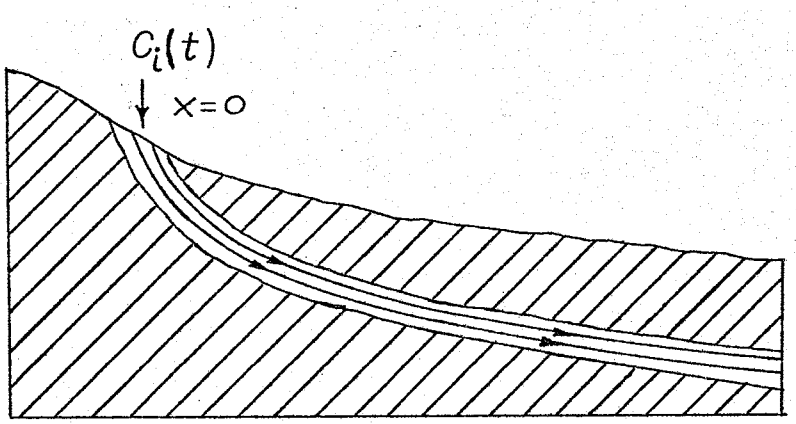
$C_i(t)$
x=0

$$\frac{\partial c'}{\partial t} + \frac{\partial c'}{\partial \tau} = \frac{\alpha}{u}\frac{\partial^2 c'}{\partial \tau^2} - Kc' \tag{1.78}$$

Making use of the spectral representation theorem results in the ordinary differential equation

$$\frac{\alpha}{u}\frac{d^2}{d\tau^2}(dZ_c) - \frac{d}{d\tau}(dZ_c) - (i\omega+K)\,dZ_c = 0 \tag{1.79}$$

Solving for $dZ_c(\tau,\omega)$ results in the frequency response function for (1.72)

$$\frac{dZ_c(\tau,\omega)}{dZ_{c_i}(\omega)} = H(\tau,\omega) \tag{1.80}$$
$$= c_2 \exp\left[\frac{x}{2\alpha} - \frac{1}{2}\sqrt{\frac{x}{\alpha}}\left[\frac{x}{\alpha} + 4K\tau + 4i\omega\tau\right]^{\frac{1}{2}}\right]$$

where c_2 is evaluated using boundary condition (1.73) or (1.74)

$$c_2 = \begin{cases} 1 \;;\; \text{B.C. (1.73)} \\ \left(\frac{\alpha}{2x}\right)^{-1}\left[\frac{x}{\alpha} + \sqrt{\frac{x}{\alpha}}\left(\frac{x}{\alpha} + 4K\tau + 4i\omega\tau\right)^{\frac{1}{2}}\right]^{-1} \;;\; \text{B.C.(1.74)} \end{cases}$$

and $\tau = x/u$ is the travel time from $x = 0$ to some point in the aquifer. The spectral equation or transfer function is determined using (1.9)

$$\frac{\phi_{cc}(\tau,\omega)}{\phi_{c_o c_o}(\omega)} = |H(\tau,\omega)|^2 \tag{1.82}$$
$$= |c_2|^2 \cdot \left|\exp\left[\frac{\zeta}{2} - \frac{1}{2}\zeta^{\frac{1}{2}}(\zeta+4\kappa+4i\Omega)^{\frac{1}{2}}\right]\right|^2$$

and

$$|c_2|^2 = \begin{cases} 1, \text{ B.C.(1.73)} \\ \left|\left[\frac{1}{2\zeta}\left[\zeta + \zeta^{\frac{1}{2}}(\zeta+4\kappa+4i\Omega)^{\frac{1}{2}}\right]\right]^{-1}\right|^2, \text{ B.C.(1.74)} \end{cases} \tag{1.83}$$

where $\zeta=x/\alpha$, $\kappa=K\tau$ and $\Omega=\omega\tau$ are the dimensionless dispersivity length, dimensionless rate constant and frequency, respectively. Recalling that the spectrum for a given solute describes the distribution of variance over frequency and that the transfer function is a ratio of the spectrum at an observation point X, to the input spectrum, then it is possible to examine the amplitude filtering characteristics of the system as a function of the dimensionless dispersion parameter $\zeta=x/\alpha$. Figure 1.7 illustrates the transfer function for a wide range of ζ. Both boundary conditions are shown; however there is essentially no difference when $\zeta=x/\alpha > 10$. It is immediately apparent that as the dispersivity length increases ($x/\alpha \rightarrow 0$), increasingly more high frequency input variations are filtered out. The corollary to this interpretation is that as the effect of dispersion diminishes ($x/\alpha \rightarrow \infty$) the transfer function approaches the situation of pure convection or $\alpha=0$.

The phase behavior for $c(x,t)$ and $c_i(t)$ can be used to evaluate the time lag for different frequencies in the input. The general form for the phase spectrum (as shown previously) is given by

$$\theta(\omega) = -\mathrm{Tan}^{-1}\left[\frac{Q_{cc_i}(\omega)}{L_{cc_i}(\omega)}\right] \qquad (1.84)$$

where Q_{cc_i}, the quadrature spectrum, and L_{cc_i} the co-spectrum, are the complex and real parts of the cross-spectrum which is given by

$$\phi_{cc_i}(\tau,\omega) = \phi_{c_ic_i}(\omega)\, H(\tau,\omega) = L_{cc_i}(\tau,\omega) - iQ_{cc_i}(\tau,\omega). \qquad (1.85)$$

Both L_{cc_i} and Q_{cc_i} were determined by using a complex algebra package on a Dec-20 computer, and the phase was calculated from (1.84). A plot of

Figure 1.7. Theorertical transfer function for convective-dispersive transport versus Ω. The dashed lines indicate a flux type boundary condition (1.74) and the solid lines are the concentration type boundary condition (1.73).

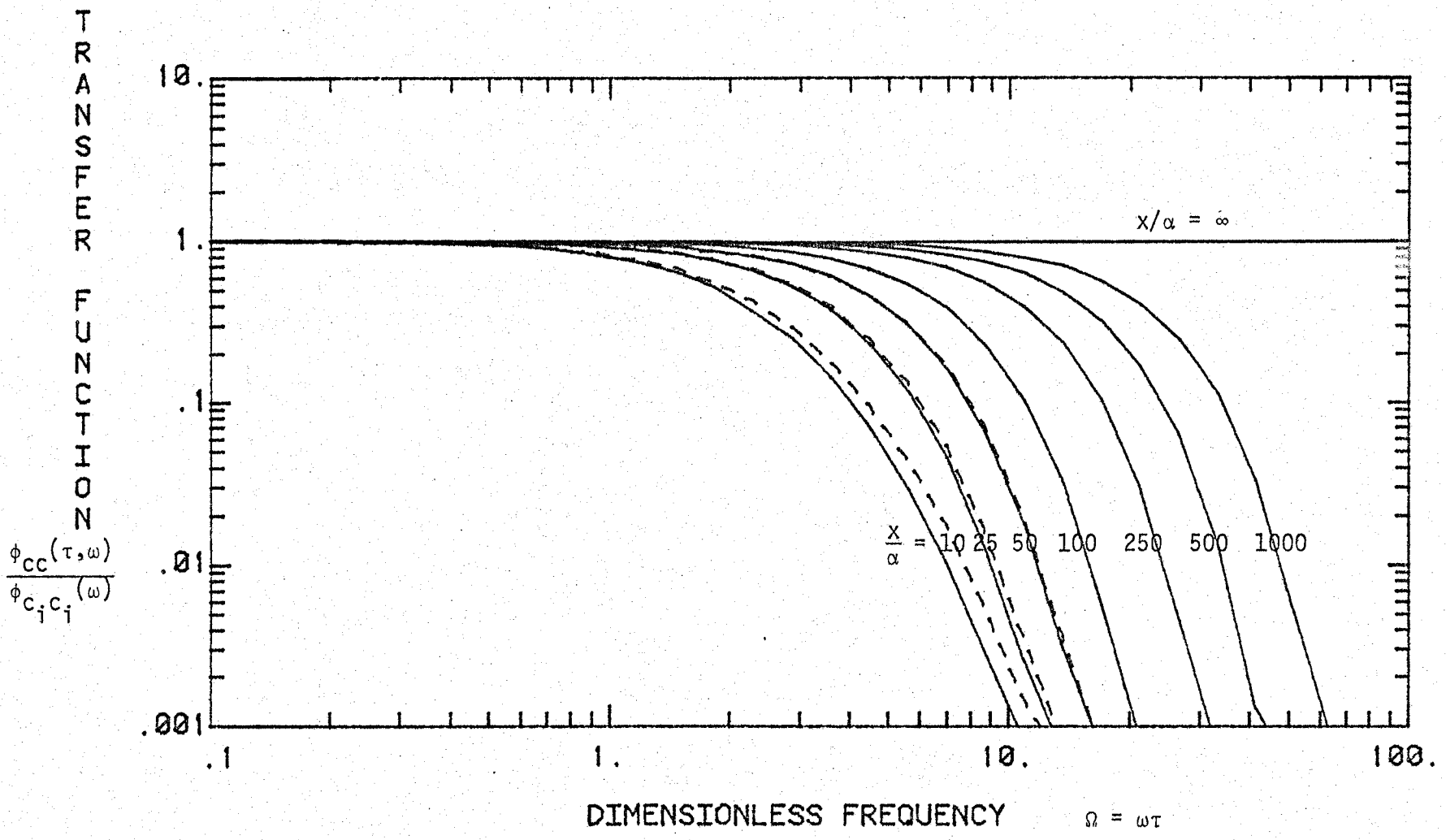
TRANSFER FUNCTION
$\frac{\phi_{cc}(\tau,\omega)}{\phi_{c_i c_i}(\omega)}$
10.
1.
.1
.01
.001
.1
1.
10.
100.
$x/\alpha = \infty$
$\frac{x}{\alpha}$ = 10 25 50 100 250 500 1000
DIMENSIONLESS FREQUENCY $\Omega = \omega\tau$

Figure 1.8. Theoretical phase (radians) for convective-dispersive transport versus Ω. The dashed lines indicate a fluxtype boundary condition (1.74), and the solid lines indicate concentration type boundary condition (1.73).

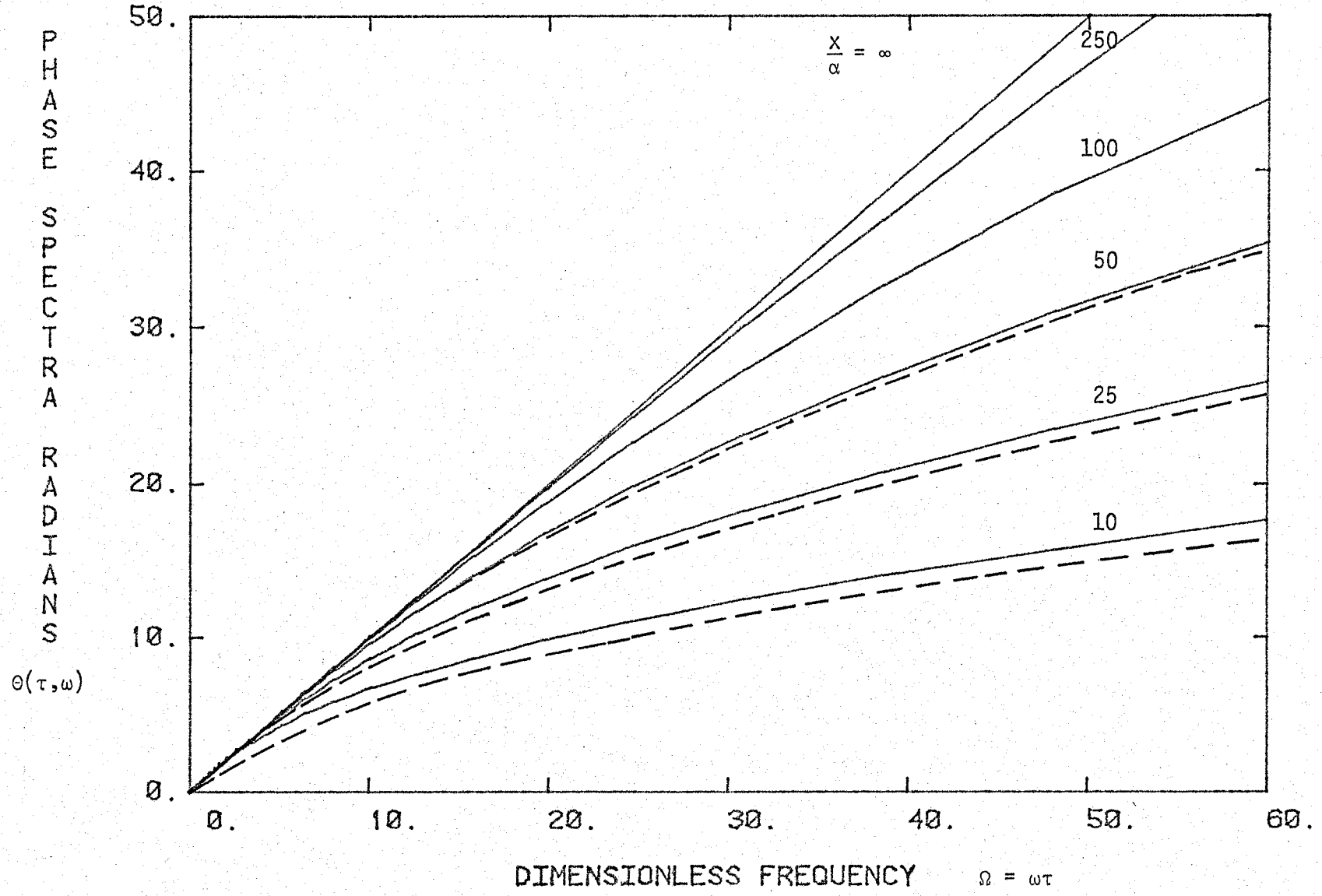
PHASE SPECTRA RADIANS
θ(τ,ω)
50.
40.
30.
20.
10.
0.
0.
10.
20.
30.
40.
50.
60.
DIMENSIONLESS FREQUENCY Ω = ωτ
X/α = ∞
250
100
50
25
10

the phase spectra versus dimensionless frequency is shown in Figure 1.8. Dispersion has the effect of decreasing the negative phase lag for high frequency components of the input. The limiting case of pure convection (α=0) is indicated as a straight line.

For this simple case of convective-dispersive transport the phase and transfer function will describe the dynamic relation between input and output water quality variations.

The decay of a radioactive solute can have a significant impact on the transfer function. Figure 1.9 illustrates how increasing the dimensionless rate constant $\kappa=K\tau$ reduces the transfer function over the entire range of frequency. The effect of κ can be approximated simply by multiplying (1.82) by $\exp(-2K\tau)$. This simplification allows us to use the result in Figure (1.9) if the abscissa is replaced by

$$\exp(-2K\tau) \cdot \frac{\phi_{cc}(\tau,\omega)}{\phi_{c_i c_i}(\omega)}$$

It was found that this approximation was satisfactory for any value of $K\tau$ when $x/\alpha > 50$, and for $K\tau > 1$ if, $25 < x/\alpha < 50$. In the case of the phase spectrum it was found that the parameter $K\tau$ had no effect at all. Thus the phase angle is unaltered by radioactive decay.

The influence of dispersion on the concentration variance can be evaluated with the general result demonstrated in Chapter 1 (1.19)

$$\sigma_c^2 = \int_{-\infty}^{\infty} \phi_{cc}(\tau,\omega)d\omega = \int_{-\infty}^{\infty} \left|H(\tau,\omega)\right|^2 \phi_{c_i c_i}(\omega)d\omega \qquad (1.19)$$

where $H(\omega,\tau)$ is given by (1.80). To integrate (1.19) it is necessary to

Figure 1.9. Transfer function versus dimensionless frequency for exact and approximate form of convective-dispersive transport with chemical interaction and/or radioactive decay.

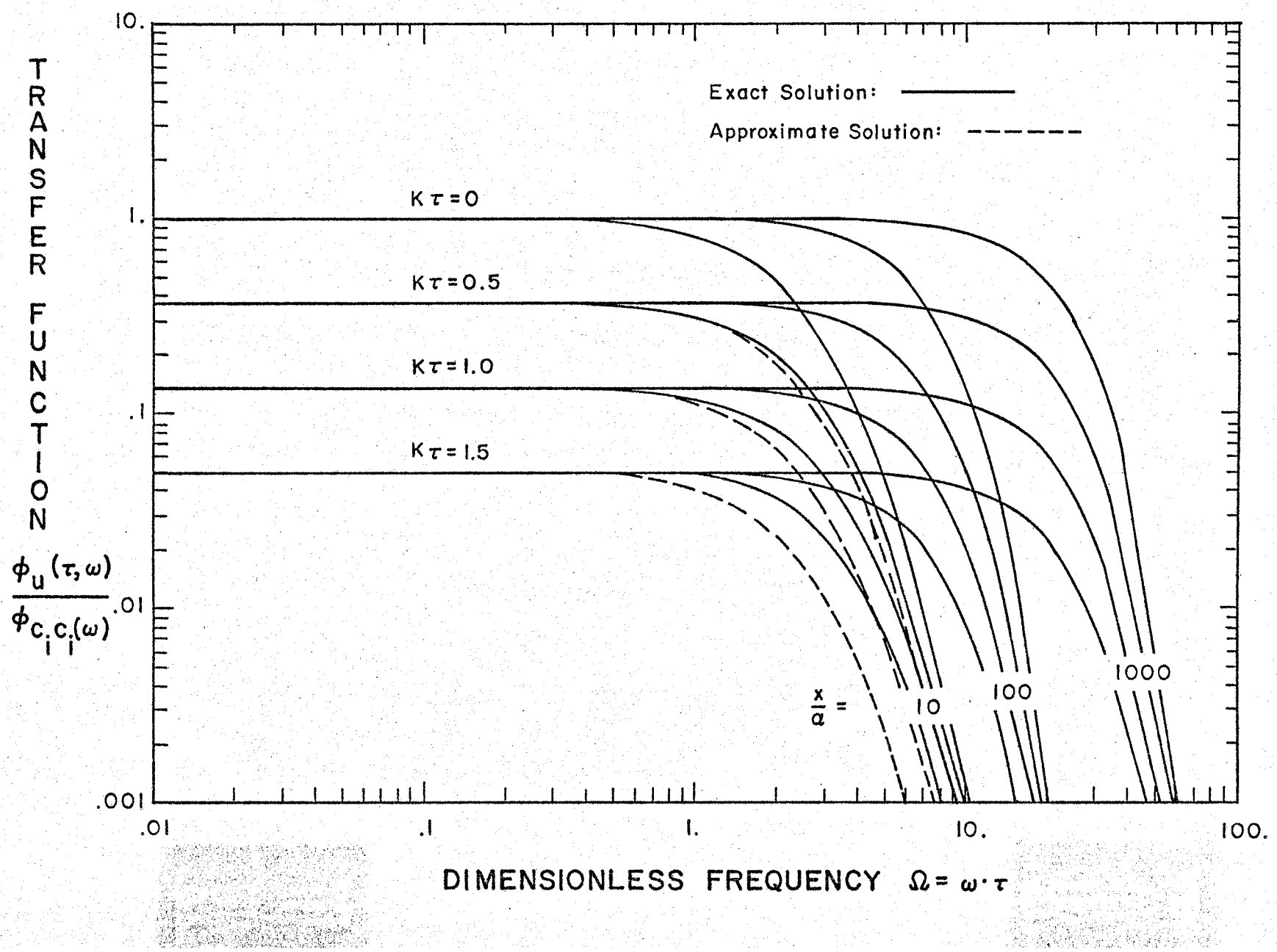
TRANSFER FUNCTION
$\frac{\phi_u(\tau,\omega)}{\phi_{c_i c_i}(\omega)}$
10.
1.
.1
.01
.001
.01
.1
1.
10.
100.
Exact Solution:
Approximate Solution:
Kτ=0
Kτ=0.5
Kτ=1.0
Kτ=1.5
$\frac{x}{a}$ =
10
100
1000
DIMENSIONLESS FREQUENCY Ω = ω·τ

know the form of the input spectrum $\phi_{c_i c_i}(\omega)$. A convenient form is given by

$$\phi_{c_i c_i}(\omega) = \frac{\lambda \sigma^2_{c_i}}{\pi(1+\lambda^2\omega^2)} \tag{1.20}$$

The parameter λ is the correlation scale of the input process $c_i(t)$. Substituting (1.20) into (1.19) and rewriting the variance equation in a dimensionless form we get

$$\frac{\sigma^2_c}{\sigma^2_{c_i}} = \frac{2T_\tau}{\pi} \int_0^\infty \frac{|H(\Omega)|^2}{(T^2_\tau+\Omega^2)} \, d\Omega \tag{1.87}$$

where $T_\tau = \tau/\lambda$ is a dimensionless travel time, $\Omega = \omega\tau$ is dimensionless frequency with K taken to be zero in this case. Evaluation of (1.87) was accomplished by numerical integration and is shown in Figure 1.10. The figure points out that input variability is attenuated as the influence of dispersion increases (x/α decreases), and that decreasing the input correlation scale λ will produce a reduction in the output variance for a given x/α.

Figure 1.10. Output/input variance ratio for convective-dispersive transport problem.

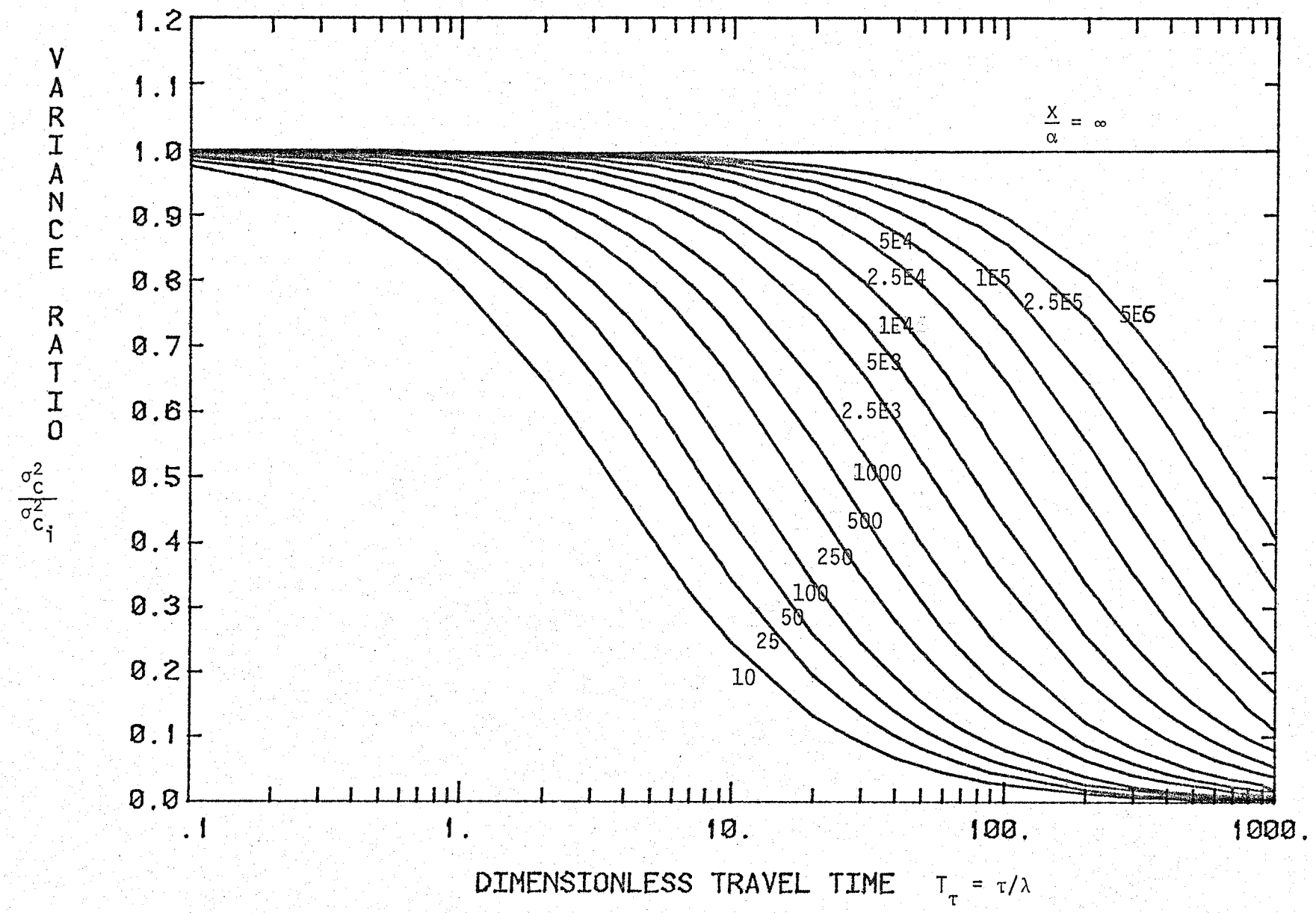
VARIANCE RATIO
$\frac{\sigma_c^2}{\sigma_{c_i}^2}$
1.2
1.1
1.0
0.9
0.8
0.7
0.6
0.5
0.4
0.3
0.2
0.1
0.0
.1
1.
10.
100.
1000.
$\frac{X}{\alpha} = \infty$
5E4
2.5E4
1E5
2.5E5
5E5
1E4
5E3
2.5E3
1000
500
250
100
50
25
10
DIMENSIONLESS TRAVEL TIME $T_\tau = \tau/\lambda$

Discussion of Results

The principal design of this chapter is to demonstrate the application of the spectral analysis procedure for analyzing continuous and time variable water quality series, via frequency domain solutions to equations of solute transport. In the case of time domain solutions we are generally restricted to simple forms of input events, such as a pulse or step. These may be readily applied to controlled field experiments or tracer tests, but they may not be easily applied to time variable situations of pollution or natural tracers already in the environment. By going to the frequency domain and spectral methods we can examine the behavior of a continuous sequence of events over a wide range of frequencies, to arrive at an 'average' estimate of the system parameters. In addition, the method will provide a theoretical estimate of the input-output variance ratio if the system parameters are known.

The second aspect of this discussion relates to the diagnostic capabilities of the frequency response function for appraising the nature of the groundwater flow system itself. That is, the shape of the field estimated transfer function and phase can be compared to the theoretical curves for solute transport in several groundwater flow systems. If the filtering characteristics of the different transport models are unique, then this would present a method for matching the most appropriate model to the field situation.

Figure 1.11 illustrates the theoretical transfer function and phase for each system previously developed. The linear reservoir model (Fig. 1.11a), which represents a distributed source of solute, has the properties of a typical 'low pass' filter (Jenkins and Watts, 1968, p.42). That is, high frequency amplitudes in the transfer function are

Figure 1.11. Frequency response characteristics for: (a) linear reservoir, (b) convection in a curvilinear flow (pumping well adjacent to a river), (c) convection in a uniform flow, and (d) convective-dispersive transport.

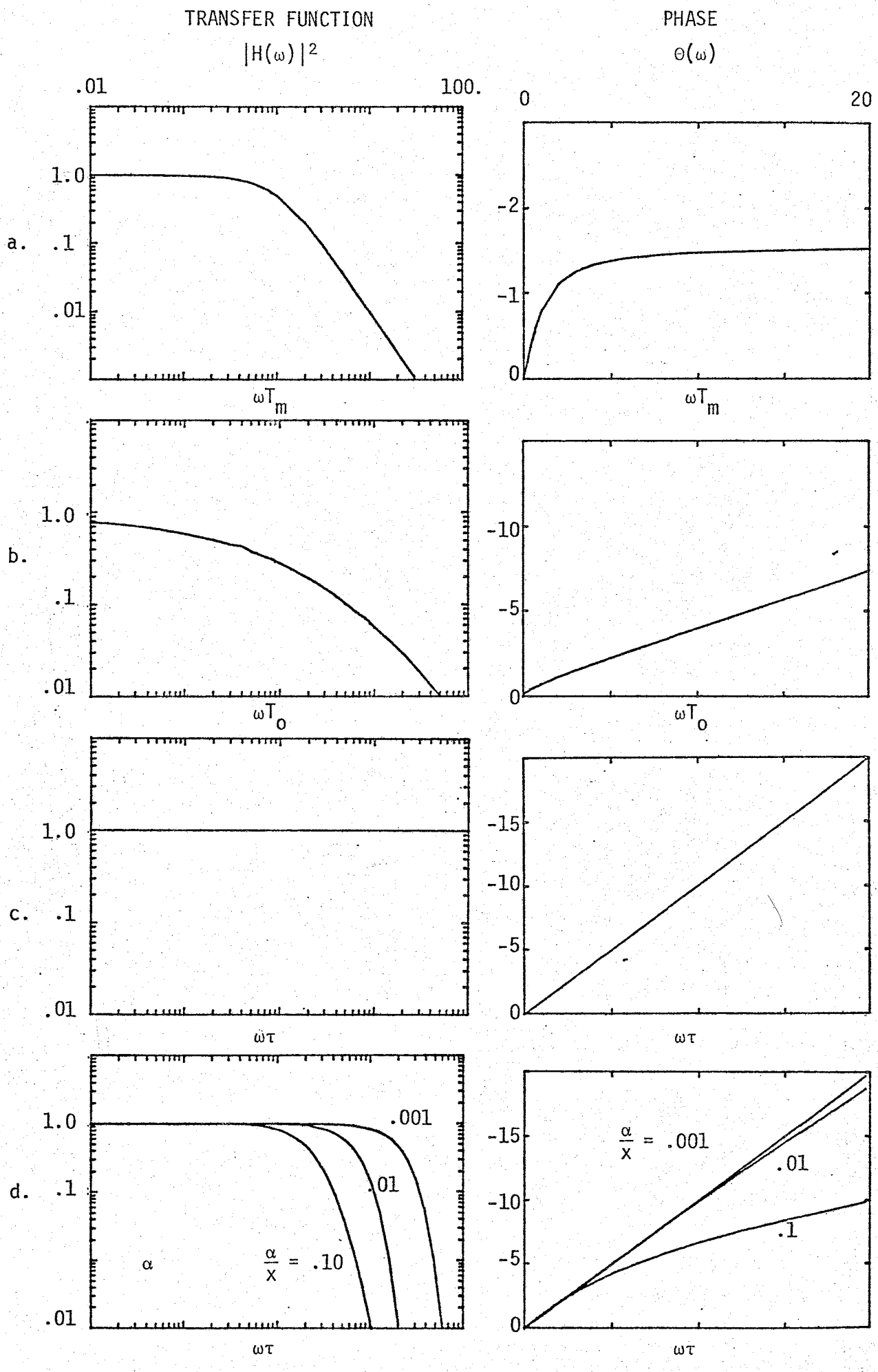
TRANSFER FUNCTION
$|H(\omega)|^2$
PHASE
$\Theta(\omega)$
.01
100.
0
20
a.
1.0
.1
.01
-2
-1
0
ωT_m
ωT_m
b.
1.0
.1
.01
-10
-5
0
ωT_o
ωT_o
c.
1.0
.1
.01
-15
-10
-5
0
$\omega\tau$
$\omega\tau$
d.
1.0
.1
.01
.001
.01
α
$\frac{\alpha}{X}$ = .10
-15
-10
-5
0
$\frac{\alpha}{X}$ = .001
.01
.1
$\omega\tau$
$\omega\tau$

attenuated, and the phase approaches a constant of $-\pi/2$ radians. The case of pure convection in a uniform flow (Figure 1.11c) demonstrates the situation of an 'all pass' filter, where the amplitude of the signal passes through the system unaltered, and the negative phase spectrum increases linearly with frequency. For convection in a curvilinear flow (Figure 1.11b), we observe an intermediate result. The filter would still be termed 'low pass' but with significantly more amplitude filtering in the low frequency range ($\omega T_o < 1$), and slightly less attenuation in the higher range ($\omega T_o > 1$). The negative phase spectrum increases linearly for $\omega T_o > 1$, similar to Figure 1.11b, but the slope is much less.

To examine convective-dispersive transport (Figure 1.11d) under uniform flow conditions it is necessary to include the dimensionless parameter α/x. We see that increasing the dispersion parameter also increases the amplitude filtering in the high frequency range, and the negative phase spectrum is reduced as α/x increases. When α/x becomes small, or dispersion becomes insignificant, the situation of convection dominates. Overall we can say that convective-dispersive transport with a plane source input does not display the broad band filtering evident in cases a and b.

Based on this comparison it is reasonable to expect that individual groundwater flow systems will have distinctive frequency response characteristics, and that spectral analysis and linear filters may provide an additional tool for understanding the mechanisms of solute transport in groundwater.

2. SPATIAL VARIATIONS OF WATER QUALITY

Introduction

In the last section a situation of convective-dispersive transport subject to transient changes in the source strength was examined. It was assumed that the variables were depth-averaged quantities and the coefficients of the equation (u,D) were considered constants for a uniform flow situation (ie. parallel flow boundaries, homogeneous and isotropic K and constant hydraulic gradient (J) and porosity (n)). The purpose of this chapter is to examine the effects of a nonuniform, vertically bounded flow field on the transport process, where the velocity u(x) is taken to be a spatial stochastic process in x. The nonuniform velocity field is assumed to be composed of a mean value and a perturbation caused by local changes in the longitudinal aquifer characteristics (ie. transmissivity, thickness, hydraulic gradient and effective porosity) in the mean flow direction. The analysis is thought to apply to field situations subject to natural groundwater flow variations on a regional scale, perhaps using environmental isotopes as tracers. The approach is not felt to be suitable for local mass transport situations where the solute is measured near the source. A derivation of the depth-averaged mass transport equation is shown to produce terms which correspond to the asymptotic macrodispersion coefficient recently suggested by Gelhar et al. (1979) and Matheron and DeMarsily (1980). From the stochastic theory, the effect of a variable velocity on the mean transport equation produces an overall reduction in the convective velocity, and a corresponding increase in the dispersion coefficient. The stochastic theory also provides a means of estimating the concentration variance for the mean transport equation.

A brief review of research pertaining to the analytical description of macrodispersion in ground water would include the recent work of Gelhar et al. (1979), and Matheron and DeMarsily (1980) who have demonstrated by means of somewhat different techniques that the coefficient of dispersion can theoretically be related to the heterogeneities of the porous media. Both authors consider a two-dimensional flow field in a stratified aquifer of infinite extent (x and z), with the mean flow parallel to bedding. The stratification is assumed to produce a statistically homogeneous velocity field which varies in the vertical direction, while remaining constant within a particular layer ($u(z)=\bar{u}+u'(z)$). The stochastic velocity field is itself generated by a likewise stochastic permeability field $K(z)=\bar{K}+K'(z)$, from the Darcy equation and steady flow assumption. Variations in the effective porosity are taken to be small, and thus n=constant. In the paper by Gelhar et al. the transport equation is separated into two parts by means of a first order perturbation: (1) the partial differential equation describing the global or mean dispersion process, and (2) the zero-mean stochastic differential equation describing the locally fluctuating transport process. The latter was solved using a spectral analysis technique for spatial variables (Lumley and Panofsky, 1967). The results of the stochastic analysis were used to demonstrate the following effects of a stratified aquifer on the mean or global dispersion process:

(1). The mean transport process does become Fickian (i.e. the usual convection-dispersion equation would apply), but only for large displacement or time.

(2). Significant departure from Fickian behavior is expected in the early and intermediate stages of mass transport as a result of the time dependence of the dispersivity during this period.

(3). The asymptotic or large time value of the dispersivity is given by

$$\alpha = a_L + a_\infty \tag{2.1}$$

where α is the effective or depth averaged dispersivity, a_L is the local longitudinal dispersivity, a_∞ is the asymptotic ($\bar{x}$ or t-->large) dispersivity which depends on the statistical properties of the medium. The asymptotic dispersivity a_∞ will always be much larger than a_L under field conditions, with the latter taken to be similar to laboratory scale measurements. The dependence of a_∞ on the statistical properties is expressed by Gelhar et al. (1979) as

$$a_\infty = \frac{\sigma_k^2 \ \ell_z^2}{3\bar{K}^2 \ a_T} \tag{2.2}$$

where $(\sigma_k^2 / \bar{K}^2)$ is the square of the coefficient of variation for K, ℓ_z is the vertical length scale of the stratified medium, and a_T is the local transverse dispersion coefficient.

The paper of Matheron and DeMarsily (1980) constructs a problem similar to the stratified aquifer of Gelhar et al. However their analysis uses an equivalent representation of the two-dimensional transport equation, which they call a random motion model (Kolmogorov, 1931). The conclusions of this research relevant to the present work are:

(1). For flow parallel to stratification Fickian transport is not possible unless local transverse dispersion is significant. Under this condition the usual dispersion equation will apply but only after large displacement or time.

(2). For flow not strictly parallel to stratification Fickian transport will occur and the asymptotic dispersivity is greatly reduced.

(3). The influence of vertical aquifer boundaries may reduce the large time or displacement requirement for the Fickian transport equation to apply.

It is evident from these results that the use of a Fickian form of the dispersion equation (ie. a constant dispersivity) may not be suitable for early time applications of the equation. The developing dispersion process requires 'sufficient' time for the asymptotic behavior to be reached. In addition, according to these authors, even at large time Fickian behavior may not be achieved unless a special form of the covariance of hydraulic conductivity is used (see Equation (27), Gelhar et al., 1979). However, the theory describing an early time dependence of the dispersivity does provide a satisfying explanation of the 'scale' effect observed in tracer experiments, where the dispersivity apparently increases with distance away from the source (Molinari et al., 1977).

In the present research we will restrict the analysis to a vertically bounded, nonuniform flow where it is assumed that the transverse and longitudinal components of velocity and concentration will mix the solute in a plane normal to the flow. Nir (1964) calls this a condition of complete transverse mixing. The following assumptions will also apply:

(1). The usual convection-dispersion equation is applicable under the restriction that only 'large time' behavior is observed.

(2). It is expected that boundary effects and local vertical velocity variations will tend to accelerate transverse mixing and thus somewhat reduce the large time requirement in (1).

(3). That the statistical properties of the medium control the magnitude of the effective dispersivity.

Derivation of the Depth-Averaged Transport Model

It is generally recognized that the concentration c of a dilute solute (tracer or contaminant) in a steady, saturated flow can be described by (Bachmat and Bear, 1964)

$$\frac{\partial c}{\partial t} = \frac{\partial}{\partial X_i}(D_{ik}\frac{\partial c}{\partial X_k} - u_i c) \tag{2.3}$$

where x_i (i=1,2,3) are cartesian coordinates, u_i are the three components or seepage velocity (L/T) and D_{ik} is the dispersion tensor of second order. We expect (2.3) to apply to any conservative solute (no reaction or decay) which is neutrally buoyant in the fluid medium. For this study molecular diffusion is taken to be a small part of the dispersion process and will be neglected.

In the particular case of a two dimensional flow in the vertical plane, the equation of mass transport can be written

$$\frac{\partial c}{\partial t} + \frac{\partial}{\partial x}(uc) + \frac{\partial}{\partial z}(vc) = \frac{\partial}{\partial x}\left(D_L\frac{\partial c}{\partial x}\right) + \frac{\partial}{\partial z}\left(D_T\frac{\partial c}{\partial z}\right) \tag{2.4}$$

where the longitudinal and transverse components of the dispersion tensor are assumed to coincide with the principal axes x and z respectively, with

$$D_{11} = D_L$$

$$D_{33} = D_T \quad , D_{ij} = 0 \quad i \neq j$$

$$D_{22} = 0$$

u and v are horizontal and vertical velocities respectively.

In the case of natural aquifers which are relatively thin in the vertical dimension but extensive in axial extent, it is convenient to consider a depth averaged version of (2.4). The integration over the aquifer thickness (a<z<b) is given by (Holley, 1975)

$$\int_a^b \frac{\partial c}{\partial t}\,dz + \int_a^b \frac{\partial}{\partial x}(uc)dz + \int_a^b \frac{\partial}{\partial z}(vc)dz = \int_a^b \frac{\partial}{\partial x}\left(D_L \frac{\partial c}{\partial x}\right)dz + \int_a^b \frac{\partial}{\partial z}\left(D_T \frac{\partial c}{\partial z}\right)dz \tag{2.5}$$

Applying Leibnitz's rule for differentiation under the integral sign we get

$$\int_a^b \frac{\partial c}{\partial t}\,dz + \frac{\partial}{\partial x}\int_a^b (uc)dz - uc\Big|_b \frac{\partial b}{\partial x} + uc\Big|_a \frac{\partial a}{\partial x} + vc\Big|_b - vc\Big|_a$$

$$= \frac{\partial}{\partial x}\int_a^b D_L \frac{\partial c}{\partial x}dz - D_L \frac{\partial c}{\partial x}\Big|_b \frac{\partial b}{\partial x} + D_L \frac{\partial c}{\partial x}\Big|_a \frac{\partial a}{\partial x} + D_T \frac{\partial c}{\partial z}\Big|_b - D_T \frac{\partial c}{\partial z}\Big|_a \tag{2.6}$$

which is simplified by recognizing that each integral over z can be written as

$$h\bar{\Phi} = \int_a^b \Phi dz \quad .$$

The overbar denotes depth average, and h is the aquifer thickness. Rewriting (2.6) produces

$$h\frac{\partial \bar{c}}{\partial t} + \frac{\partial}{\partial x}(h\overline{uc}) - \frac{\partial}{\partial x}h\overline{D_L \frac{\partial c}{\partial x}} =$$

$$c_b\left[u_b \frac{\partial b}{\partial x} - v_b\right] + c_a\left[-u_a \frac{\partial a}{\partial x} + v_a\right] \tag{2.7}$$

$$+ \left[J_x\Big|_b \frac{\partial b}{\partial x} - J_z\Big|_b\right] + \left[-J_x\Big|_a \frac{\partial a}{\partial x} + J_z\Big|_a\right]$$

with

$$J_x = -D_L \frac{\partial c}{\partial x} \quad , \quad J_z = -D_L \frac{\partial c}{\partial z} \quad . \tag{2.8}$$

The terms in brackets on the right hand side of (2.7) are the vector components of dispersive flux $\tilde{J}$ and velocity $\tilde{u}$ which are parallel to the

boundaries at a and b. These terms must vanish since

$$\tilde{u}\cdot\tilde{n} = \tilde{J}\cdot\tilde{n} = 0 \tag{2.9}$$

where $\tilde{n}$ is the normal vector at the upper and lower limits of the aquifer given by

$$\tilde{n} = \begin{cases} z = b\ , \ \dfrac{\partial b}{\partial x}\tilde{i} - \tilde{j} \\ z = a\ , \ \dfrac{\partial a}{\partial x}\tilde{i} + \tilde{j} \end{cases} \tag{2.10}$$

In order to express $\overline{uc}$ and $\overline{D_L \frac{\partial c}{\partial x}}$ in terms of individual depth averages rather than depth averaged products, requires that we write each variable in terms of a depth average and a local vertical fluctuation

$$\overline{uc} = \overline{(\bar{u} + u'(z))\ (\bar{c} + c'(z))} = \bar{u}\bar{c} + \overline{u'c'} \tag{2.11}$$

$$\overline{D_L \frac{\partial c}{\partial x}} = \overline{(D_L + D_L'(z))\ \frac{\partial}{\partial x}\ (\bar{C} + C'(z))} = \bar{D}_L \frac{\partial \bar{c}}{\partial x} + D_L' \frac{\partial c'}{\partial x} \tag{2.12}$$

keeping in mind that the averages are taken in the vertical. This allows us to write (2.7) in the following form

$$h\frac{\partial \bar{c}}{\partial t} + \frac{\partial}{\partial x}(h\bar{u}\bar{c}) = \frac{\partial}{\partial x}\left(h\bar{D}_L \frac{\partial \bar{c}}{\partial x}\right) + \frac{\partial}{\partial x}\left(-h\overline{u'c'} + h\overline{D_L' \frac{\partial c'}{\partial x}}\right) . \tag{2.13}$$

To complete the derivation, the perturbation products on the right hand side of (2.13) must be simplified to a more usable form. For dispersion in streams Holley (1975) suggests that mixing is complete over the depth. He then goes on to argue that the perturbation terms can be absorbed into respective gradient and diffusion terms, producing Fickian behavior. In the case of ground water flow, recent evidence suggests that the perturbation terms are the predominant mechanism determining macro-dispersivity (Gelhar et al., 1979). For large displacement or time the terms can be expressed as

$$\overline{u'c'} = -a_\infty \bar{u} \frac{\partial \bar{c}}{\partial x} \tag{2.14}$$

$$\overline{D_L' \frac{\partial c'}{\partial x}} = \frac{3}{2} a_L \bar{u} a_\infty \frac{\partial^2 c}{\partial x^2} \tag{2.15}$$

where a_∞ was given in Equation (2.2). Both (2.14) and (2.15) were evaluated using the spectral analysis procedure, the details of which are given in Gelhar et al. (1979).

To conclude the present development, all that remains is to determine the depth-averaged version of the continuity equation by integration as before

$$\int_a^b \frac{\partial u_i}{\partial x_i} dz = \frac{\partial}{\partial x} (h\bar{u}) = 0 \tag{2.16}$$

$$i = 1,2$$

Inserting (2.14) through (2.15) into (2.13) and neglecting terms of order three or higher, produces the classical form of the dispersion equation (with overbars deleted), which includes a physical interpretation of the dispersion coefficient

$$\frac{\partial c}{\partial t} + u \frac{\partial c}{\partial x} = D \frac{\partial^2 c}{\partial x^2} \quad . \tag{2.17}$$

D is the depth averaged dispersion coefficient which can also be written as (Gelhar et al., 1979)

$$D = \alpha \cdot u(x) = u(x)(a_L + a_\infty) \quad .$$

Thus α assumes the role of effective dispersivity, in the one dimensional, depth-averaged mass transport equation, which is the subject of the present research.

Formulation of the Problem

Having derived the equation of mass transport in such a way as to

include the influence of vertical heterogeneities of the medium, we can now consider how longitudinal changes in the depth-averaged velocity may influence the dispersion process. An appropriate geologic setting for this analysis would be a gently dipping sandstone aquifer with outcrop located along the mountain front as shown in Figure 2.1 . For this situation the solute would encounter its vertical boundaries in a short time relative to the overall travel time of the tracer, making the vertically mixed condition a reasonable assumption.

To conceptualize how variations in the velocity field are produced it is only necessary to examine the Darcy equation for one-dimensional flow

$$u(x) = \frac{T(x)\ J(x)}{n(x)\ b(x)} \tag{2.18}$$

where T is the depth averaged transmissivity, J is the hydraulic gradient and nb is the cross-sectional area to flow, composed of the effective porosity and the saturated thickness. In natural aquifers it is conceivable that nb, the transmissivity, and the hydraulic gradient will all combine in some complex way to alter the velocity u(x) along the direction of flow. It is also true that these factors will not necessarily compensate to produce a uniform flow condition as is usually assumed. In this manner we will consider u(x) to be a spatial stochastic process composed of properties which can be measured in the field.

In the previous chapter on time series analysis the Fourier representation theorem was developed considering time as the independent variable, while the space dimension was carried along as a parameter. The interpretation of spatial stochastic processes is identical, except that x becomes the independent variable of interest with time held as a parameter. In addition, the necessary assumption of stationarity in time is now properly referred to as homogeneity in space.

Figure 2.1. A. Regional solute transport in a nonuniform flow.
B. Conceptual displacement of a tracer in a nonuniform flow.

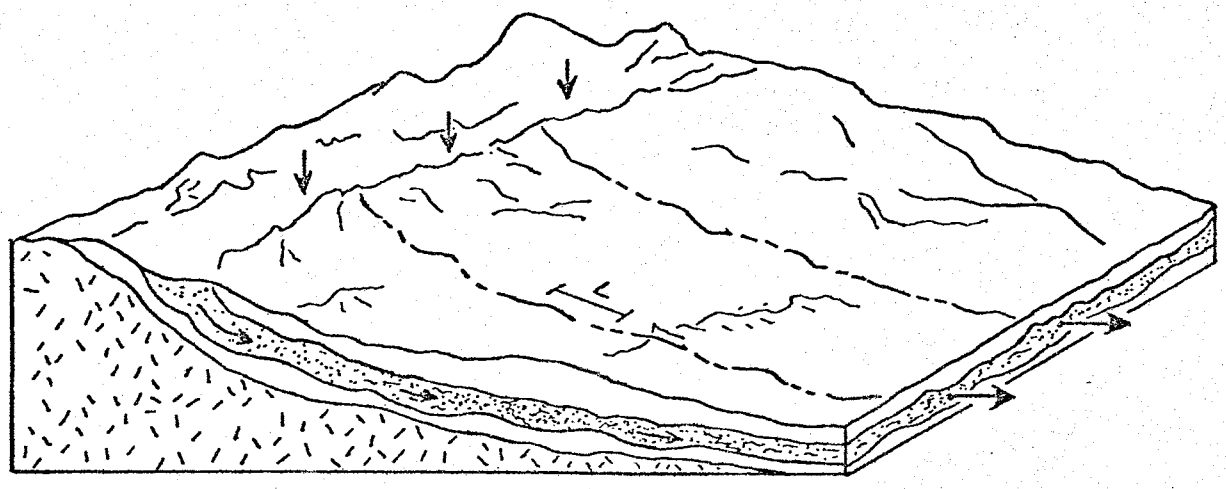

A.

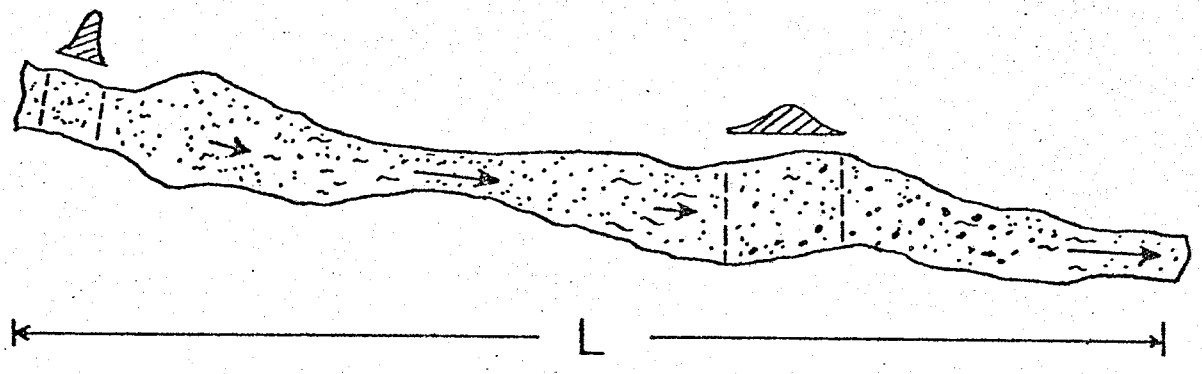

B.

In order to represent each depth averaged variable of the transport equation as homogeneous processes the solute concentration, velocity and dispersion coefficient of (2.17) are each expressed in terms of a mean condition (overbars now denote mean in x), and a fluctuation about the mean

$$D_L = \bar{D}_L + D_L'(x)$$

$$u(x) = \bar{u} + u'(x) \tag{2.19}$$

$$c(x,t) = \bar{c}(x,t) + c'(x,t)$$

with $E(u')=E(D')=E(c')=0$, and the expectation is with respect to x. The mean solute concentration $\bar{c}(x,t)$ is assumed to be a slowly varying process relative to the fluctuation $c'(x,t)$. Substituting these expressions into (2.17) and taking the expected value produces the mean equation for one-dimensional mass transport

$$\frac{\partial \bar{c}}{\partial t} + \bar{u}\frac{\partial \bar{c}}{\partial x} - \bar{D}\frac{\partial^2 \bar{c}}{\partial x^2} = \overline{-u'\frac{\partial c'}{\partial x}} + \overline{D'\frac{\partial^2 c'}{\partial x^2}} \tag{2.20}$$

The right-hand side of (2.20) represents the additional convective and dispersive flux terms resulting from longitudinal heterogeneities in the porous medium.

The zero-mean equation is a stochastic differential equation with a random forcing function and it is written

$$\frac{\partial c'}{\partial t} + \bar{u}\frac{\partial c'}{\partial x} - \alpha\bar{u}\frac{\partial^2 c'}{\partial x^2} = u' \cdot g \tag{2.21}$$

$$g = \left(-\frac{\partial \bar{c}}{\partial x} + \alpha\frac{\partial^2 \bar{c}}{\partial x^2}\right) . \tag{2.22}$$

The Stochastic Solution

Solving the stochastic differential equation (2.21) provides a means of evaluating the influence of velocity variations on the mean transport equation. As will be shown later, the solution will also provide a theoretical expression for the concentration variance.

In order to solve the stochastic differential equation (2.21) we first define the spectral representation theorem for any homogeneous stochastic process as

$$Y(x,t) = \int_{-\infty}^{\infty} e^{ikx}\, dZ_y(k,t) \tag{2.23}$$

where the dZ is the Fourier amplitude of the process with properties outlined previously (Chapter 1.), k is wave number, and the time dimension is carried along as a parameter. This implies that Y is homogeneous in space while varying in time. Substituting this representation for the primed quantities in (2.21) yields

$$\frac{d}{dt}\, dZ_c(k,t) + \Gamma\, dZ_c = g\, dZ_u(k) \tag{2.24}$$

where

$$\Gamma = \bar{u}(\alpha k^2 + ik) \tag{2.25}$$

and g is taken to be approximately constant for a slowly varying mean concentration.

For a plane source boundary condition c'=0, (x=0) with the initial condition $dZ_c = 0$ (t=0), the solution to (2.24) can immediately be written as

$$dZ_c(k,t) = dZ_u(k)\, \frac{g}{\Gamma} \left[1-e^{-\Gamma t}\right]. \tag{2.26}$$

Applying the properties of the dZ's (1.9) and concerning ourselves only with the large time result produces the spectral relation between c' and u'

$$\phi_{cc}(k) = \phi_{uu}(k) \cdot g^2/[\bar{u}^2k^2(1+\alpha^2k^2)] \quad . \tag{2.27}$$

In the previous section on time series analysis it was demonstrated that the spectrum decomposes the variance of the series into contributions from a continuous range of frequencies or wave number. Integration of (2.27) produces the overall variance of the fluctuating process c'

$$\sigma_c^2 = \int_{-\infty}^{\infty} \phi_{cc}(k)dk = \int_{-\infty}^{\infty} \frac{g^2\phi_{uu}(k)}{\bar{u}^2k^2(1+\alpha^2k^2)}\, dk \quad . \tag{2.28}$$

In order to remove the singularity at k=0 it is necessary to assume a particular form for $\phi_{uu}(k)$ (Bakr et al., 1978)

$$\phi_{uu}(k) = \frac{2}{\pi} \frac{\sigma_u^2 \ell_x^3 k^2}{(1+\ell_x^2k^2)^2} \quad . \tag{2.29}$$

Using (2.29) implies that the autocovariance for u' is given by

$$R_{uu}(\xi) = \sigma_u^2 \left(1 - \frac{|\xi|}{\ell_x}\right) e^{-|\xi|/\ell_x} \tag{2.30}$$

where ξ is the lag distance. Substituting $\phi_{uu}(k)$ into (2.28) and integrating yields

$$\sigma_c^2 = \frac{\sigma_u^2}{\bar{u}^2} g^2\ell_x^2 \left[\frac{1+2\alpha/\ell_x}{(1+\alpha/\ell_x)^2}\right] \quad . \tag{2.31}$$

Notice that σ_c depends on the coefficient of variation of the velocity, the length scale, and the term g, which is a function of the first and second derivatives of the mean concentration. Similarly, the right-hand side of the mean transport equation can be evaluated by recognizing that the terms appear as covariance expressions which can be evaluated as follows:

$$E\left(u'\frac{\partial c'}{\partial x}\right) = \int_{-\infty}^{\infty} \phi_{u\dot{c}}(k)dk = -\bar{u}A\frac{\partial \bar{c}}{\partial x} - \bar{D}A\frac{\partial^2 \bar{c}}{\partial x^2} \tag{2.32}$$

and

$$E\left(D'\frac{\partial^2 c'}{\partial x^2}\right) = \alpha \int_{-\infty}^{\infty} \phi_{u\ddot{c}}(k)dk = -\bar{D}\frac{A}{\ell_x}\left(\frac{\alpha}{\ell_x} + 2\right)\frac{\partial \bar{c}}{\partial x} \tag{2.33}$$

where

$$A = \frac{\sigma_u^2}{\bar{u}^2}\left[\frac{1}{1 + \alpha/\ell_x}\right]^2 \tag{2.34}$$

ℓ_x = the length scale of u(x) and

$$\phi_{uc} = E(dZ_u \cdot dZ_c^*) \tag{2.35}$$

is the cross-spectrum between u' and c'; $\phi_{u\dot{c}}$ is the cross-spectrum between u' and $\partial c'/\partial x$ and $\phi_{u\ddot{c}}$ is the cross-spectrum between u' and $\partial^2 c'/\partial x^2$. Details of the integrations are shown in Appendix 1. The significance of a heterogeneous medium along the direction of flow is demonstrated by substitution of (2.32) and 2.33) into the mean transport equation

$$\frac{\partial \bar{c}}{\partial t} + u^*\frac{\partial \bar{c}}{\partial x} = D^*\frac{\partial^2 \bar{c}}{\partial x^2} \tag{2.20a}$$

where the coefficients u* and D* are now given by

$$u^* = \bar{u}\left(1 - \frac{\sigma_u^2}{\bar{u}^2}\right) \tag{2.36}$$

$$D^* = \bar{u}\cdot\alpha\left[1 + \frac{\sigma_u^2}{\bar{u}^2}\left(\frac{1}{1 + \alpha/\ell_x}\right)^2\right] . \tag{2.37}$$

Thus u* and D* represent the velocity and dispersion coefficients when the medium is vertically bounded and longitudinally heterogeneous. In addition, the effects of vertical stratification can be included when α

is expressed as a macrodispersivity by (2.1) and (2.2).

The Effect of u'(x) on Mass Transport

The process of dispersive transport for a longitudinally nonuniform flow produces some interesting behavior which deserves further discussion. First of all, the resulting equation (2.20a) is cast in the usual Fickian form for dispersive transport. In addition, the coefficients of the equation (u^* , D^*) are interpreted in terms of the flow characteristics of the medium. The convective velocity term indicates that a retardation of the solute will occur as the degree of longitudinal nonuniformity ($\sigma_u / \bar{u}$) is increased. This reduction in the convective velocity can be attributed to the properties of the medium since u'(x) = f(T,J,nb). The dispersion coefficient is altered by longitudinal heterogeneity as well, with D^* increasing as $\sigma_u/\bar{u}$ increases.

The above effects can be illustrated by solving (2.20a) for a pulse input of solute ($\bar{c}(x,o) = M\delta(x)$)

$$\bar{c} = \frac{M}{\sqrt{2\pi}\,\sigma_x} \exp\left[-\tfrac{1}{2}\left(\frac{x-\bar{u}t}{\sigma_x} + \frac{\bar{u}t}{\sigma_x}\frac{\sigma_u^2}{\bar{u}^2}\right)^2\right] \tag{2.38}$$

where $\sigma_x = (2D^*t)^{1/2}$ is the standard deviation of the normal probability curve, and M is the mass per net area. Writing (2.38) in terms of a normalized concentration and the spatial coordinate $x/\bar{x}$ gives

$$c^* = \bar{c}\,\frac{(4\pi\alpha x)^{1/2}}{M} = \frac{1}{\sqrt{B}} \exp\left[-\frac{\left(x/\bar{x} - \left(1 - \sigma_u^2/\bar{u}^2\right)\right)^2}{4B\alpha/\bar{x}}\right] \tag{2.39}$$

where B is given by

$$B = 1 + \frac{\sigma_u^2}{\bar{u}^2}\left(\frac{1}{1 + \alpha/\ell_x}\right)^2 \tag{2.40}$$

The standard deviation of concentration σ_c (2.31) can also be written in terms of c*

$$\sigma_{c^*} = \frac{\sigma_c (4\pi\alpha\bar{x})^{\frac{1}{2}}}{M} = |g^*| \frac{\ell_x}{\bar{x}} \frac{\sigma_u}{\bar{u}} \left[\frac{1 + 2\alpha/\ell_x}{(1 + \alpha/\ell_x)^2} \right]^{\frac{1}{2}} \tag{2.41}$$

with

$$|g^*| = \left| - \frac{\partial c^*}{\partial (x/\bar{x})} + \frac{\alpha}{\bar{x}} \frac{\partial^2 c^*}{\partial (x/\bar{x})^2} \right| \tag{2.42}$$

The influence of u'(x) on the spatial distribution of c* is shown in Figure 2.2 where (2.39) and (2.41) are plotted versus $x/\bar{x}$. Case a is for $\sigma_u^2/\bar{u}^2 = 0$, and case b is for $\sigma_u^2/\bar{u}^2 = 0.3$. It is evident that even for modest values of $\sigma_u/\bar{u}$ significant retardation of the maximum concentration relative to the mean fluid velocity would occur. In addition the maximum concentration is attenuated by the factor $1/\sqrt{B}$. The significance of nonuniform flow to the dispersion process can be observed by writing D* in terms of the rate of growth of the dispersed zone

$$\sigma_x/\bar{x} = \sqrt{2(\alpha/\bar{x})B} \tag{2.43}$$

where σ_x is normalized by $\bar{x}$ to conform to (2.39). If the width of the plume is defined as $2\sigma_x/\bar{x}$, then the impact of $\sigma_u^2/\bar{u}^2$ on the dispersion process is

Case a: $2\sigma_x/\bar{x} = 0.4$

Case b: $2\sigma_x/\bar{x} = 0.44$

or a 10% increase in the normalized width of the plume. The net result is that convection and dispersion are effected by u'(x) in an inverse manner, with a smaller displacement of c* corresponding to a wider dispersed zone when $\sigma_u/\bar{u}$ is increased.

Figure 2.2. The spatial distribution of concentration c* versus the normalized spatial coordinate $x/\bar{x}$. Case a is for $\sigma_u^2/\bar{u}^2 = 0.0$, and case b is for $\sigma_u^2/\bar{u}^2 = 0.3$. The dashed lines in case b are $\pm \sigma_{c^*}$ given by (2.41).

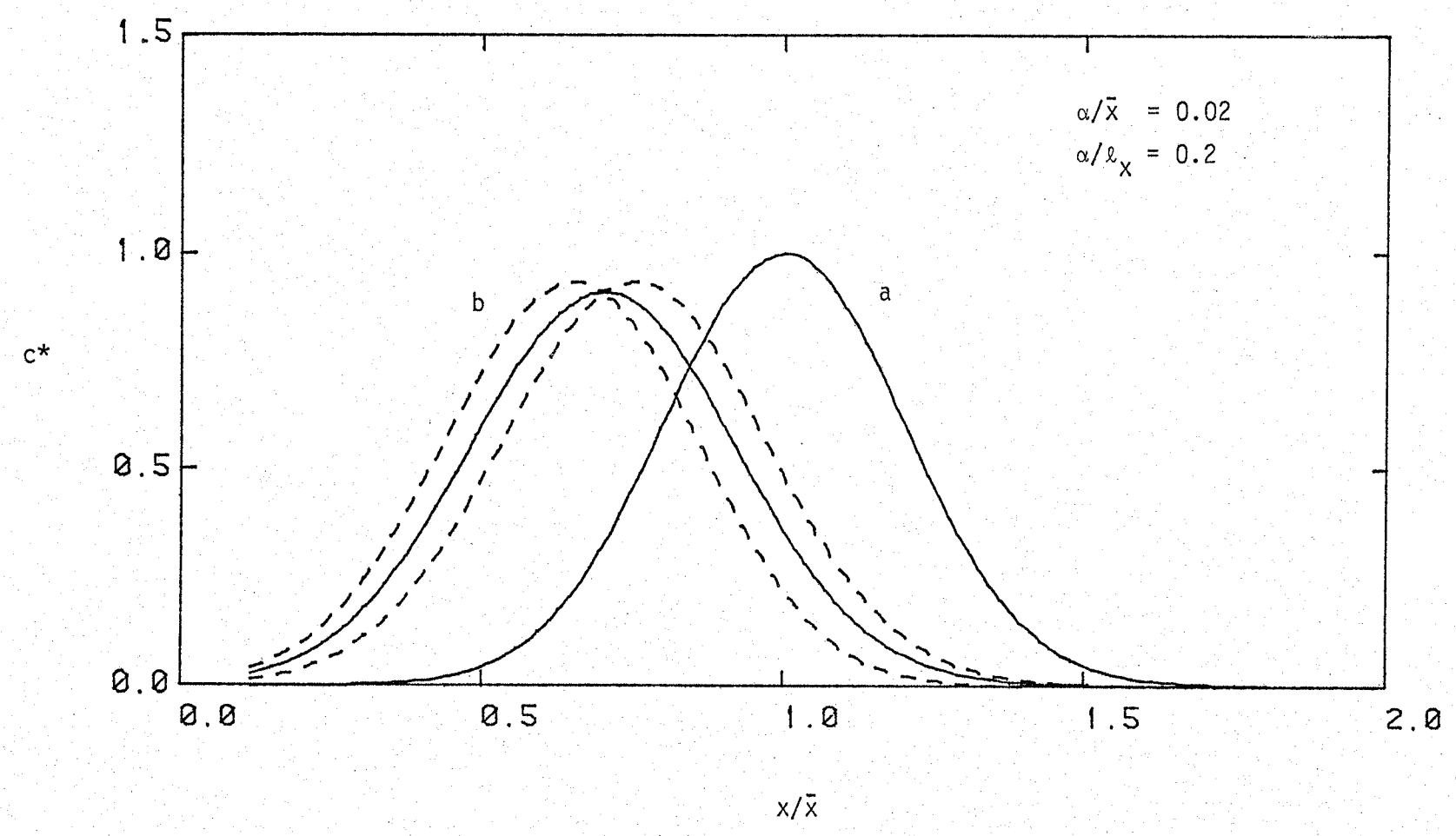
1.5
1.0
0.5
0.0
c*
0.0
0.5
1.0
1.5
2.0
x/x̄
α/x̄ = 0.02
α/ℓx = 0.2
a
b

For the case of a fixed location in space, say at an observation well, the time distribution of the solute becomes important. Here we use the transformation $x = \bar{u}t_o$, where t_o denotes the travel time to the well located at point x. In this case the normalized concentration is

$$c^* = \frac{\bar{c}\ (4\pi\alpha\bar{x})^{\frac{1}{2}}}{M} = \frac{1}{\sqrt{B}} \exp\left[- \frac{\left[1-\frac{t}{t_o}\left(1 - \frac{\sigma_u^2}{\bar{u}^2}\right)\right]^2}{4B(\alpha/x)(t/t_o)} \right] \tag{2.44}$$

where the parameter α/x is a constant. The standard deviation of concentration in this case is written

$$\sigma_{c^*} = \frac{\sigma_c(4\pi\alpha x)^{\frac{1}{2}}}{M} = |g^{**}|\ \frac{\sigma_u}{\bar{u}}\ \frac{t}{t_o}\ \frac{\ell_x}{x}\left[\frac{1+2\alpha/\ell_x}{(1+\alpha/\ell_x)^2}\right]^{\frac{1}{2}} \tag{2.45}$$

where

$$g^{**} = \left| - \frac{\partial c^*}{\partial(t/t_o)} + \frac{\alpha}{x}\ \frac{t}{t_o}\ \frac{\partial^2 c^*}{\partial(t/t_o)^2} \right| \tag{2.46}$$

Figure 2.3 illustrates c^* versus t/t_o when $\sigma_u^2/\bar{u}^2 = 0$ and 0.3. Case b demonstrates the increased travel time that arises when there is nonuniform flow. Thus we can expect the time breakthrough at c^*_{max} to be significantly later ($t/t_o = 1.43$) in this case. The 'tailing' of the pulse for case b is much more dramatic than case a, indicating an even larger retardation for the 75%-95% concentration breakthrough to pass the observation point. This additional spreading is due entirely to the effect of nonuniform flow. The dashed lines again indicate $\pm\ \sigma_{c^*}$ calculated from (2.45).

The significance of the dashed lines in Figures 2.2 and 2.3 becomes apparent if σ_{c^*} is thought of as a measure of uncertainty in c(x,t) produced by a nonuniform, heterogeneous flow field. It is worthwhile then

Figure 2.3. The temporal distribution of c* versus normalized time, t/t_o. Case a is for $\sigma_u^2/\bar{u}^2 = 0.3$, and case b is for $\sigma_u^2/\bar{u}^2 = 0.0$. The dashed lines in case b are $\pm \sigma_{c*}$ given by (2.45).

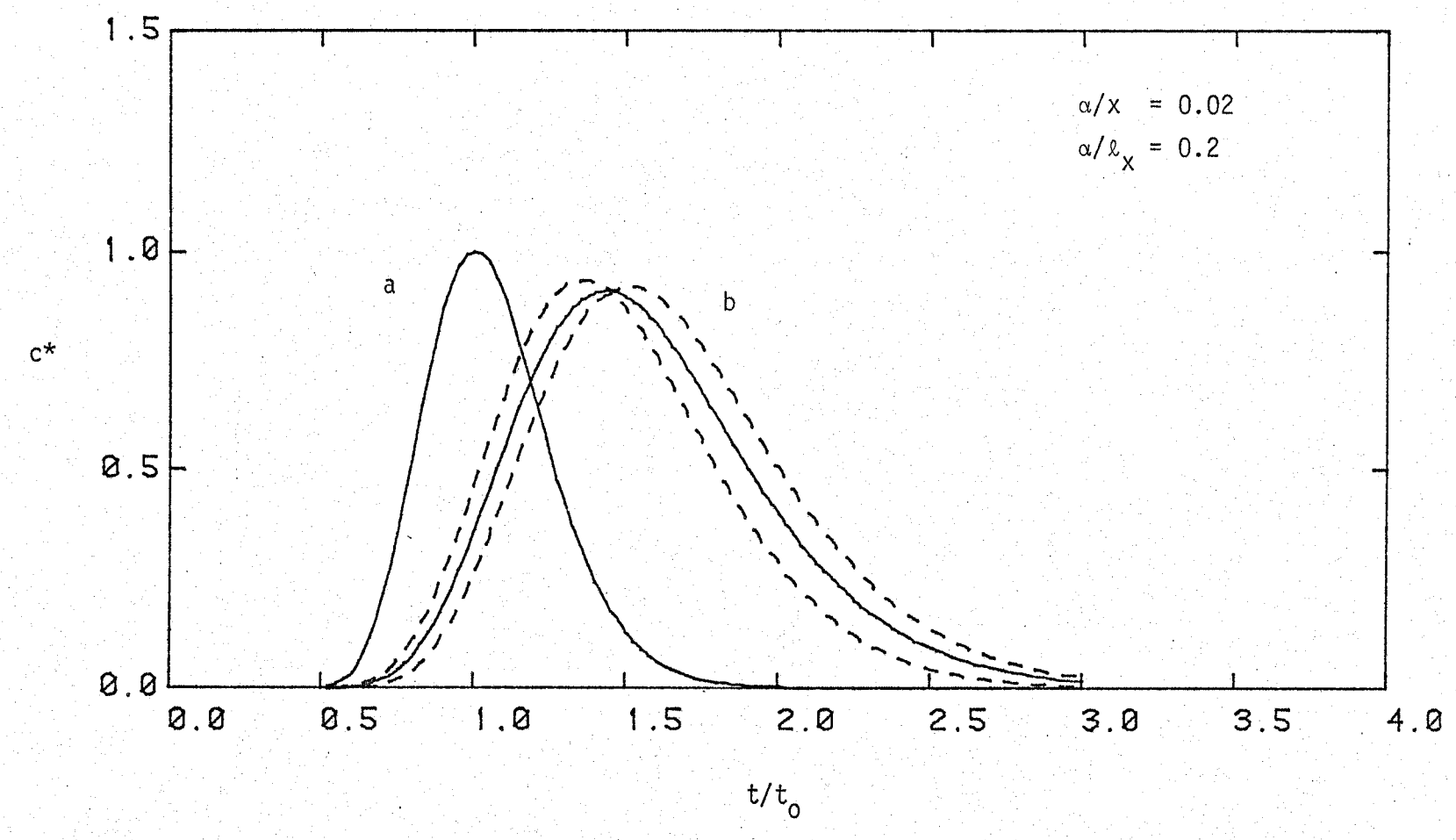
1.5
1.0
0.5
0.0
c*
α/x = 0.02
α/ℓx = 0.2
a
b
0.0
0.5
1.0
1.5
2.0
2.5
3.0
3.5
4.0
t/to

to list the factors which influence σ_{c^*}:

1. σ_{c^*} is strongly dependent on the mean concentration gradient and, to a lesser extent, the second derivative of c*. That is, we can expect the solute fluctuations to be the greatest in regions where $\partial c^*/\partial x$ and/or $\partial^2 c^*/\partial x^2$ are large.
2. The correlation scale of the velocity variation is directly proportional to the magnitude of σ_{c^*}.
3. $\sigma_u/\bar{u}$, the coefficient of variation of the velocity is also directly proportional to σ_{c^*}.
4. The magnitude of the dispersivity α has a smaller impact on σ_{c^*} than factors 1-3.

From a practical point of view it is of considerable interest to know whether the kind of phenomenon described by this theory actually occurs under natural conditions, and if so to what degree. There are several mechanisms which are known to produce retardation of a solute. For example the transport of adsorbing chemicals has been studied using one of several linear adsorption isotherms (Wierenga et al., 1975,; Van Genuchten and Wierenga, 1976). However in these cases a reduction in the convective velocity is accompanied by a reduction in the dispersion coefficient rather than an increase, since the velocity element of the dispersion term is reduced as well. It has been suggested (Schwartz, 1975) that the convection velocity may be reduced as the flow paths of ions become more irregular (ie. the paths get longer), and/or the solute is trapped in 'dead end' pores. However a theory describing a reduced convective velocity along with an increase in the dispersion coefficient for a longitudinally heterogeneous flow field has apparently not been demonstrated previously.

The average particle velocity is identical to the form of the convective velocity u* in (2.36), thus providing an alternative argument for the retardation effect. The corresponding increase in dispersion observed in the stochastic nonuniform flow model can best be explained by comparison with a more traditional nonuniform flow field, a sinusoidal velocity field. Gelhar and Collins (1971) have given a solution for dispersive transport in an oscillating flow field with u(x) given by

$$u = \bar{u}/(1+\beta \sin kS) \quad , \quad |\beta|<1$$
$$kS = 2n\pi, \; n = 1,2,....$$

where β is a constant parameter controlling the amplitude of the oscillation. Their results show that an oscillatory flow produces additional dispersion over the uniform flow case, that is dependent on the amplitude of the oscillation but not on the wavelength. Table 2.1 illustrates the influence of flow nonuniformity on dispersion using σ_x, the rate of growth of the dispersed zone.

In terms of actual field experiments the results shown here have apparently not been observed. However, this may be due to the fact that the solute itself is generally used to calculate the velocity and thus the effects presented here would be lost. A recent paper by Smith and Schwartz (1980) does suggest this kind of mechanism in the context of a two dimensional Monte Carlo experiment. Their analysis points out that as the heterogeneity of the medium is increased ($\sigma_{\log K}$ increases) the mean travel time of the particles (t_{50}) increases, or in other words the mean convective velocity decreases. In addition an increase in $\sigma_{\log K}$ produces a corresponding increase in the width of the dispersed zone. Since the hydraulic conductivity is directly related to the velocity, it seems reasonable that the theory presented here applies to some of their results.

An alternate approach for describing the apparent decrease in convective velocity can be illustrated by a simple Lagrangian experiment. Consider a column of porous material with stratification in a plane normal to the mean flow direction. The stratifications are constructed in such a way that the fluid velocity will vary along the length of the column as

$$u(x) = \bar{u} + u'(x)$$

where $\bar{u}$ is the average fluid velocity for the entire column, and $u'(x)$ is a random process with mean, $E(u') = 0$, and variance, σ_u^2. If a series of particles are introduced at $x = 0$ and allowed to travel a fixed distance $\bar{x}$, the expected value of the travel time $\bar{t}$ for the particles is given by

$$E(t) = \bar{t} = E\left(\frac{\bar{x}}{u(x)}\right) = E\left(\frac{\bar{x}}{\bar{u} + u'(x)}\right)$$

which can be expressed as

$$\bar{t} = E\left(\frac{\bar{x}}{\bar{u}}\left(1 - \frac{u'}{\bar{u}} + \frac{u'^2}{\bar{u}^2} - \ldots\ldots\right)\right)$$

Taking the expected value inside the brackets, the mean travel time for particles to move the distance $\bar{x}$ is approximately

$$\bar{t} \simeq \frac{\bar{x}}{\bar{u}}\left(1 + \frac{\sigma_u^2}{\bar{u}^2} - \ldots.\right)$$

By the same token the average particle velocity can be determined from

$$\frac{\bar{x}}{\bar{t}} = \frac{1}{E\left(\frac{1}{u(x)}\right)} = \frac{\bar{u}}{\left(1 + \frac{\sigma_u^2}{\bar{u}^2} - \ldots.\right)} \approx \bar{u}\left[1 - \frac{\sigma_u^2}{\bar{u}^2}\right]$$

as long as $\sigma_u^2/\bar{u}^2 < 1$. This result indicates that the harmonic mean is the appropriate way of averaging velocities along a streamline.

Flow Field	u(x)	σ_x^2
uniform	$\bar{u}$	$2\alpha\bar{u}t$
sinusoidal	$\bar{u}/(1+B \sin ks)$	$2\alpha\bar{u}tA$; $A = (1+B^2/2)$
stochastic	$\bar{u} + u'(x)$	$2\alpha\bar{u}tB$; $B = 1+\sigma_u^2/\bar{u}^2\left(\frac{1}{1+\alpha/\ell_x}\right)^2$

Table 2.1. The effect of the velocity field on σ_x^2.

Finally it should be pointed out that the spectral procedure developed in this chapter will only apply for small perturbations of the velocity field. It is expected that $\sigma_u^2/\bar{u}^2 < 0.5$ might be a reasonable maximum. It is clear that values greater than 1.0 will produce negative convective velocities which would of course be unreasonable. As was mentioned earlier in the introduction to this chapter, the spectral solution will only be valid at a considerable distance downstream from the source.

3. APPLICATION AND INTERPRETATION OF FIELD DATA

Introduction

In order to demonstrate how spectral methods can be applied to field problems of mass transport, several examples have been taken from the literature. Although a great deal of research effort has been directed towards understanding mass transport in ground water, there are still relatively few studies with large enough record lengths to apply the spectral procedure. A data set with one hundred samples is probably the minimum length to produce a good spectral estimator. However this will ultimately depend on the correlation scale and variance of the series. Some of the data sets to be examined here would be considered too short by the one hundred sample criterion just mentioned. However, the data sets were chosen to demonstrate the utility of the spectral method to a wide range of mass transport problems, rather than as detailed case studies.

Transport of salts in an irrigated watershed: Rio Grande Valley, New Mexico (a linear reservoir application)

The ground water below irrigated agriculture receives considerable quantities of soluble salts which originate for the most part from irrigation water, but also from the natural geochemistry of the regional groundwater system. In arid regions excess irrigation water is applied over and above the crop requirements to prevent accumulation of precipitated salts in the soil zone. With regard to the groundwater reservoir, the contamination is considered a distributed or areal source of pollution. The leaching process, although necessary for

productive agriculture, has a significant impact on downstream users, since much of the excess salt reappears in drains or rivers as 'irrigation return flow.' As a typical example, the seasonal application of one meter of irrigation water with a total dissolved solids concentration of 500 mg/l would supply 5000 Kg of salt for each hectare under irrigation. It is easy to understand why it is necessary to leach this salt below the roots. The central dilemma to management of these watersheds is striking a balance between maintenance of a suitable environment for crop growth, while exporting the minimum amount of salt to downstream users.

In order to be able to predict how farm management and irrigation practices might affect the quality of irrigation return flow, it is first necessary to have a model of the hydraulics and solute behavior for the system. The most elementary model which can be applied to a distributed source of contamination is the linear reservoir model. A comprehensive study on the validity and application of this model for non-point sources of contamination is given by McLin (1981). In this study he has shown, by comparison with spatially distributed models, that the 'well-mixed' assumption of the linear reservoir will provide a good approximation for modeling input-output behavior as long as the longitudinal extent of the aquifer is large compared to the saturated thickness. The study also included two applications of the method to large irrigated basins in the Western United States.

In the present application we are interested in the interpretation of time series of soluble salts in a small irrigated watershed. The field site is located in the Middle Rio Grande region of New Mexico, near the village of San Acacia. The geology of the Rio Grande valley

can be described as a down-faulted structure filled with alluvial sediments. Agriculture takes place on the alluvial soils adjacent to the river, which is the main source of irrigation water. The aquifer at the field site is composed of Quaternary alluvial deposits (0-20 meters of sands, gravels with some clay lenses or thin beds), overlain by a thin layer of soil (~ 1.5 meters, typically consisting of clay loam-loam-sand). Figure 3.1 illustrates a plan view of the watershed, which occupies a 20.2 hectare area. A good deal of hydrologic information is available at this site, since it has been the object of a long term study on the impact of agriculture on irrigation return flow (EPA Grant No. R-806092, New Mexico State Environmental Improvement Div. No. 66/665.52/04). Wierenga et al. (1979) have described the nature of the groundwater flow and chemical quality at the field site. Gelhar et al. (1980) have demonstrated several modeling applications at the site, including a deterministic model of chloride ion using the Linear Reservoir, and a stochastic model characterizing the hydraulics of irrigation and drainage at the site. Recently Simonett (1981) in a M.S. thesis at NMIMT examined a multi-celled linear reservoir model for the purpose of including the influence of flow and chemical quality of the regional groundwater system.

The result of these studies indicate a highly transient groundwater flow system, with the hydraulic response time T_h, on the order of 5-7 days. The hydraulic response time T_h indicates the average time for the groundwater level to decay to the e^{-1} level after a recharge event. The small value of T_h for this system is the result of permeable alluvial soils, and a shallow depth to the groundwater table (<2 meters). The solute response time or residence time for this system is

Figure 3.1. Irrigated watershed at San Acacia, New Mexico showing the effective drainage area of the middle drain (20.2 hectares).

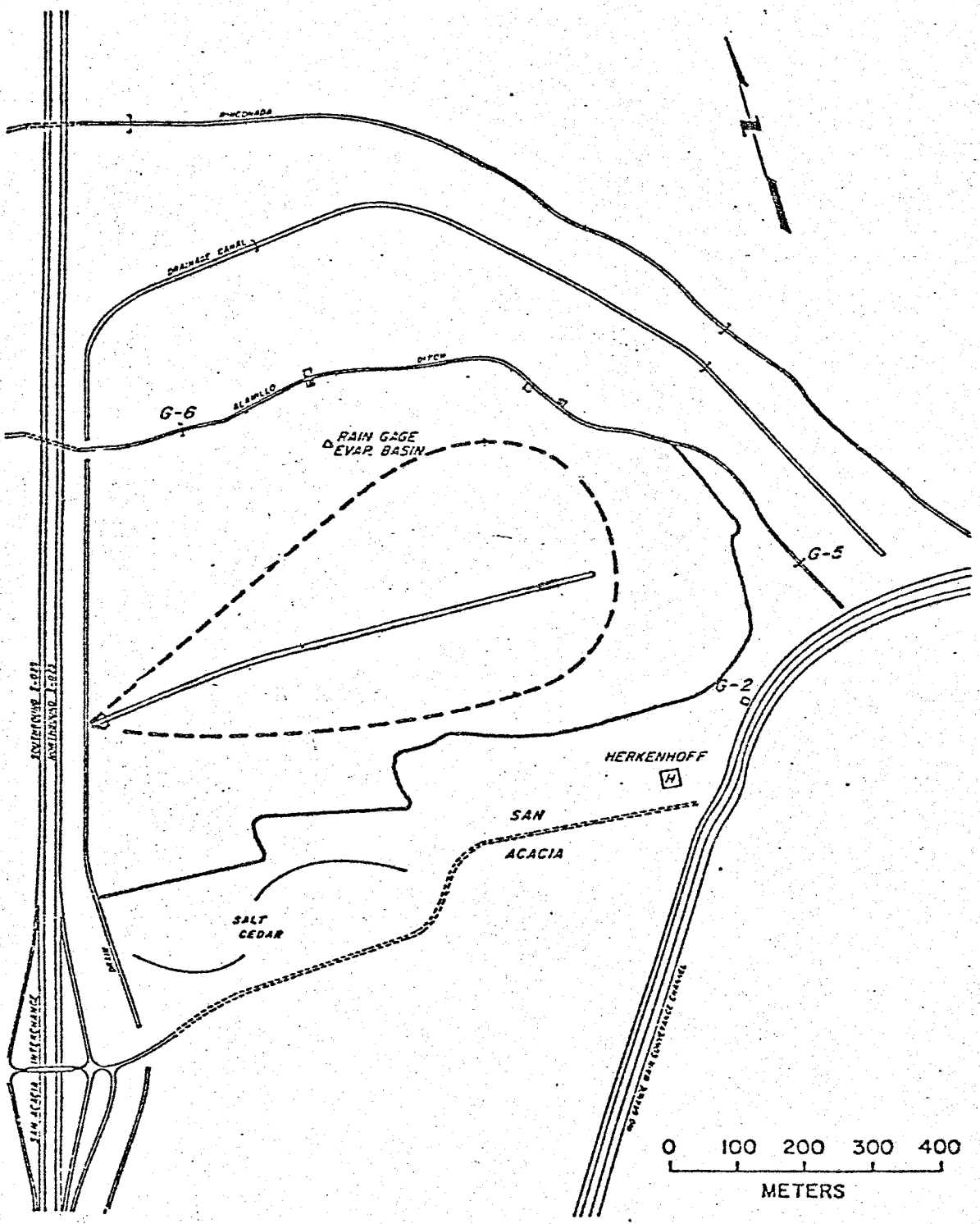
PINCONADA
DRAINAGE CANAL
DITCH
ALAMILLO
G-6
RAIN GAGE
EVAP. BASIN
G-5
G-2
HERKENHOFF
H
SAN
ACACIA
SALT
CEDAR
INTERSTATE 10
SAN ACACIA INTERCHANGE
0 100 200 300 400
METERS

apparently much larger, with T_c on the order of 2 years or greater (Simonette, 1981). The combination of large residence times with small hydraulic response times, produces some interesting behavior in the time variability of the total mass of salts in the drain. Even though the concentration of total dissolved solids (TDS) was found to remain fairly constant over the irrigation season, the highly transient nature of the flow system produces large changes in the mass flux of TDS. This points out distinctly, that for well-mixed systems, the total mass flux of salts is the important parameter for modeling the salt load in irrigation return flows.

The objectives of this application are: (1) to demonstrate the mass flux approach to well-mixed groundwater reservoirs, (2) to illustrate an application of the stochastic time series method by evaluating the frequency characteristics of the system and (3) to determine the appropriate parameters of the groundwater reservoir from (2).

The equation describing a linear reservoir for a particular solute was previously given by (1.27). In the development of (1.27) we were concerned with the time variations of the solute in a steady-state flow system. In the present situation, groundwater recharge or deep percolation is considered to be highly variable, and the steady flow assumption is not suitable. Thus a modification of the equation is necessary. The mass flux form of the linear reservoir equation is written

$$\frac{dM}{dt} = m_i - m_o + m_r \tag{3.1}$$

where M, as given in Chapter 1, is the total mass of salts in the aquifer, m_i is the applied irrigation water mass flux, m_o is the output

or drain mass flux, m_r is the mass flux contribution from the regional groundwater system. Recall now that the drainflow q is linearly related to the average head in the aquifer by the expression

$$q = a(\bar{h} - h_o) \tag{3.2}$$

where a is the outflow coefficient and h_o is the drain coefficient. Writing (3.2) in terms of a mass flux of solute c we get

$$m_o = qc = a\bar{h}c - ah_oc \tag{3.3}$$

Rearranging (3.3) in terms of the total mass of salts in the aquifer produces

$$M(t) = n\bar{h}c = T_m \cdot m_o + nh_oc \tag{3.4}$$

where $T_m = n/a$ is the response time for the mass flux of solute c. It should be pointed out that the hydraulic response time $T_h = S/a$ (S = specific yield) governing the linear reservoir flow model is quite similar to T_m. The difference between T_m and T_h stems from the difference between the effective porosity n and the specific yield, S. In many situations this difference will be considerable. Substituting (3.4) into equation (3.3) yields

$$\frac{dM}{dt} = T_m \frac{dm_o}{dt} + nh_o \frac{dc}{dt} = m_i - m_o + m_r \tag{3.5}$$

the mass balance for total dissolved solids (TDS) in the system. Figure 3.2 illustrates the mass flux version of the linear reservoir model.

Having modified the linear reservoir theory to a mass flux form we can proceed with the data analysis. The mass flux for the output series ($m_o = q \cdot c$) was calculated by multiplying the average daily drainflow per unit of irrigated area by the TDS concentration c(t). Drainflow is continuously recorded at the site. Electrical conductivity (EC) was used as a measure of total dissolved solids (TDS). Water quality

Figure 3.2. Linear reservoir model for mass flux at the San Acacia site.

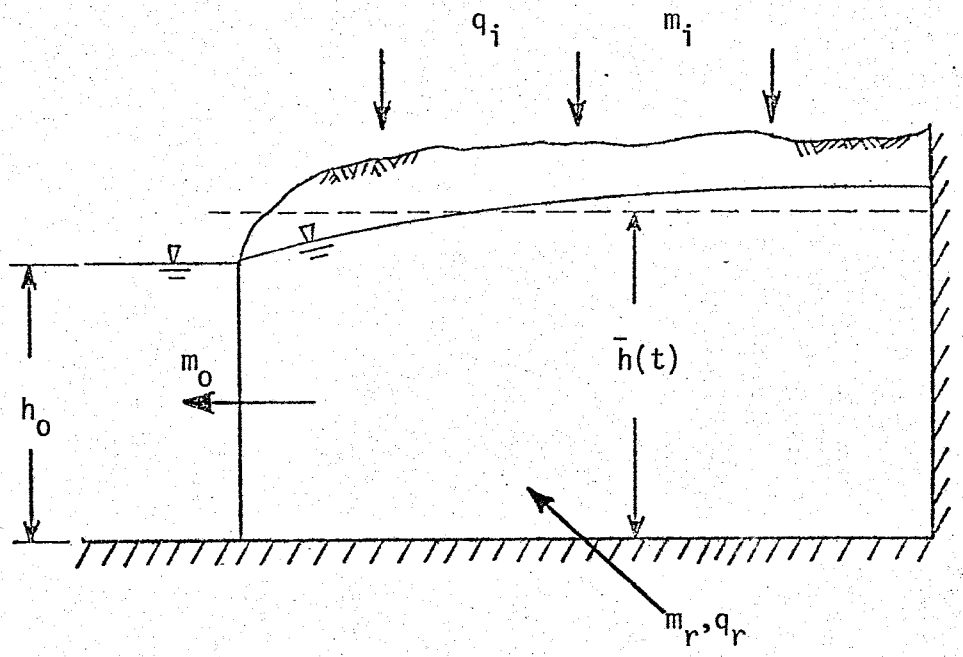
q_i
m_i
m_o
h_o
$\bar{h}(t)$
m_r, q_r

samples were taken on a monthly basis and analyzed for major ions, pH and EC (see Wierenga et al., 1979, 1981). The relationship between TDS and EC was established by performing linear regression on 104 drain samples taken from four locations in the vicinity of San Acacia during the period, April 1977-March 1979. The regression equation was found to be

$$\text{Drain: TDS (mg/l)} = 660.6 \cdot \text{EC (mmhos/cm)} + 74.8$$

with a correlation coefficient of $r = 0.97$. The same procedure was performed for the irrigation diversion water, with the following results

$$\text{Diversion: TDS (mg/l)} = 752.3 \cdot \text{EC (mmhos/cm)} - 18.49$$

The correlation coefficient was found to be $r = 0.96$.

To determine the time variability of EC, closely spaced samples in time were taken at several periods during the irrigation season. It was found that the groundwater component of the drain concentration showed very little time variability, except during the initial stages of an irrigation when some dilution would occur. The dilution was primarily due to direct runoff (or 'tailwater') into the drain, as well as a contribution from ponded water which accumulated adjacent to the drain. Figure 3.3 illustrates an eight day period where EC and q were measured at two-hour intervals. During the initial stages of the irrigation, direct runoff from the field was logged by the field technician at one location on the south side of the drain. This direct runoff is shown in Figure 3.3. Since the EC concentration of the irrigation water is on the order of 1.0 (mmhos/cm), this produced a maximum dilution in the drain of 1.5 (mmhos/cm). As more land became irrigated, ponded conditions were observed at several locations

Figure 3.3. Electrical conductivity (mmhos/cm) and discharge (l/sec) at the outflow drain, demonstrating the various contributions to salinity and flow before-during-and after an irrigation.

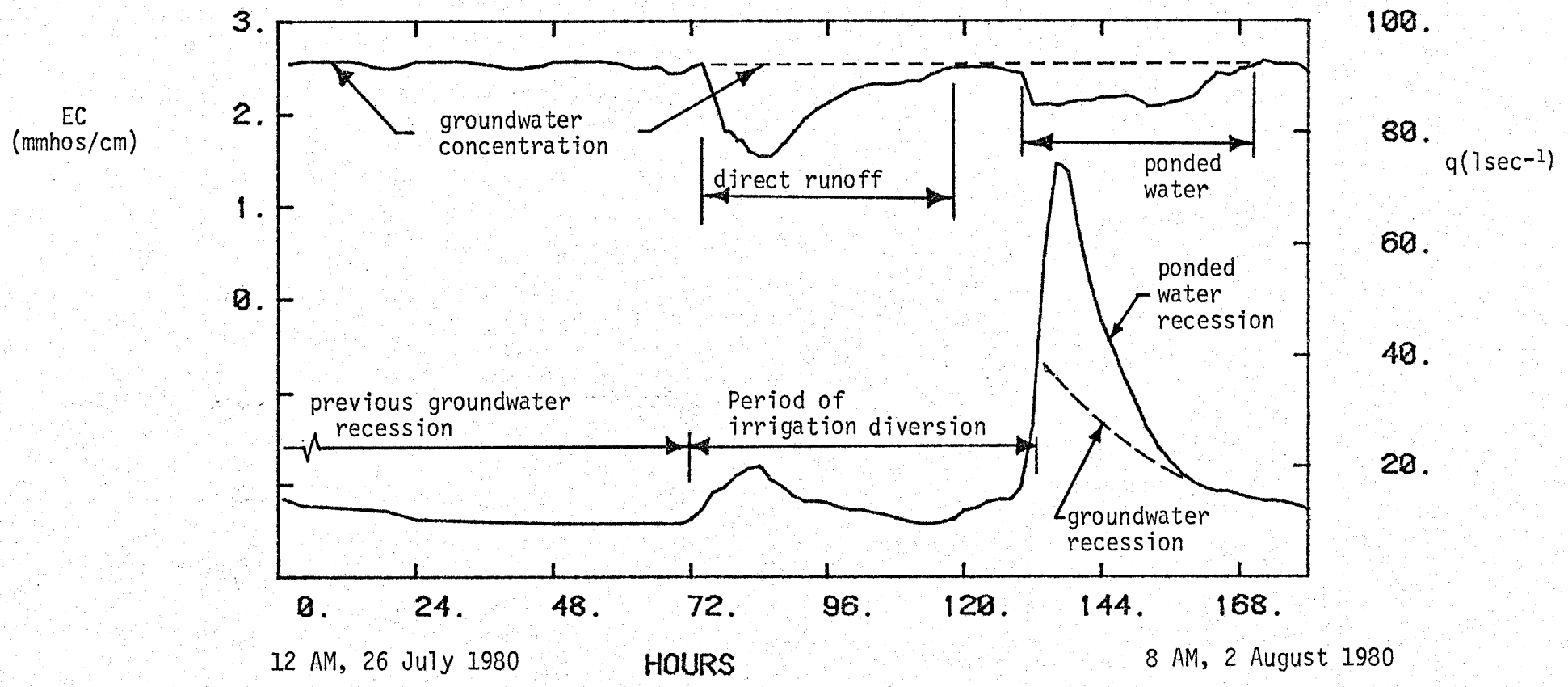
EC
(mmhos/cm)
3.
2.
1.
0.
100.
80.
60.
40.
20.
q(lsec-1)
groundwater
concentration
direct runoff
ponded
water
ponded
water
recession
previous groundwater
recession
Period of
irrigation diversion
groundwater
recession
0.
24.
48.
72.
96.
120.
144.
168.
12 AM, 26 July 1980
HOURS
8 AM, 2 August 1980

adjacent to the drain. The ponded water infiltrates quickly and mixes with the groundwater close to the drain, producing an EC concentration of about 2.1 (mmhos/cm). It was determined from experiments of this sort, that overall, the groundwater contribution to drainflow TDS was reasonably constant on a daily basis, and thus weekly samples of EC were found to be suitable to describe the groundwater TDS concentration. The daily TDS concentration was determined by interpolation. The mass flux for the input series $m_i = q_i c_i$ was calculated by multiplying the average daily diversion volume per unit area by the TDS concentration of the diversion, the same as for $m_o(t)$. It is significant in this case that nearly all the time variability in the mass flux quantities is produced by the transient nature of the flow system itself, and not the TDS concentration. From the linear reservoir theory it can also be demonstrated that during one irrigation season the outflow solute concentration will change very little, since the residence time T_c in this system is expected to be on the order of years.

Making use of the fact that TDS should not vary appreciably over one irrigation season we can simplify (3.5) by setting $dc/dt \cong 0$. Following the procedure of Chapter 1, the perturbation form of (3.5) is given by

$$T_m \frac{d}{dt} (\bar{m}_o + m_o') = \bar{m}_i + m_i' - \bar{m}_o + m_o' + \bar{m}_r \tag{3.6}$$

where the regional aquifer mass flux $m_r = q_r c_r$ is taken to be constant over the period of interest. Equation (3.6) can then be separated into a steady-state or expected value contribution

$$\begin{aligned} \bar{m}_o &= E(m_o) = E(m_i) + E(m_r) \\ &= \bar{m}_i + \bar{m}_r \end{aligned} \tag{3.7}$$

and a time variable process given by

$$T_m \, dm_o'/dt + m_o' = m_i' . \tag{3.8}$$

Notice that (3.8) does not depend on the regional mass flux into the irrigated system, since $E(m_r'(t)) = 0$. The perturbation equation for mass flux (3.8) has the same form as the solute equation (1.27), except that the T_m replaces the solute response time T_c. The transfer function, phase and variance results are respectively

$$\frac{\phi_{m_o m_o}(\omega)}{\phi_{m_i m_i}(\omega)} = \frac{1}{1 + \omega^2 T_m^2} \tag{3.9}$$

$$\Theta(\omega) = - \, TAN^{-1}(\omega T_m) \tag{3.10}$$

and

$$\frac{\sigma^2_{m_o}}{\sigma^2_{m_i}} = \frac{1}{1 + T_m/\lambda_m} \tag{3.11}$$

where λ_m is the correlation time scale of the input process $m_i(t)$.

In Figure 3.4 is plotted the estimated daily time series of mass flux m_o (Kg/ha/day) and TDS concentrationsc (g/l) at the outflow drain for the 1978 irrigation season (214 days). Figure 3.5 illustrates the applied irrigation mass flux (Kg/ha/day) for the same period. The mean (μ) and variance (σ^2) for each series is also given.

Estimation of the spectra and phase for the bivariate stochastic processes $m_i(t)$ and $m_o(t)$ was accomplished using the Timanl Spectral and Cross-spectral analysis program developed at New Mexico Institute of Mining and Technology for a Dec. 20 computer. The estimated spectra for $m_i(t)$ and $m_o(t)$ are shown in Figures 3.6 and 3.7. The

Figure 3.4. The outflow drain mass flux and total dissolved solids concentration for 15 March-15 October, 1978.

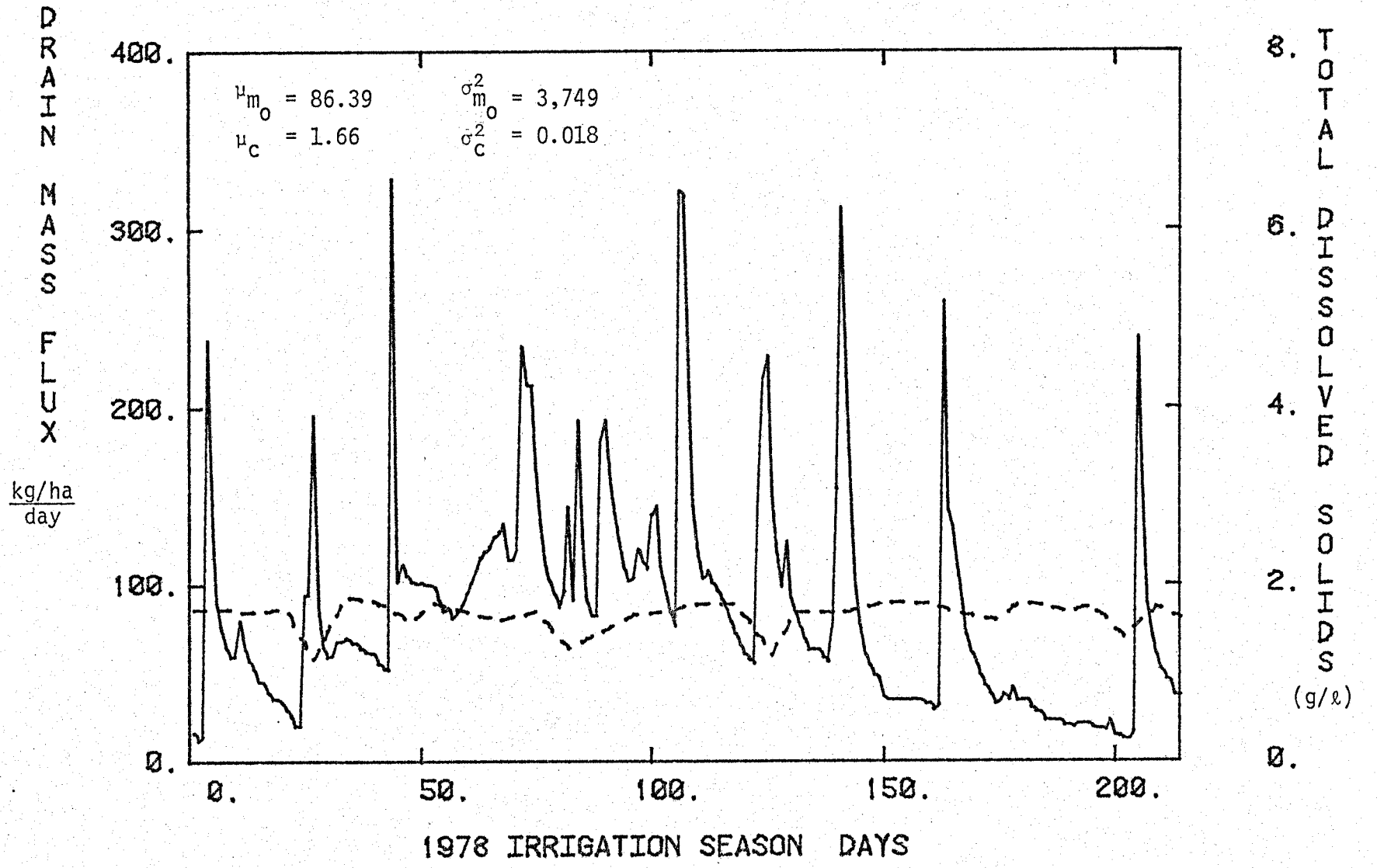
DRAIN MASS FLUX
kg/ha
day
400.
300.
200.
100.
0.
μ_{m_o} = 86.39
$\sigma^2_{m_o}$ = 3,749
μ_c = 1.66
σ^2_c = 0.018
0.
50.
100.
150.
200.
1978 IRRIGATION SEASON DAYS
8.
6.
4.
2.
0.
TOTAL DISSOLVED SOLIDS
(g/ℓ)

Figure 3.5. Applied irrigation mass flux for 15 March-15 October, 1978. The irrigations are numbered.

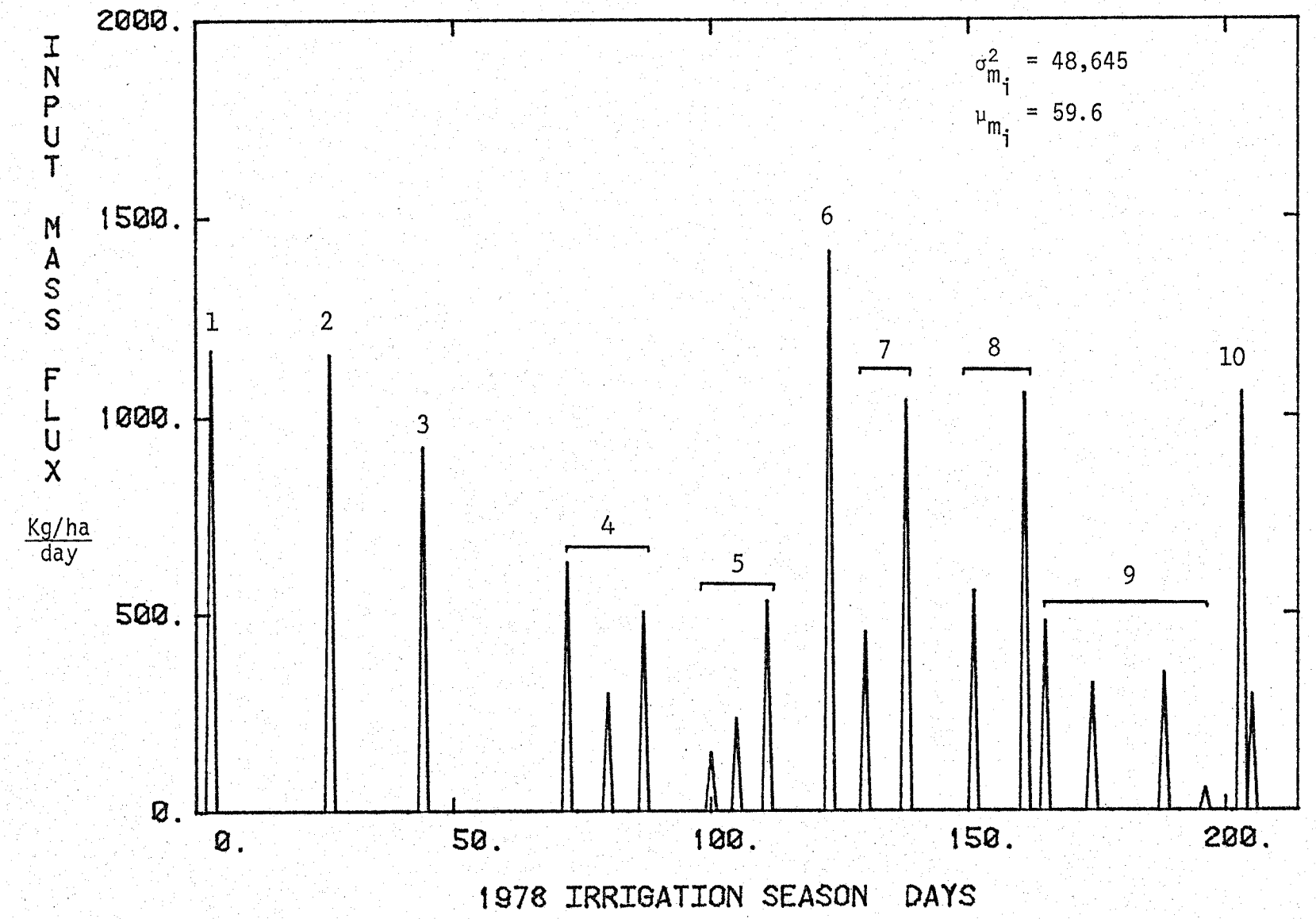
INPUT MASS FLUX
Kg/ha
day
2000.
1500.
1000.
500.
0.
$\sigma^2_{m_i}$ = 48,645
μ_{m_i} = 59.6
1
2
3
4
5
6
7
8
9
10
0.
50.
100.
150.
200.
1978 IRRIGATION SEASON DAYS

Figure 3.6. Input spectrum for mass flux $\phi_{m_i m_i}(f)$ versus ordinary frequency f.

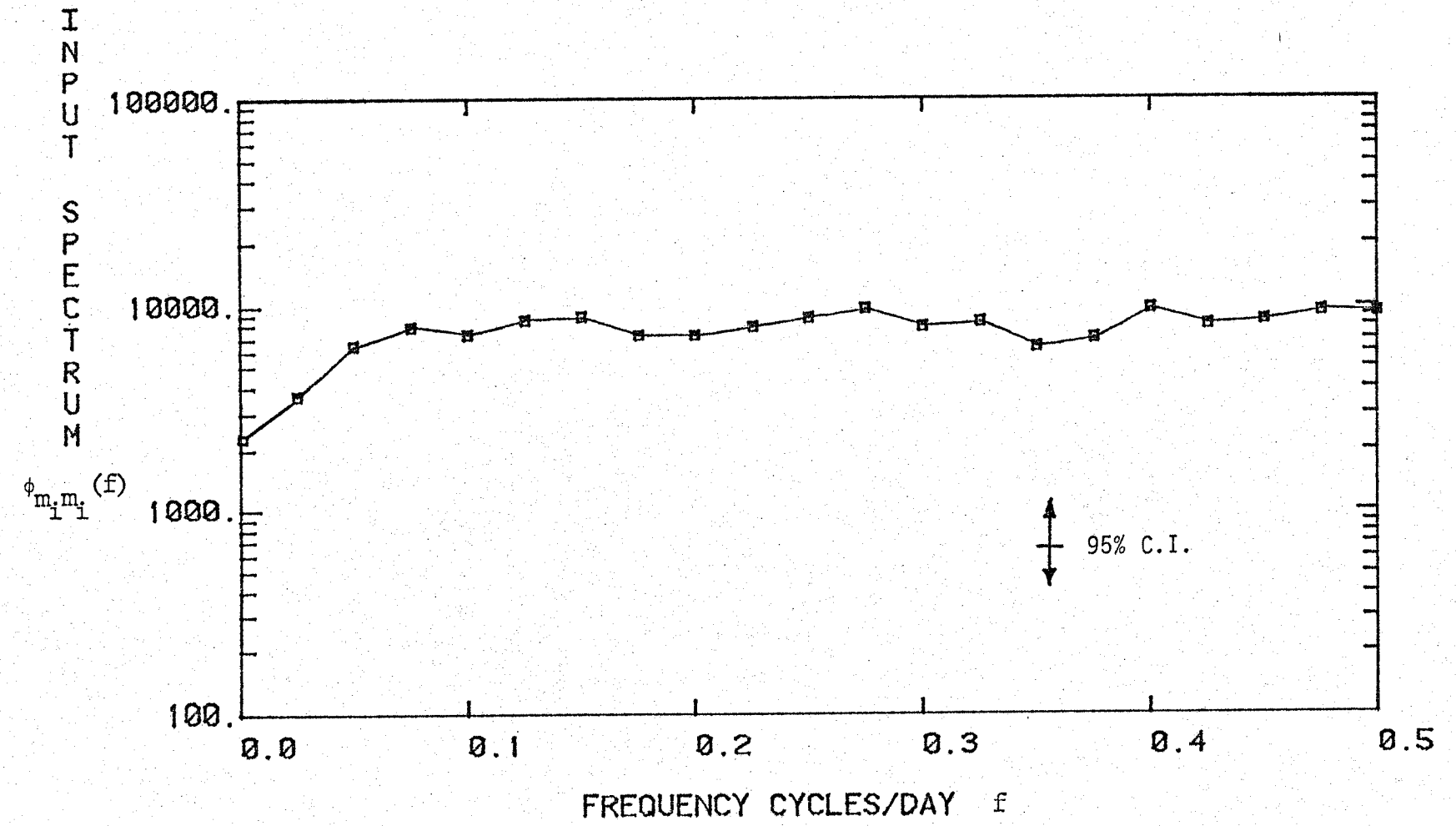
INPUT SPECTRUM
$\phi_{m_i m_i}(f)$
100000.
10000.
1000.
100.
95% C.I.
0.0
0.1
0.2
0.3
0.4
0.5
FREQUENCY CYCLES/DAY f

Figure 3.7. Output spectrum for mass flux $\phi_{m_o m_o}(f)$ versus ordinary frequency f.

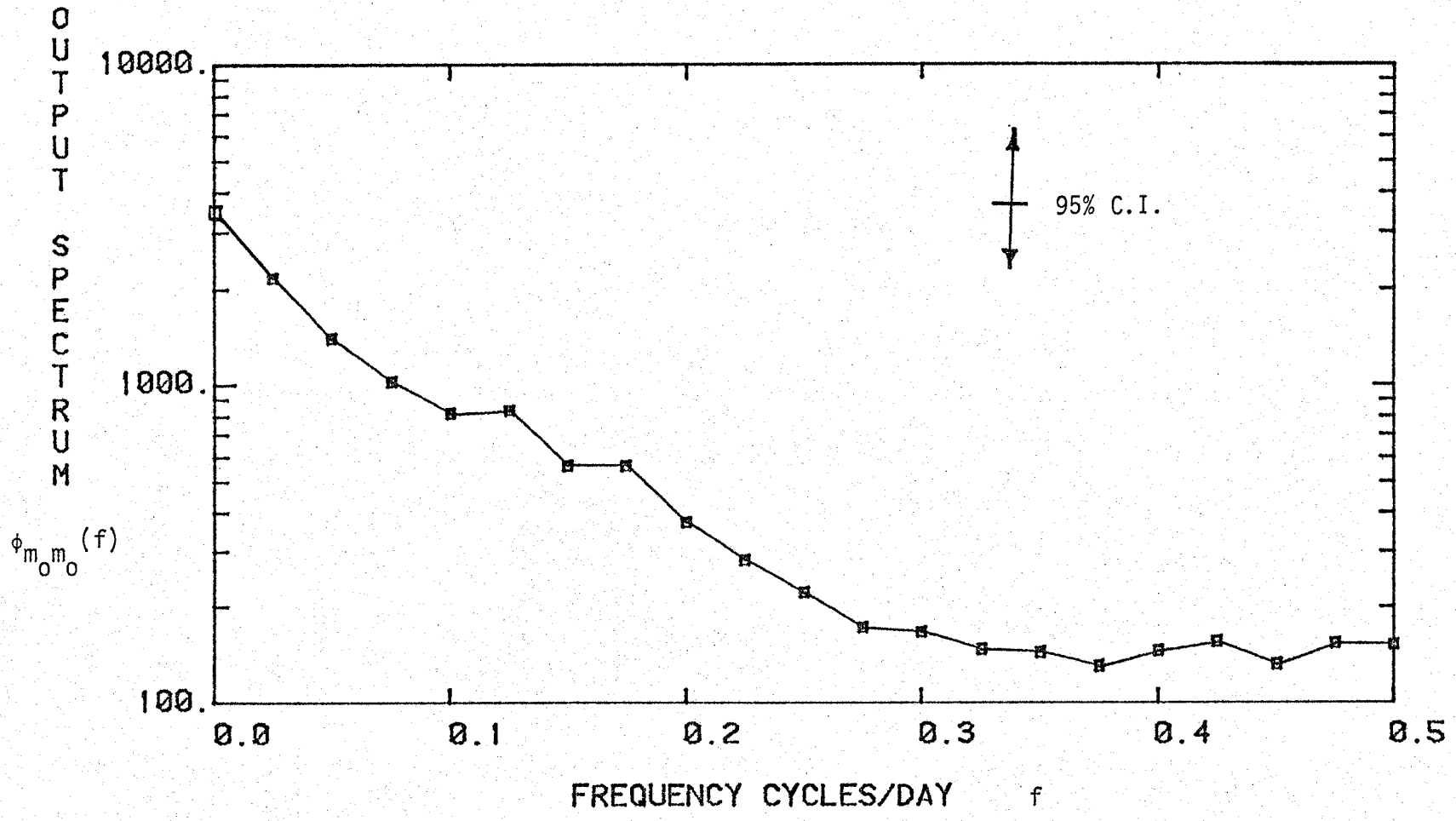
OUTPUT SPECTRUM
$\phi_{m_o m_o}(f)$
10000.
1000.
100.
95% C.I.
0.0
0.1
0.2
0.3
0.4
0.5
FREQUENCY CYCLES/DAY f

natural log of the spectrum is plotted versus ordinary frequency f (cycles/day) in order to produce a constant confidence interval for each spectral estimate. Details of the confidence interval calculation are found in Jenkins and Watts (p. 254). The input spectrum is remarkably flat, and is not significantly different from a 'white noise' signal (independent events). The filtering characteristics of the groundwater system on the input $m_i(t)$ is evident from the spectrum for $m_o(t)$. Notice a gradual decrease in the estimated output spectrum at higher frequencies. This is to be expected for 'low pass' filters, where higher frequency variations tend to be attenuated while low frequency variations tend to pass through the system unaltered.

To demonstrate the use of the spectral approach for estimating the system parameters, a curve matching procedure was performed using the estimated and theoretical transfer function and phase. The result of the curve matching procedure are shown in Figures 3.8 and 3.9, with the best fit (by eye) determined to be T_m = 5.5 days. Confidence intervals on both the transfer function and the phase are also given. For some estimates the confidence interval could not be determined due to lack of correlation between input and output at these frequencies. For details of these calculations see Jenkins and Watts (1968, p. 434).

The estimated transfer function behaves quite similar to the theoretical result except in the high frequency range. This points out why a curve matching procedure was used here, as opposed to a least squares fitting technique. Since CI's are wide or nonexistent for the high frequency spectral estimates, more weight was given to the lower frequency range, where the confidence interval is tighter. The phase estimates are reasonably close to the theoretical curve in the range

Figure 3.8. The theoretical and estimated transfer function versus frequency. The response time was estimated to be 5.5 days.

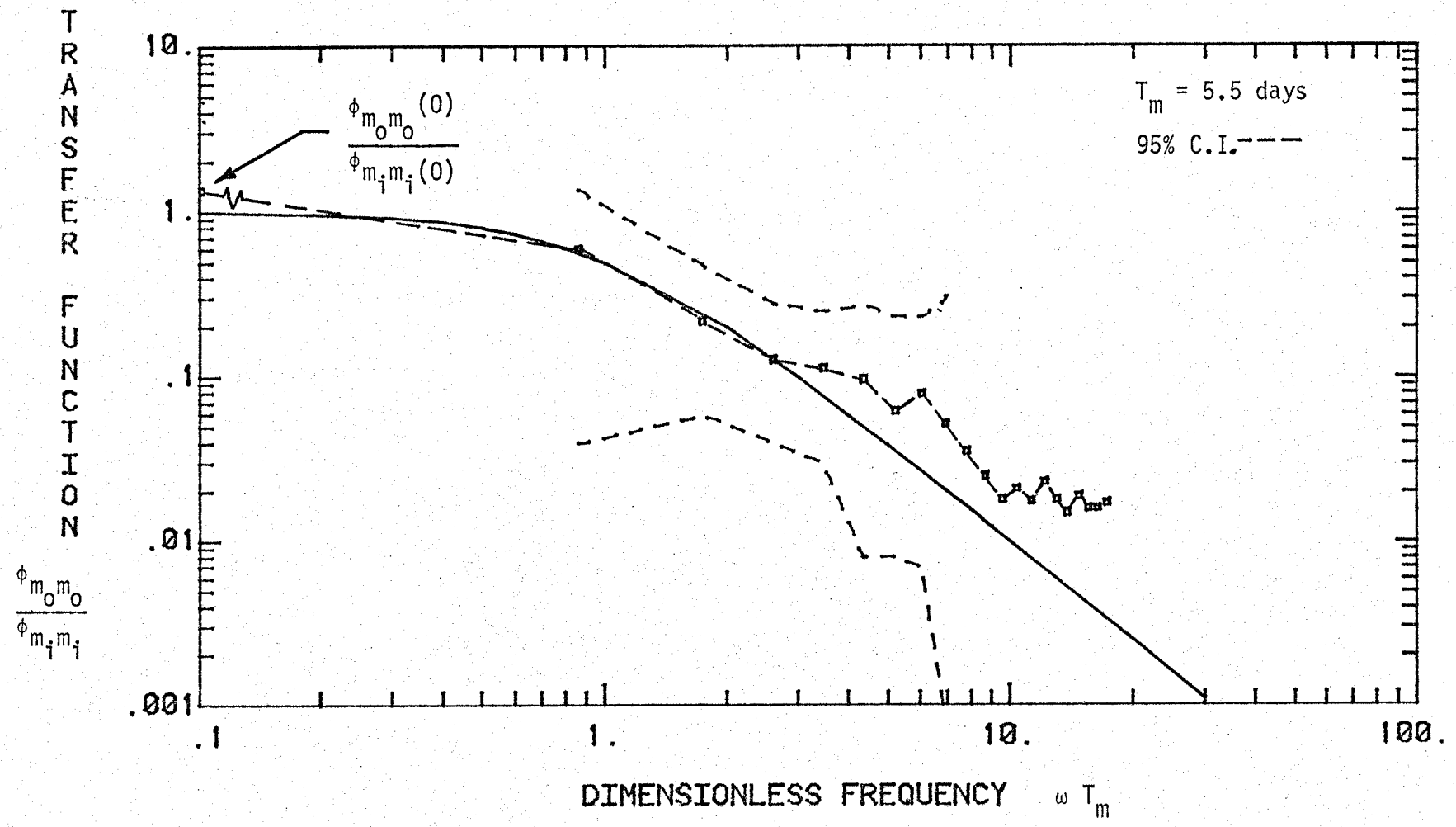
TRANSFER FUNCTION
$\frac{\phi_{m_o m_o}}{\phi_{m_i m_i}}$
10.
1.
.1
.01
.001
.1
1.
10.
100.
$\frac{\phi_{m_o m_o}(0)}{\phi_{m_i m_i}(0)}$
T_m = 5.5 days
95% C.I.---
DIMENSIONLESS FREQUENCY ωT_m

3.9. The theoretical and estimated phase spectra versus frequency. The response time was estimated to be 5.5 days.

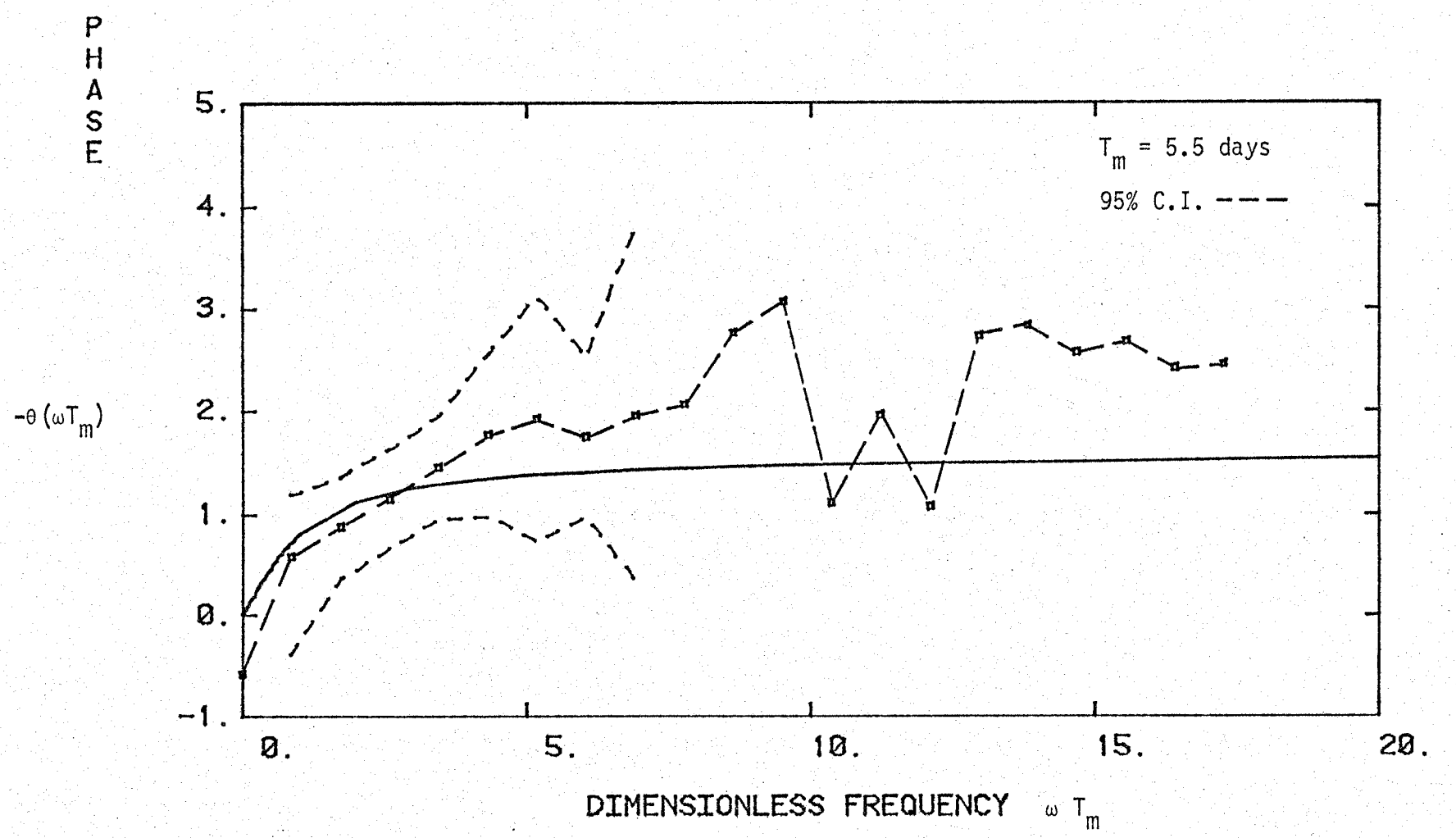
PHASE
$-\theta(\omega T_m)$
5.
4.
3.
2.
1.
0.
-1.
0.
5.
10.
15.
20.
T_m = 5.5 days
95% C.I. ---
DIMENSIONLESS FREQUENCY ωT_m

$0 < \omega T_m < 7.0$, however much larger departures from the theory appear again in the high frequency range $\omega T_m > 7.0$. In each case the high frequency estimates provide no information, and appear to be noise, unexplainable by the kind of model assumed here. In terms of the field site, 'tailwater' and ponded conditions are often observed in the vicinity of the outflow drain. This ponded condition would be expected to contribute to the early stages of drainflow, and thus might explain the high frequency behavior. However, a more complicated model and much more detailed temporal data would be necessary to examine this condition.

It is also of interest to examine the estimated and theoretical input-output variance ratio. The estimated variances for input and output are shown in Figures 3.4 and 3.5. The theoretical variance ratio plotted against T_m/λ_m is shown in Figure 3.10, along with the field estimates. Using T_m = 5.5 days the correlation time scale of the input series was found to be ~0.5 days. Although this value is likely not accurate for the daily data given here, it does point out that very little (if any) autocorrelation exists in this input series.

To summarize, the spectral technique was applied to a 'well-mixed' groundwater reservoir subject to transient changes in groundwater flow and the mass flow of salts. It was demonstrated that the mass flux approach is the only suitable means for describing the input/output salt load in highly transient groundwater flow situations. Using the stochastic time series method it was possible to determine the response time parameter T_m for the mass flux of dissolved salts at this site. Once the response time parameters is known, any time domain solution can be constructed simply by returning to the convolution equation and specifiying the input and initial condition. The spectral analysis

Figure 3.10. The output/input variance ratio versus T/λ_m. The variance ratio from the field data is also shown.

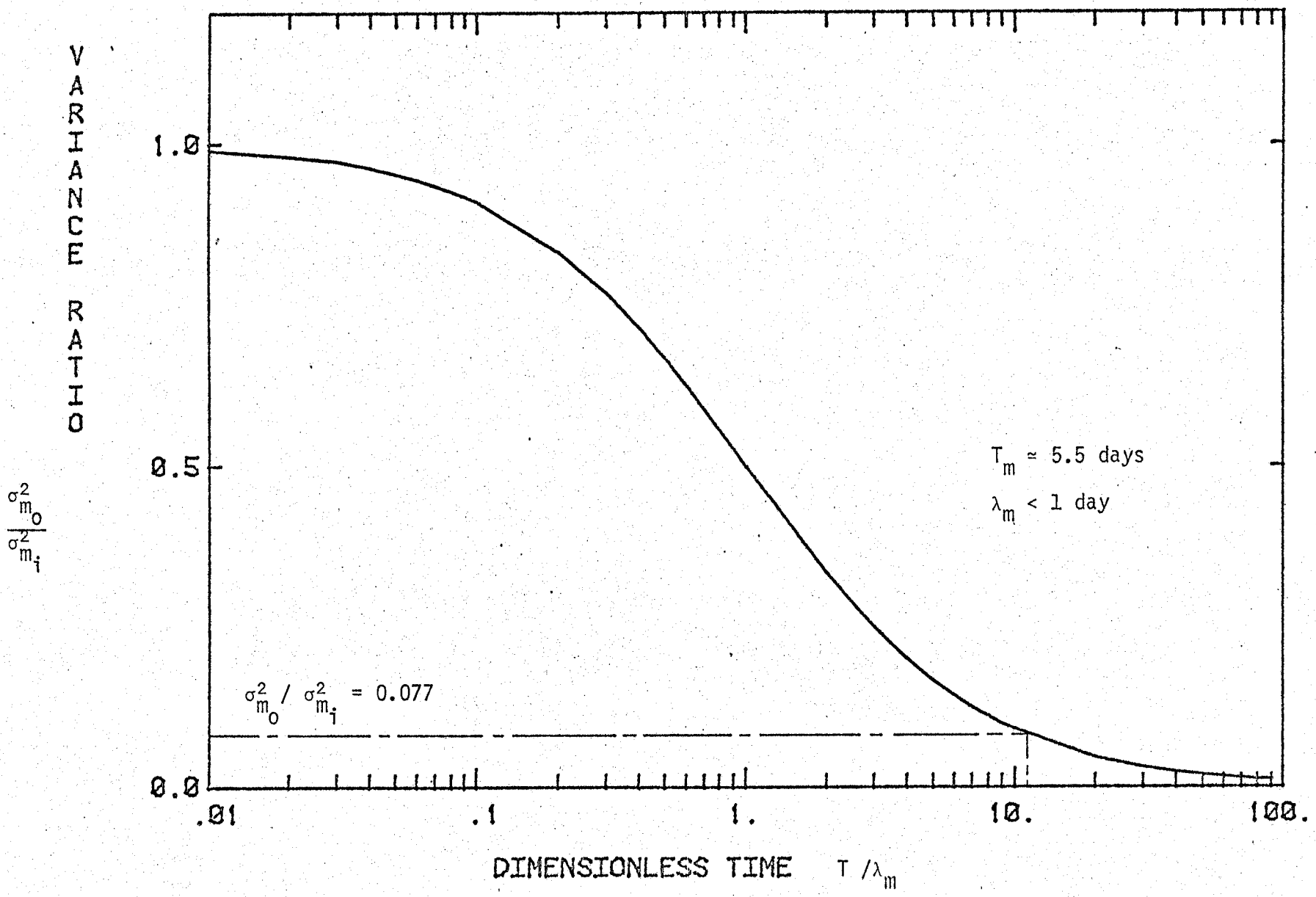
VARIANCE RATIO
$\frac{\sigma^2_{m_o}}{\sigma^2_{m_i}}$
1.0
0.5
0.0
.01
.1
1.
10.
100.
$T_m \simeq 5.5$ days
$\lambda_m < 1$ day
$\sigma^2_{m_o} / \sigma^2_{m_i} = 0.077$
DIMENSIONLESS TIME T/λ_m

procedure provides an additional tool for analyzing the impact of non-point sources of salinity in agricultural watersheds.

The influence of river salinity on the quality of municipal wells: Strasbourg, France (a convective transport application)

An illustration of industrial contamination of a river in an alluvial valley and the resulting influence on nearby groundwater supplies is presented here and analyzed with the spectral theory for convective transport previously developed. Application of the theory for a pumping well adjacent to the contaminated river is shown to provide a reasonable explanation for the variable concentration of chloride ion in the well. The procedure demonstrates that both the transfer function and the phase are necessary to fully evaluate the frequency behavior of the system. The geometry of the stream-aquifer system is shown in Figure 1.4.

Contamination of the Rhine River between France and Germany and the hydraulically connected alluvial aquifer of the Rhine valley, has been the subject of intense study for some time, because of its importance as a source of municipal and industrial water supply (Brunotte et al. 1970). Since 1945 a considerable increase in the sodium chloride concentration of the groundwater has been observed. This increase is due in part or in whole to the accumulation of potash mine spoils in the region. There are apparently two mechanisms for salt contamination of groundwater. An intense local pollution has occurred directly under the mining spoils themselves from infiltration of dissolved NaCl. In addition surface runoff gradually drains the saline effluent into the Rhine River, which subsequently affects the salinity of the Rhine's

alluvial aquifer through streambed infiltration. This application is primarily concerned with evaluating the influence of river quality on adjacent municipal well water supplies, using the stochastic theory previously developed.

The impact of the river salinity on the aquifer can readily be observed in Figure 3.11, where the monthly chloride concentration for a municipal well and the Rhine River at Strasbourg, France are shown. The data were taken from a report by the Institut de Mechanique des Fluides, Universite Louis Pasteur, de Strasbourg (1977). The chloride time series at the well, which is located some 450 meters from the river, appears to be a smoothed and lagged version of the river series. Spectral analysis was performed on the data, with the results shown in Figures 3.12 and 3.13. The estimated 95 percent confidence interval is also shown. The transfer function and phase were estimated from the data and are given in Figures 3.14 and 3.15. The parameter T_o was determined by visually matching the estimated transfer function and phase to the theoretical curves, while also attempting to contain the theoretical results within the estimated 95 percent confidence interval. This could only be accomplished for $T_o \simeq 6$ months. The estimated transfer function in this case is consistently higher than the theoretical result, although it is still within the confidence interval. The phase estimates compare extremely well with the theoretical result over the entire frequency range. It is likely that the transfer function result is due to a failure of the model to precisely represent the field situation in this case. It is known for example that the Rhine River is naturally effluent, or it loses its flow to the alluvial aquifer, in this region. Depending on the magnitude of the river loss, this could produce a more complicated

Figure 3.11. Monthly time series of chloride ion for a municipal well and the Rhine River at Strasbourg, France. The record is for January, 1972 through December, 1976.

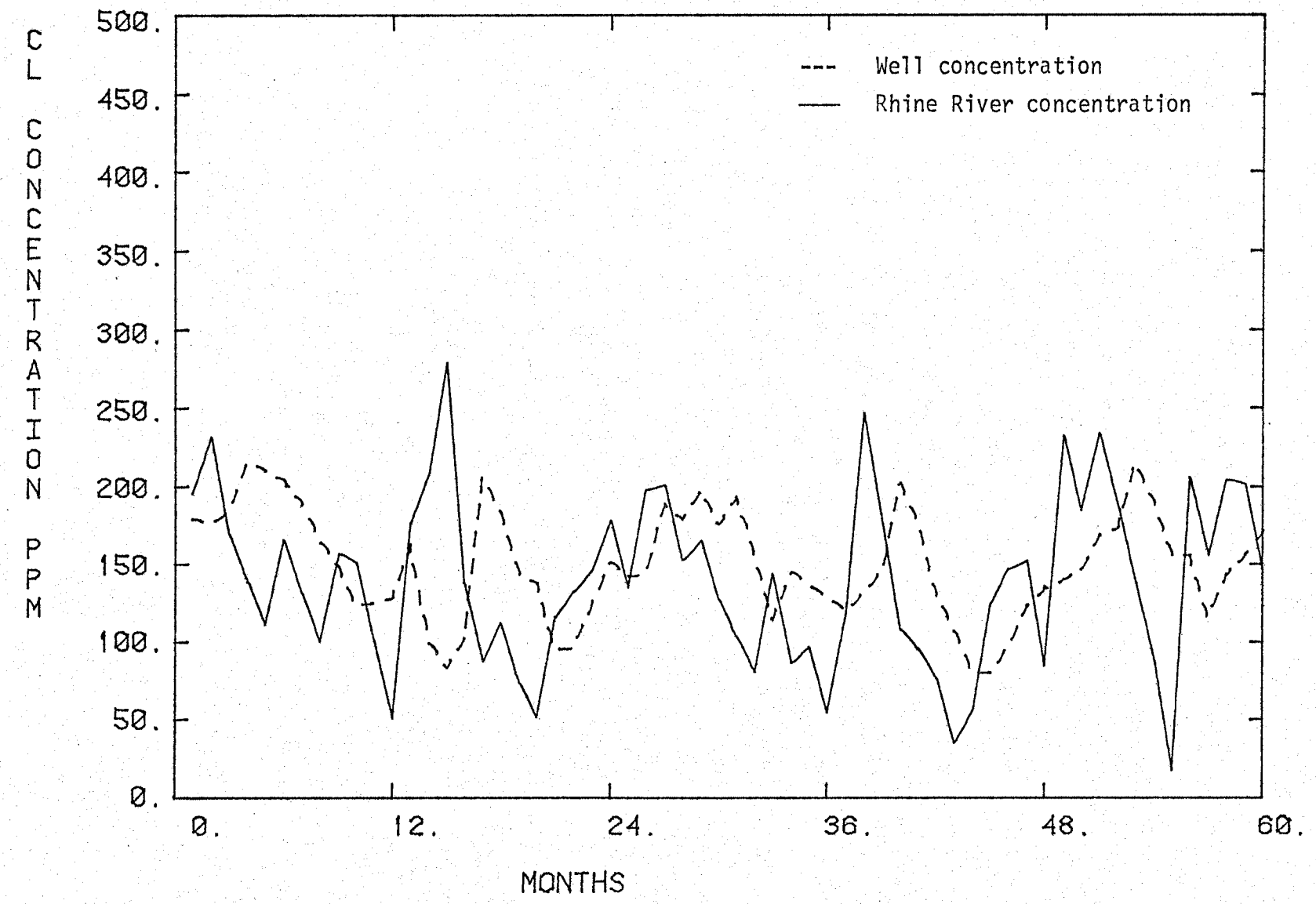
CL CONCENTRATION PPM
500.
450.
400.
350.
300.
250.
200.
150.
100.
50.
0.
0.
12.
24.
36.
48.
60.
MONTHS
Well concentration
Rhine River concentration

Figure 3.12. The estimated spectrum for the Rhine River monthly chloride time series, with the 95 percent confidence interval.

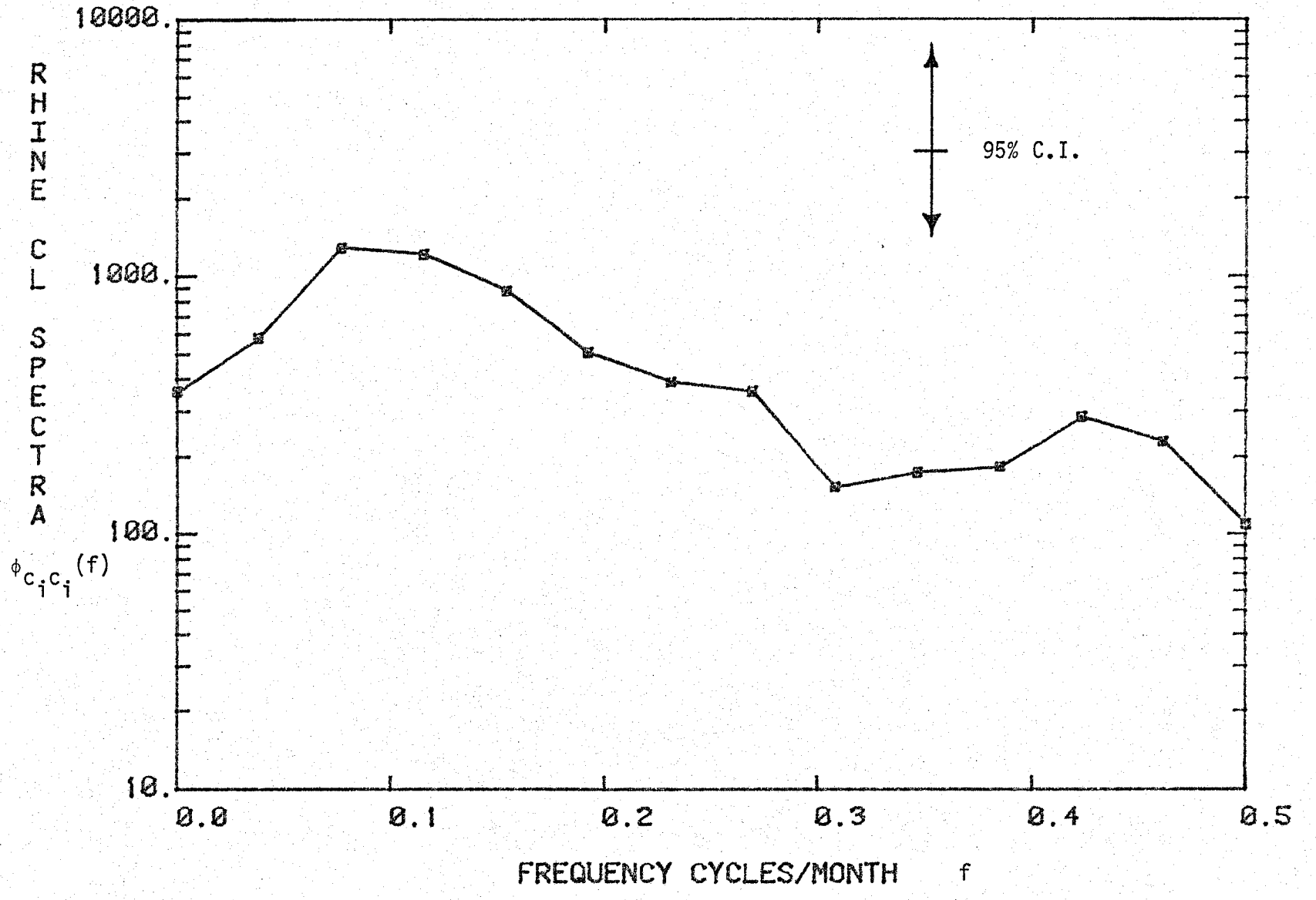
10000.
1000.
100.
10.
RHINE CL SPECTRA
$\phi_{c_i c_i}(f)$
95% C.I.
0.0
0.1
0.2
0.3
0.4
0.5
FREQUENCY CYCLES/MONTH f

Figure 3.13. The estimated spectrum for well No. 6 with the 95 percent confidence interval.

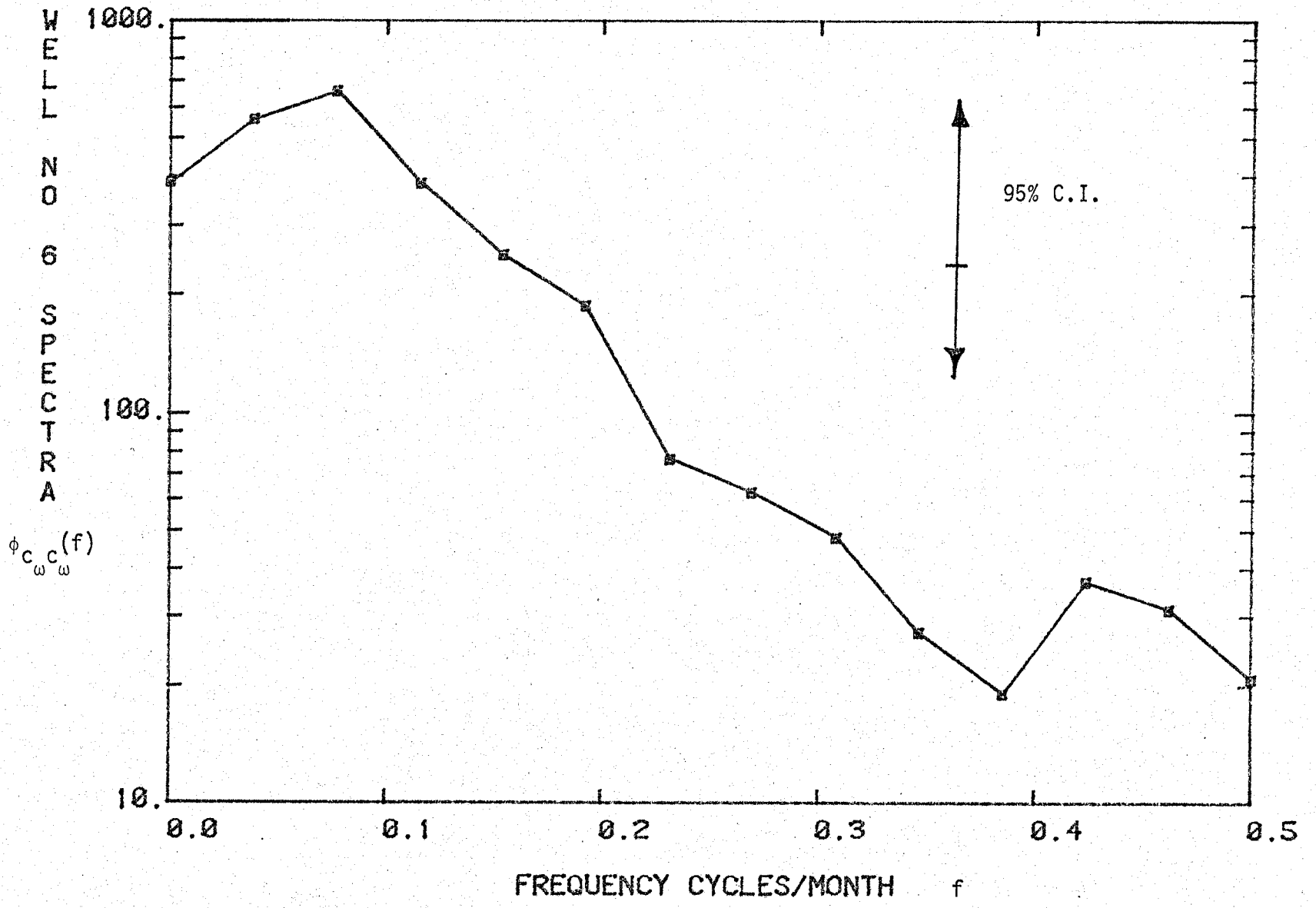
WELL NO 6 SPECTRA
$\phi_{c_\omega c_\omega}(f)$
1000.
100.
10.
95% C.I.
0.0
0.1
0.2
0.3
0.4
0.5
FREQUENCY CYCLES/MONTH f

Figure 3.14. The theoretical and estimated transfer function for the Rhine River-aquifer problem.

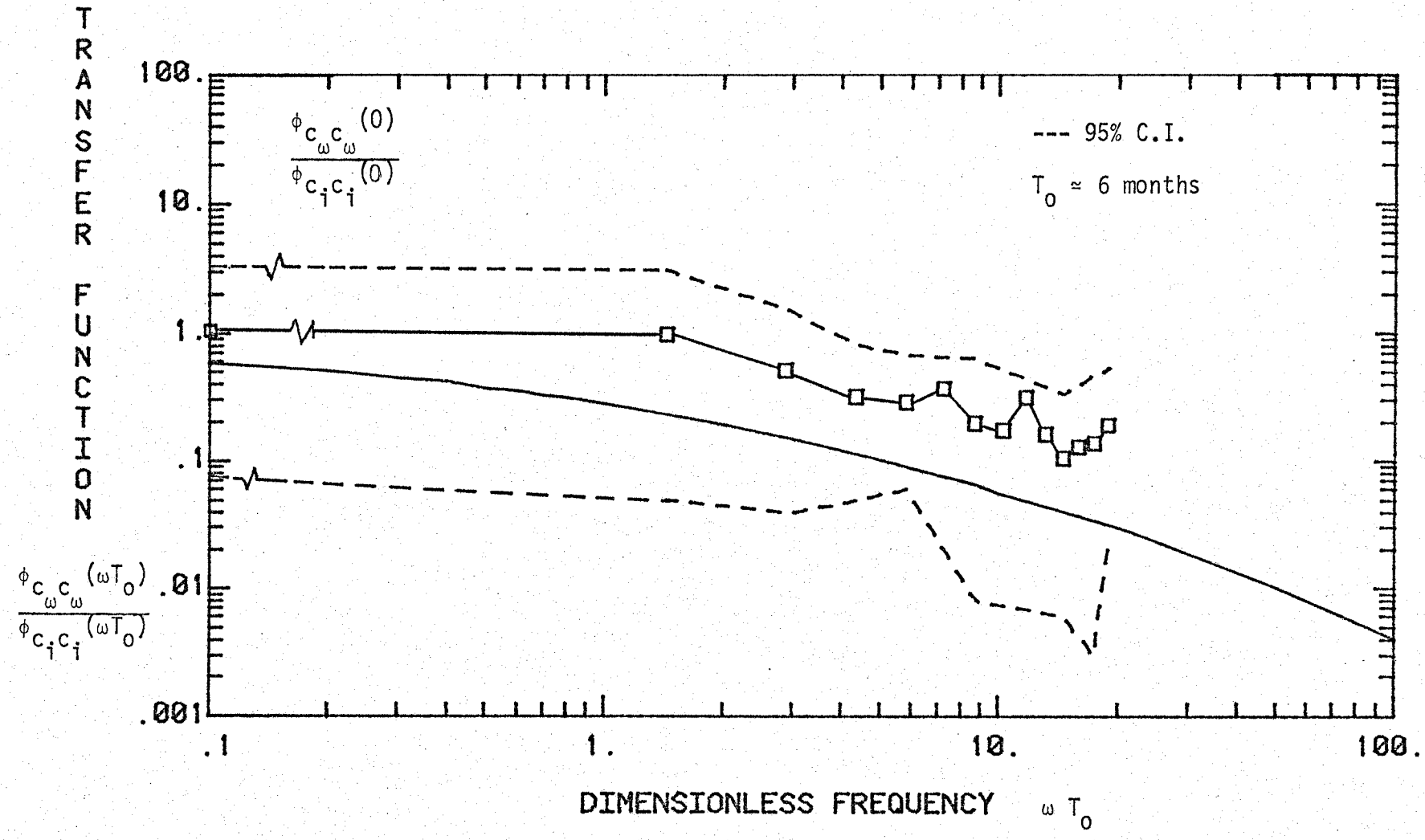
TRANSFER FUNCTION
$\frac{\phi_{c_\omega c_\omega}(\omega T_o)}{\phi_{c_i c_i}(\omega T_o)}$
100.
10.
1.
.1
.01
.001
$\frac{\phi_{c_\omega c_\omega}(0)}{\phi_{c_i c_i}(0)}$
--- 95% C.I.
$T_o \simeq$ 6 months
.1
1.
10.
100.
DIMENSIONLESS FREQUENCY ωT_o

Figure 3.15. The theoretical and estimated phase for the Rhine River-aquifer problem.

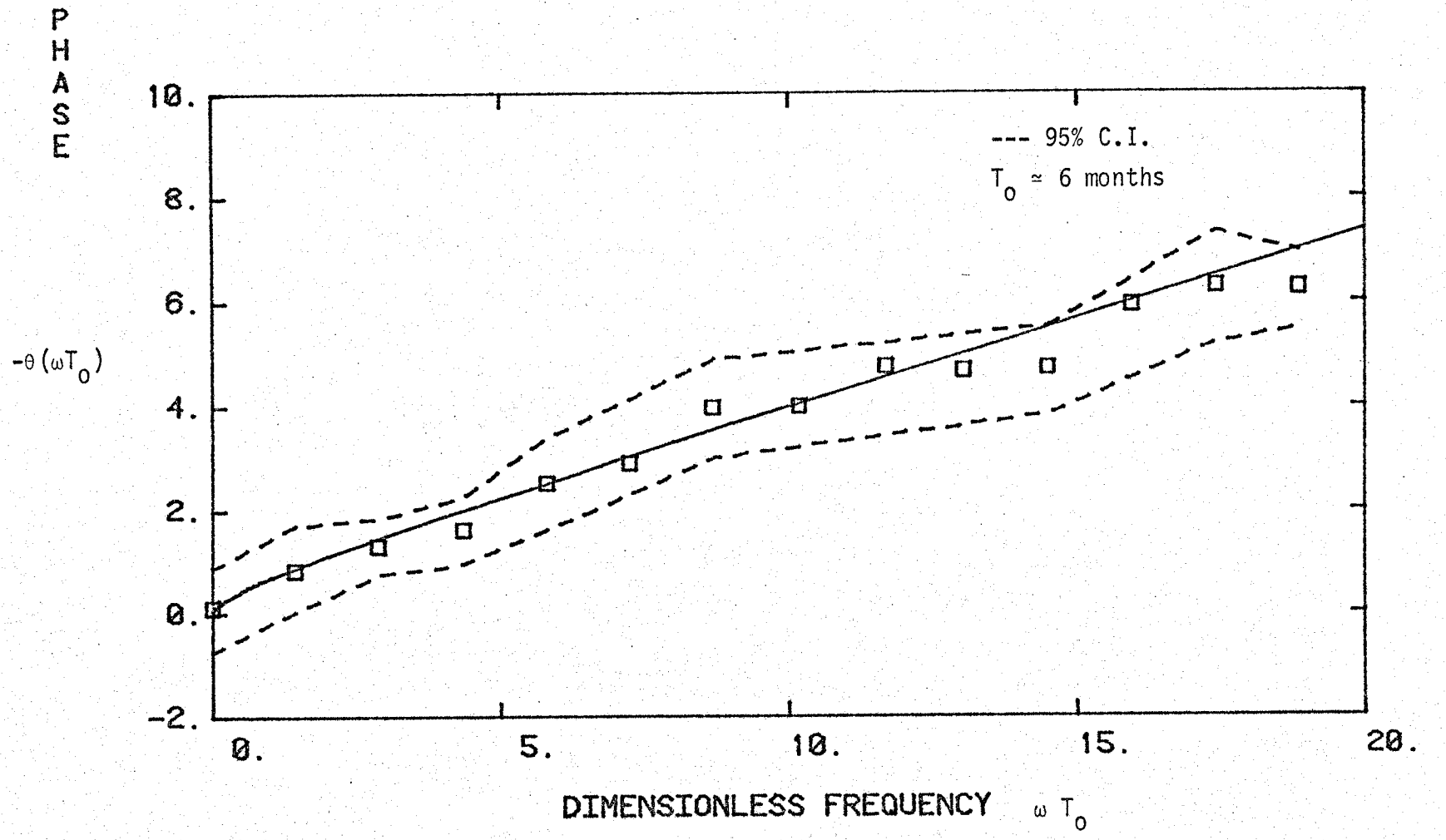
PHASE
$-\theta(\omega T_0)$
10.
8.
6.
4.
2.
0.
-2.
0.
5.
10.
15.
20.
--- 95% C.I.
$T_0 \simeq$ 6 months
DIMENSIONLESS FREQUENCY ωT_0

potential flow field than has been assumed here. In fact by superimposing a uniform flow field with a curvilinear field, it is quite possible that the transfer function would display less amplitude filtering depending on the magnitude of uniform flow component (recall that uniform flow produces no amplitude filtering of the transfer function).

Recalling that the minimum travel time to the pumping well is given by $\tau_w = T_o/3$, and using $T_o = 6$ months, we find that the first arrival of solute should occur in approximately 2.0 months. Since the phase describes the lead or lag between the input and output, we can make use of this fact to examine the average time lag for solutes to move from the river to the well as a function of frequency. In other words, does the period of the input variation have any significance on the travel time? The average time lag can be defined as (Kisiel, 1969)

$$T_L = \frac{\theta(\omega)}{\omega} = \frac{\theta(f)}{2\pi f}$$

where f is ordinary frequency in cycles/month. For $T_o = 6$ the theoretical and experimental results are shown in Figure 3.16. It is interesting that for almost the entire range of frequencies encountered, the average time lag remains near two months, or the frequency of chloride concentration in the river does not seriously affect the average time of travel to the well.

This application of convective transport in a curvilinear flow system demonstrates the spectral input-output theory from a relatively short data base (60 samples). It is encouraging that even series of this length can be diagnostic of mass transport in specific groundwater

Figure 3.16. The theoretical and estimated average travel time as a function of the frequency.

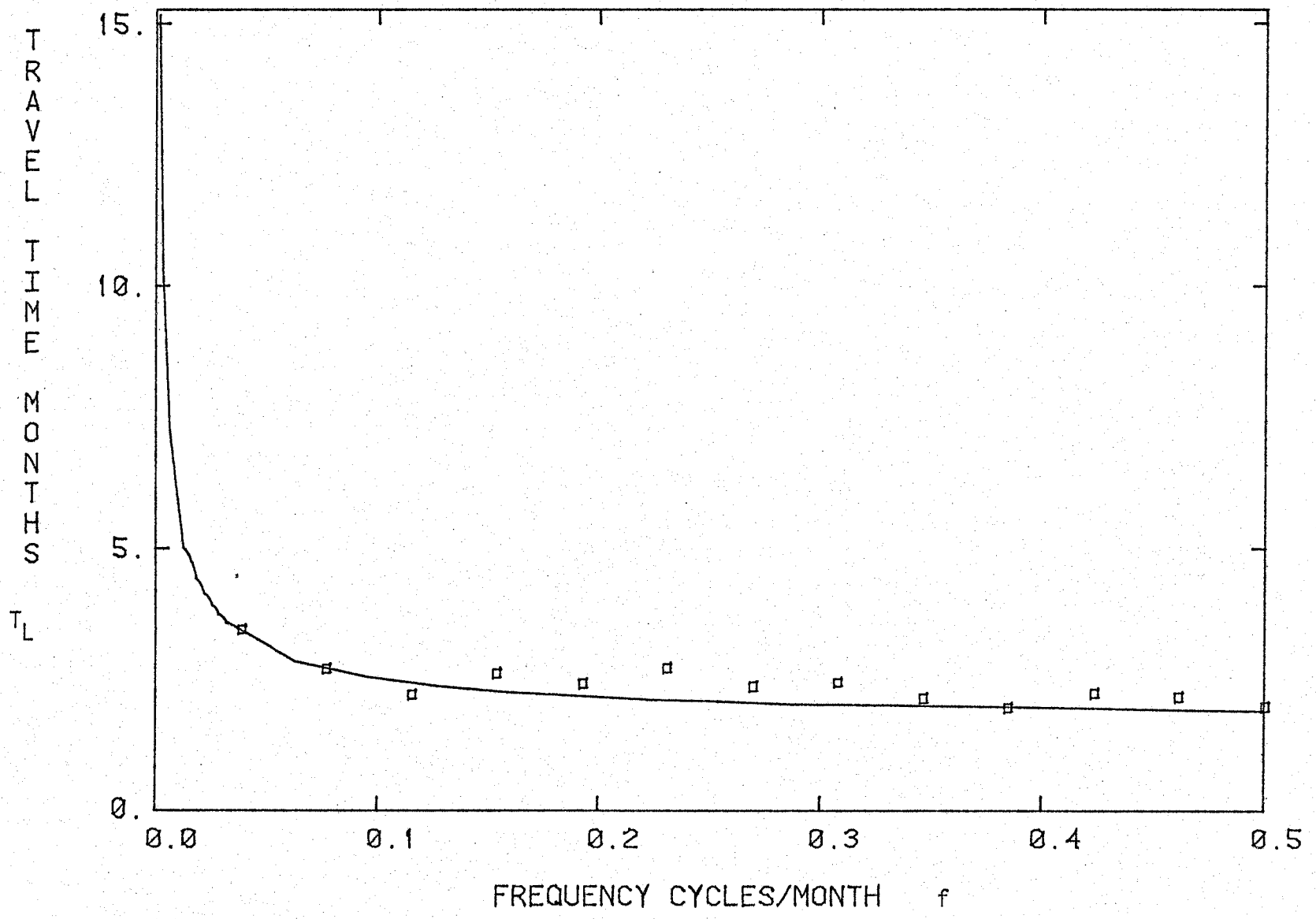
TRAVEL TIME MONTHS
T_L
15.
10.
5.
0.
0.0
0.1
0.2
0.3
0.4
0.5
FREQUENCY CYCLES/MONTH f

flow systems. The method might also be used to estimate the hydraulic parameters of the system. T_o was previously show to be

$$T_o = \frac{n\,L^2}{Q/2\pi h_o} \tag{1.66}$$

or in terms of the effective porosity

$$n = T_o Q/2\pi h_o L^2.$$

The transmissivity is approximately given by (Kirham and Affleck, 1977)

$$T = Kh_o = \frac{Q}{2\pi(h_o - h_w)} \mathrm{Ln}(2L/r_{well}).$$

These expressions provide a means of estimating the transmissivity or the porosity if the average drawdown $h_o - h_w$, the average well discharge Q and the distance to the well L are known. In this application T and n could not be determined since not all of these parameters were available.

Transport of environmental isotopes in a karst region of Rawil, Switzerland (a convection-dispersion application)

The use of environmental isotopes as natural tracers has been shown to be of considerable value to regional and local aquifer analysis (IAEA, 1967). The areas of hydrologic investigation facilitated by isotope methods include recharge estimation, groundwater velocities, and the interrelation between surface and groundwater, to name a few. Atmospheric tritium occurring both naturally and as a result of thermo-nuclear testing, displays large temporal variations which can provide a hydrologic marker for groundwater studies.

An isotope study in a karst region of the high Alps in southwestern Switzerland (U. Schotterer et al., 1980) was carried out during the

period 1973-1978. The study area was situated in a karstic-limestone formation at an altitude of 1200 to 3250 meters above sea level. According to Schotterer et al., the karst water circulation in this region is controlled primarily by synclines and secondarily by faulting. The circulation of water in karst systems can be characterized as occurring in fractured rock, in intergranular material, in dissolution features, or in some combination of these three. However, the authors did not explicitly differentiate between these flow mechanisms, instead they referred to a 'fast' response and a 'slow' response system.

Data from several springs were used in this report. Only one, the Siebenbrunnen Spring, had a long enough data record to apply the time series method. The recharge area for this spring is located a distance of ~4.13 km from the outlet. Precipitation and discharge measurements were taken continuously during the study, with tritium samples for each taken on a monthly and, in some cases, weekly basis. The tritium in precipitation was also measured at several sites, and the volume-weighted tritium input concentration was constructed. The monthly averaged tritium data taken from the report are shown in Figure 3.17.

In the present research we are concerned with the time variability of tritium in the input (precipitation and recharge), and in the output (spring), and whether it is possible to discern some elements of the convective-dispersive transport mechanisms from the frequency response characteristics of the system. Estimation of the average travel-time, the velocity and the magnitude of the karst reservoir volume are also of interest.

Spectral analysis was performed on the ^{3}H time series in precipitation and springflow given in Figure 3.17, with the resulting spectral

Figure 3.17. A. Tritium input concentration constructed by averaging several stations in the intake area of the karst region. B. Tritium in the Siebebrunnen spring constructed using a flow weighted monthly average.

A.

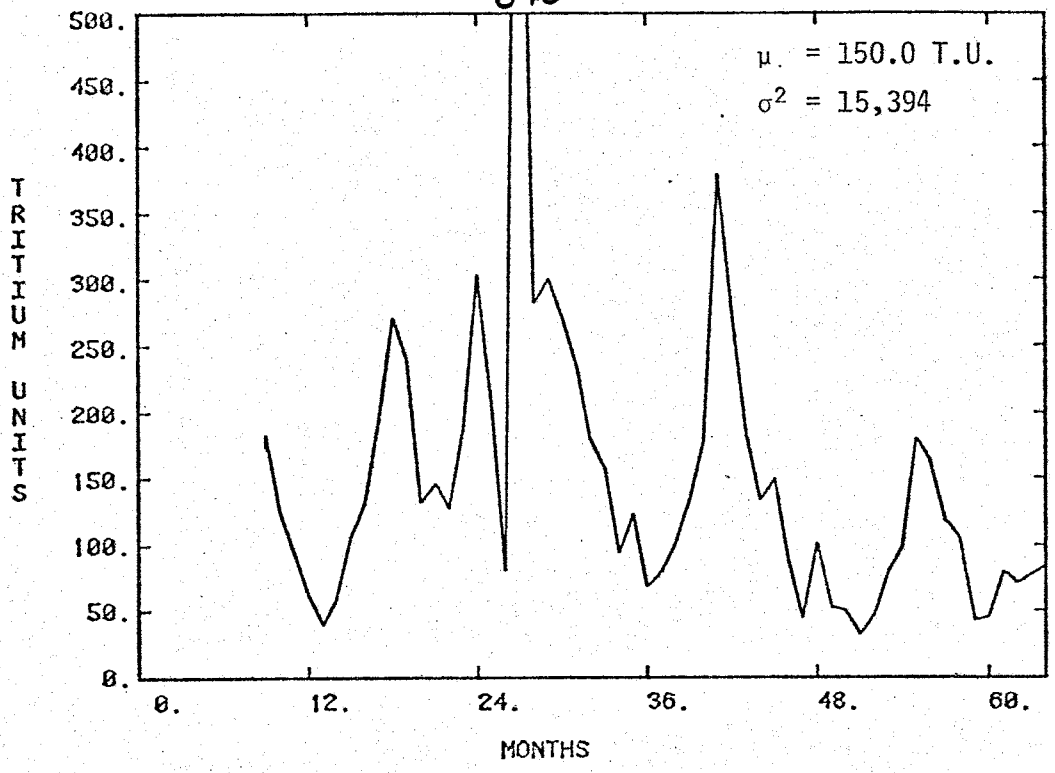
μ = 150.0 T.U.
σ² = 15,394
TRITIUM UNITS
500.
450.
400.
350.
300.
250.
200.
150.
100.
50.
0.
0.
12.
24.
36.
48.
60.
MONTHS

B.

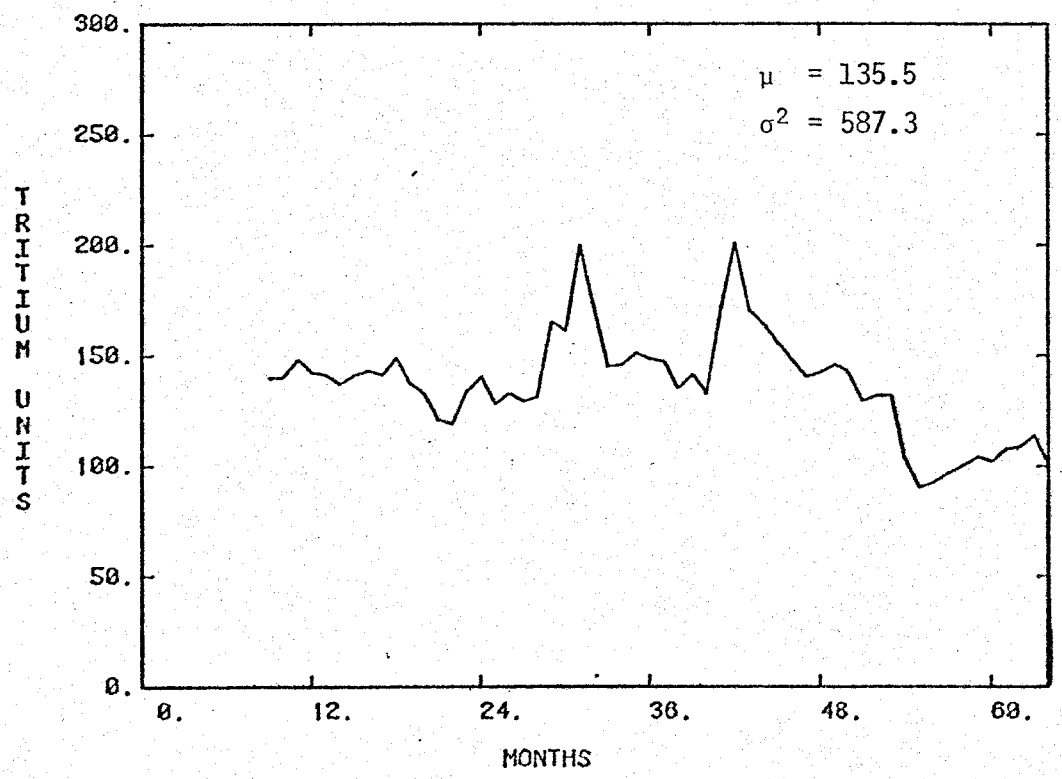
μ = 135.5
σ² = 587.3
TRITIUM UNITS
300.
250.
200.
150.
100.
50.
0.
0.
12.
24.
36.
48.
60.
MONTHS

estimates shown in Figures 3.18 and 3.19. It is significant that the spectral estimates of springflow ^3H have a ten-fold reduction in variation in the low frequency range, when compared with the input spectrum. Since the flow-through time in the primary karst system is known to be relatively fast (1 to 3 months), the large degree of amplitude attenuation could not be attributed simply to radioactive decay ($K = 0.0565$ years^{-1} for ^3H). Referring back to the report by Schotterer et al., they had determined that ^3H in the recharge water was mixing with 'older' water which was low in tritium. Their analysis concluded that the primary karst system was being diluted with low tritium inflows derived from another, and much more extensive groundwater system. At this point it was necessary to alter the convection-dispersion model developed previously to account for this lateral inflow of ^3H. The equation for convective-dispersive transport which includes lateral inflows can be written

$$\frac{\partial c}{\partial t} + u\frac{\partial c}{\partial x} = D\frac{\partial^2 c}{\partial x^2} + \frac{Q_L}{\Psi}(c_L - c) - Kc$$

where Q_L is the volumetric rate of lateral inflow to the primary karst system, c_L is the lateral inflow concentration, Ψ is the total volume of the primary system, and K is the coefficient of radioactive decay for ^3H. If we assume that c_L is approximately constant or $c_L' = 0$, then the equation for the temporal fluctuation of tritium in this example is given by

$$\frac{\partial c'}{\partial t} + u\frac{\partial c'}{\partial x} = D\frac{\partial^2 c'}{\partial x^2} - K_e c'$$

where

$$K_e = \left(\frac{Q_L}{\Psi} + K\right)$$

Figure 3.18. The estimated spectrum for the tritium input concentration (^{3}H-in tritium units^2) with the 95 percent confidence intervals indicated.

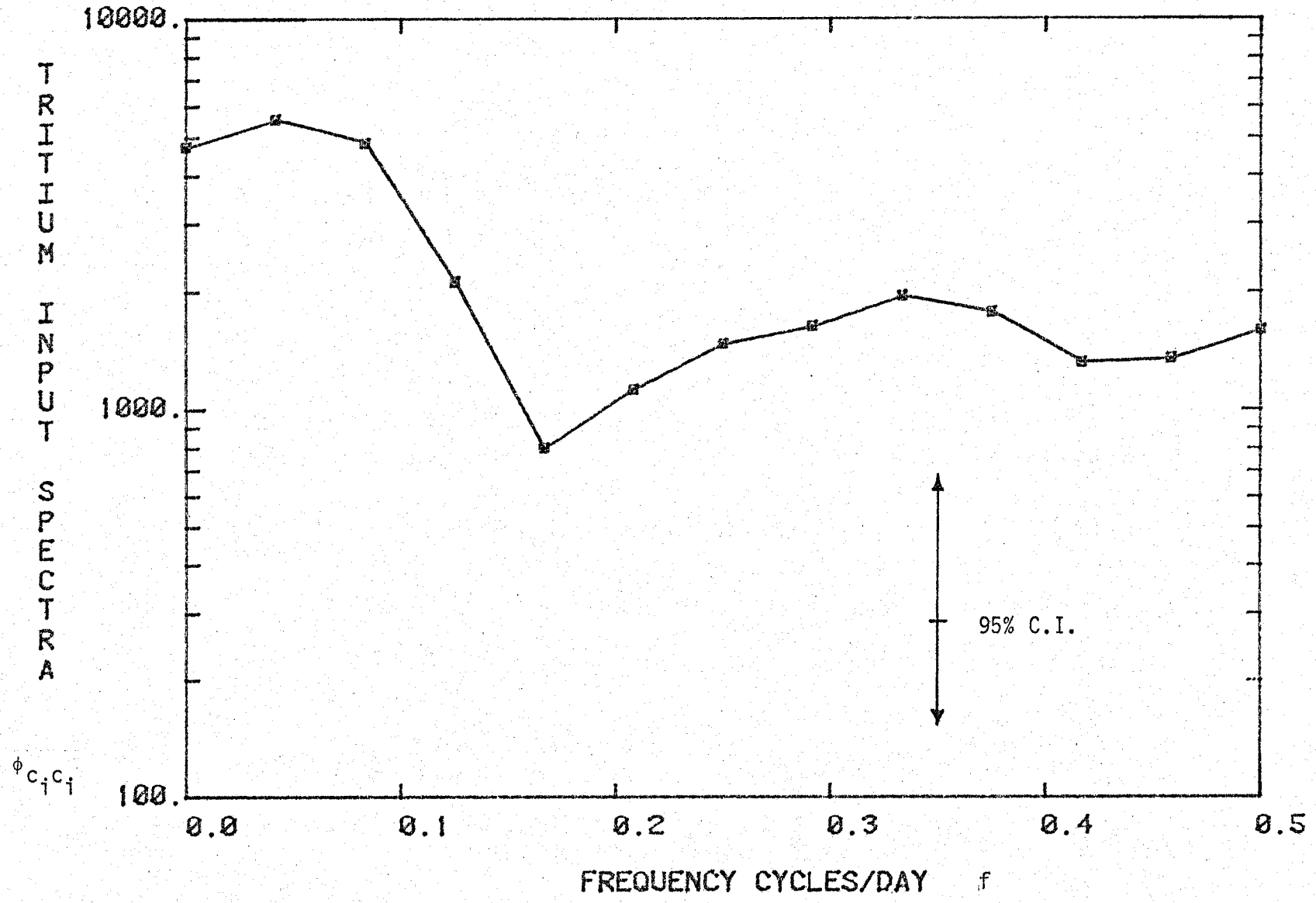
10000.
1000.
100.
TRITIUM INPUT SPECTRA
$\phi_{c_i c_i}$
95% C.I.
0.0
0.1
0.2
0.3
0.4
0.5
FREQUENCY CYCLES/DAY f

Figure 3.19. The estimated spectrum for the tritium concentration of springflow with the 95 percent confidence intervals indicated.

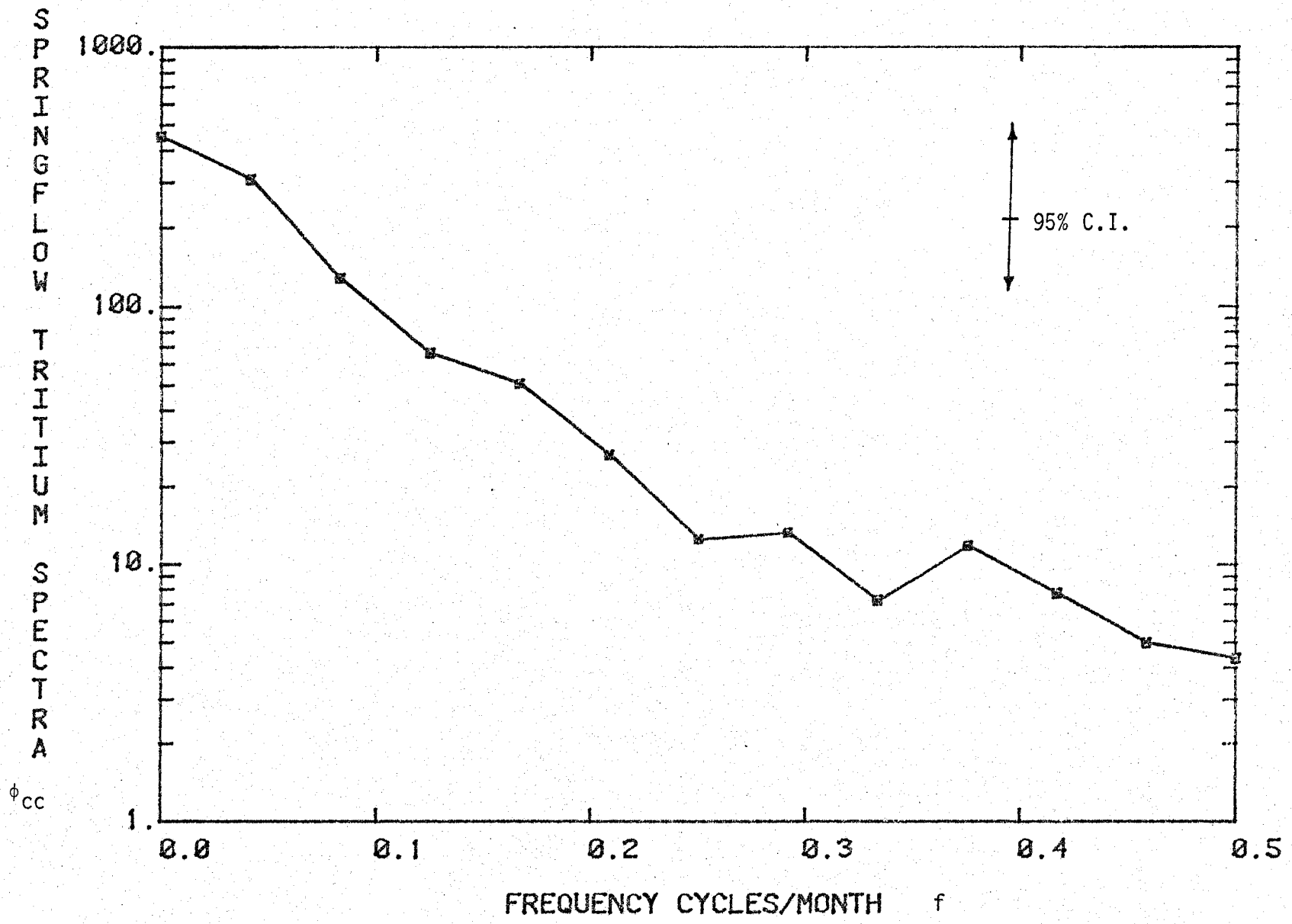
SPRINGFLOW TRITIUM SPECTRA
ϕ_{cc}
1000.
100.
10.
1.
95% C.I.
0.0
0.1
0.2
0.3
0.4
0.5
FREQUENCY CYCLES/MONTH f

is the effective rate constant. The rate constant can be removed by the following transformation on c'

$$c' = \hat{c}' \, e^{-K_e t}$$

which produces

$$\frac{\partial \hat{c}'}{\partial t} + u\frac{\partial \hat{c}'}{\partial x} = D\frac{\partial^2 \hat{c}'}{\partial x^2}$$

In terms of the output spectrum the transformation is approximately given by (see Chapter 1)

$$\phi_{cc} \cong \phi_{\hat{c}\hat{c}} \exp(-2K_e\tau)$$

Thus, the exponential term above can simply be multiplied by the usual transfer function (Equation 1.82), thereby adjusting the output for steady, lateral inflow as well as radioactive decay.

The parameters of the convection-dispersion model were estimated by curve matching both the transfer function and the phase. Since the phase is unaltered by the rate constant K_e (see Chapter 1), it was used initially to estimate the travel time τ. Figure 3.20 illustrates the phase result for a range of values for x/α. A value of $\tau = 2.2$ months was determined by curve matching the theoretical and estimated values in the low frequency range. The procedure indicated that the dispersion parameter x/α should be in the range of $10 \leq x/\alpha < 25$. The transfer function, also plotted for a range of x/α, is shown in Figure 3.21, with τ again taken to be 2.2 months. In order to match the ordinate of the estimated transfer function to the theoretical version, (1.82) was multiplied by $\exp(-2K_e\tau) = 0.065$. This allowed the calculation of the parameter K_e, which includes the lateral inflow term Q_L, and the reservoir volume $\forall$. Solving for K_e we get

Figure 3.20. The theoretical and estimated phase spectra for tritium transport in a karst region of Switzerland. The 75 percent confidence interval estimate is given, except where it could not be calculated.

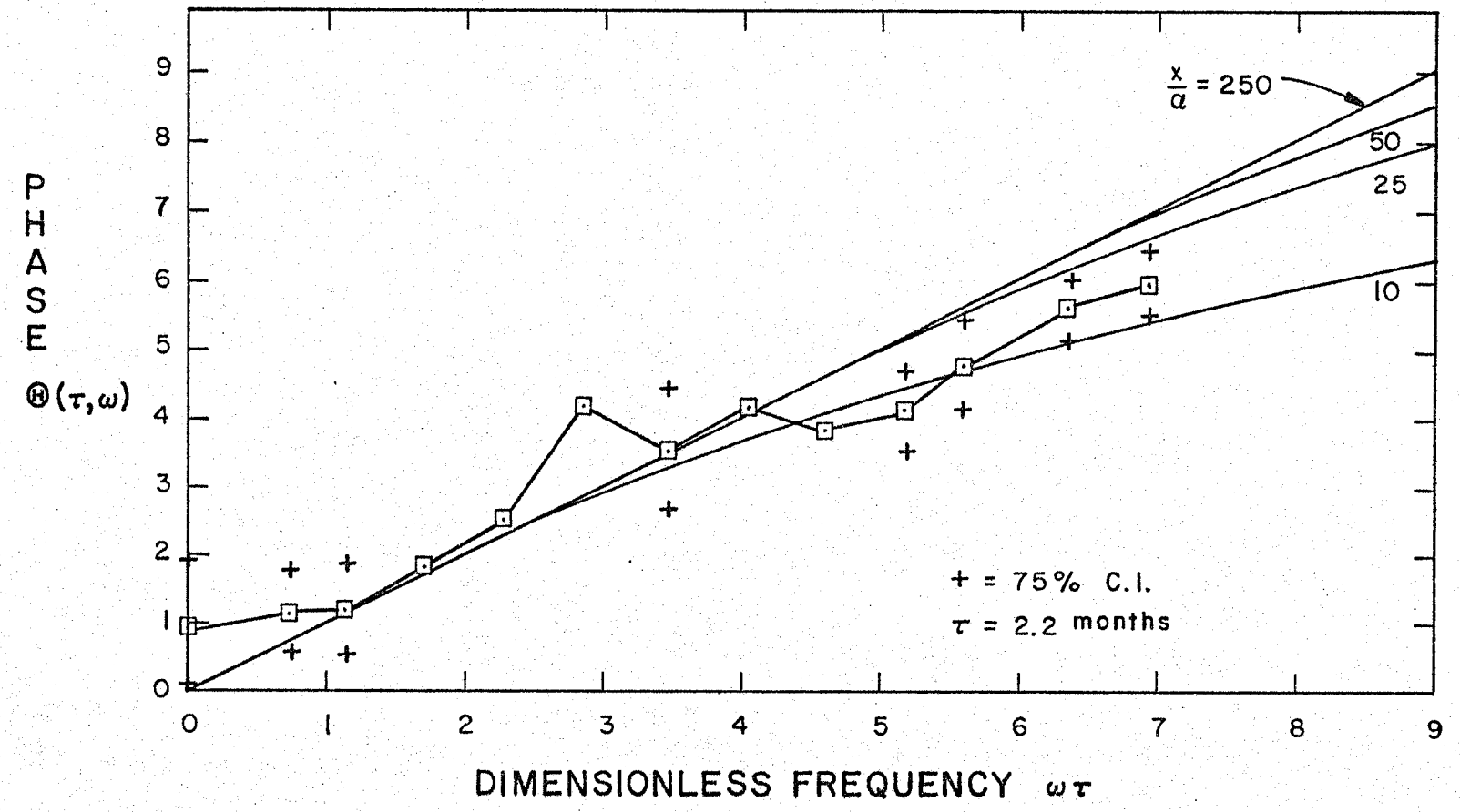
PHASE
Θ(τ, ω)
9
8
7
6
5
4
3
2
1
0
0
1
2
3
4
5
6
7
8
9
x/α = 250
50
25
10
+ = 75% C.I.
τ = 2.2 months
DIMENSIONLESS FREQUENCY ωτ

Figure 3.21. The theoretical and estimated transfer functions for tritium transport in a karst region of Switzerland. The 75 percent confidence interval estimate is given, except where it could not be calculated.

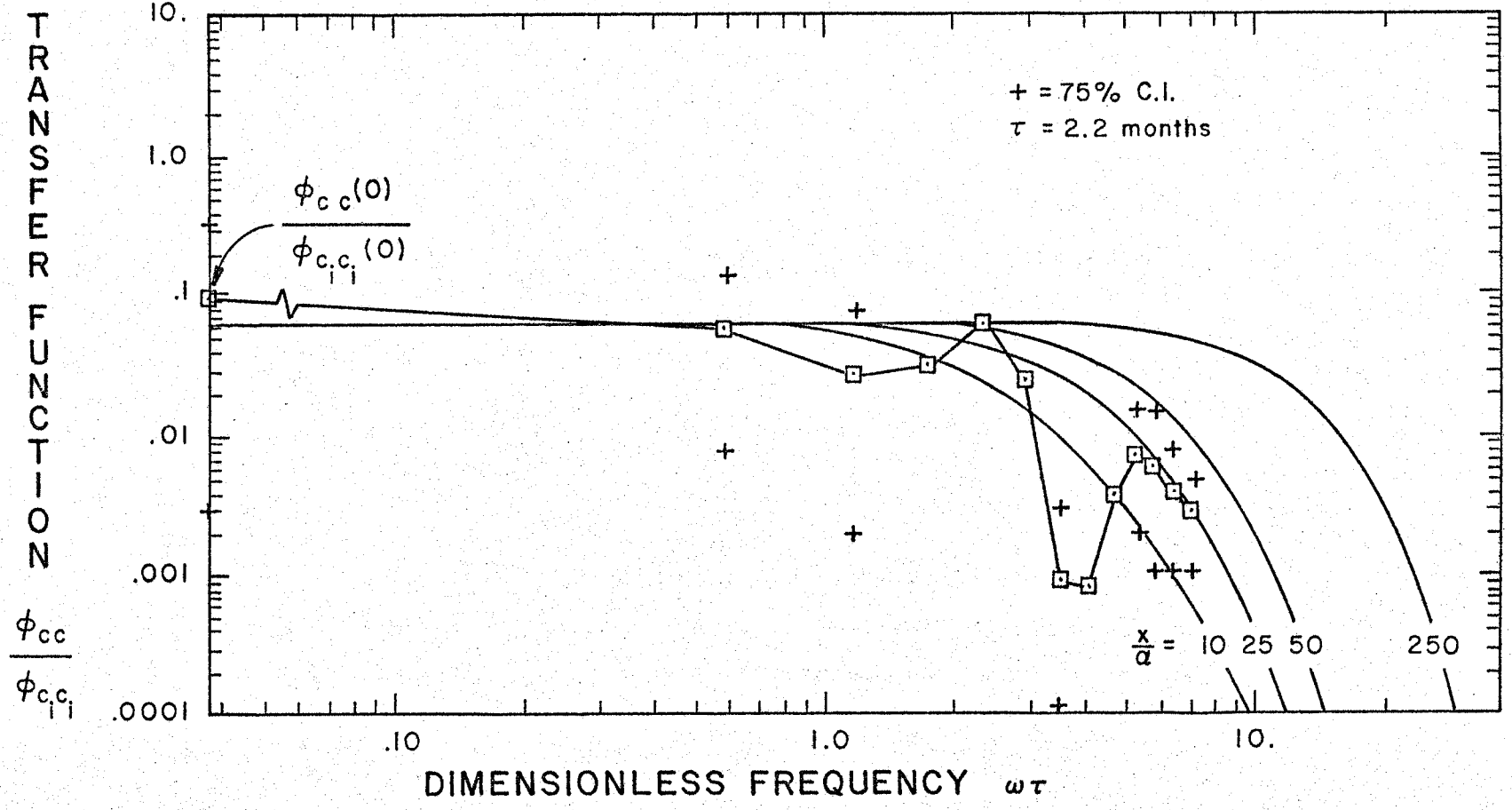
TRANSFER FUNCTION
$\frac{\phi_{cc}}{\phi_{c_ic_i}}$
10.
1.0
.1
.01
.001
.0001
.10
1.0
10.
DIMENSIONLESS FREQUENCY $\omega\tau$
+ = 75% C.I.
τ = 2.2 months
$\frac{\phi_{c\,c}(0)}{\phi_{c_ic_i}(0)}$
$\frac{x}{a}$ = 10 25 50 250

$$K_e = L_n\left(\frac{1}{.065}\right)/2\tau = 0.621 \text{ month}^{-1}$$

Using this result to evaluate $Q_L/\forall$ gives

$$Q_L/\forall = K_e - K = 0.621 - 0.005 = 0.616 \text{ months}^{-1}$$

In the Schotterer et al. report, the characteristics of the spring discharge for the period October 1973-September 1977 were:

Minimum - 0.01 m^3/s

Mean - 0.50 m^3/s

Maximum - 2.8 m^3/s

From the spring discharge record given in their report (their Figure 3), it appears that winter baseflow is consistently in the range of the minimum, Q = 0.01 m^3/s. Making the assumption that the baseflow is a constant, and identical to the lateral inflow Q_L, the volume of the primary karst reservoir is determined to be on the order of 4.21 x 10^4 m^3. The authors of the original report did not explicitly differentiate between the volume of the primary system, which carries the majority of the flow, and secondary system, which apparently contributes much less. Instead, they attempted to estimate the total volume of the karst reservoir, which they found to be 2.5 x 10^7 m^3. From the point of view of the time series approach presented here, it was not possible to determine the volume of the secondary system. The average velocity computed from the travel time estimate of τ = 2.2 months, is on the order of 60 m/day, which would be much too high for an intergranular or small scale fractured flow system. It is likely that transport occurs predominately through dissolution features and larger scale fracturing.

The dispersion characteristics of the system can also be examined from the transfer function. The dispersivity parameter x/α ranges between 10 and 25, for most of the estimates of the transfer function. Based on both the transfer function and the phase, the estimated dispersivity range for this system is $165 < \alpha < 410$ meters. The mean value for α is in the neighborhood of $\alpha = 250$ m. It is expected that longer record lengths of the input-output time series, would improve the spectral estimates, and lead to a refinement in the parameter estimation.

The significant results of this analysis can be summarized as follows:

1. Relatively short time series (<100 data points) may still be useful for preliminary data analysis, and parameter estimation.
2. It is expected that small lateral inflows of constant tritium concentration may drastically attenuate time fluctuations in the primary flow system. This may have a significant impact on using tritium peaks as a time marker in groundwater studies.
3. The phase function is unaltered by radioactive decay or lateral inflow, provided that the inflows are steady and of constant concentration.
4. The time series approach produced estimates of the volume of the primary karst reservoir, the velocity, the travel time, and the dispersivity range of the system.

4. SUMMARY AND CONCLUSIONS

The primary purpose of this research has been the application of spectral analysis and stochastic differential equations to a variety of problems of solute transport in groundwater. In Chapter 1 the spectral analysis approach is used to develop a theory for analyzing continuous and stationary solute time series for three widely applied solute transport models. Chapter 2 deals with the theoretical aspects of convective-dispersive transport in a nonuniform, stochastic velocity field. The third chapter presents an application for each of the three time series models developed in Chapter 1. The following discussion on Time Series Analysis deals with Chapters 1 and 3, while the discussion on Spatial Variability deals with Chapter 2.

Time Series Analysis: First of all, it is necessary to make some general comments on the significance of the spectral analysis procedure presented in Chapter 1. The results of this section indicate that analytical solutions to a variety of solute transport models can be obtained using a first order perturbation procedure and the spectral representation theorem for stationary, stochastic variables. In addition, the spectral solutions are presented in terms of the frequency response function, which is identical to the form which results from traditional Fourier analysis of periodic or aperiodic functions. The complex frequency response contains information about the amplitude attenuation of the system (transfer function), as well as the phase lag (phase spectrum), between each frequency component in the input and output. It should be emphasized that, in order to completely specify the frequency characteristics of water quality

'signals,' both the transfer function and the phase should be determined. Determining one or the other, will only make use of one-half the available information. A natural result of the spectral analysis method is that the output/input variance ratio can be determined theoretically, a result which would be useful for predictive modeling applications. The spectral procedure also has the advantage that higher order probability moments (3rd, 4th, etc.), as well as the underlying joint probability density functions, do not have to be determined. Thus, the spectral analysis procedure for second order stationary time series is completely specified by the mean, variance and covariance.

The linear reservoir model provides us with the most elementary approach to modeling diffuse or nonpoint sources of contamination. Application of the linear reservoir model to the problem of total salt loading from irrigation return flow, indicates that the spectral analysis procedure can be a useful tool for interpreting the time variable behavior of salinity. The response time parameter (T_m = 5.5 days) determined for this example was found to be reasonable, considering the large degree of temporal variability encountered. It was demonstrated that for a highly transient and 'well-mixed' groundwater system, that the mass flux form of the transport equation is appropriate.

The theoretical development and application of the convective transport model in a curvilinear flow field, demonstrates a situation where an explicit analytical solution for the frequency response function could not be found. The transfer function and the phase

were each determined by numerical integration. The spectral procedure was used to calculate the minimum solute travel-time from the river to the well (τ = 2 months). The theoretical phase function provided a very close comparison with field results, while the theoretical transfer function considerably underestimated the field estimates. The difference in the transfer function results were explained as due to an over simplified flow field model, which did not take into account the natural seepage from the Rhine in that area. Expressions were given for computing the effective porosity and transmissivity, but these parameters could not be determined due to lack of information on field conditions at the site.

The theory for convective-dispersive transport in a uniform flow field was applied to environmental tritium isotopes in a karst region of Switzerland. The results of this application demonstrate the effect of steady, lateral inflows of solute to the primary flow system. Even small lateral inflows were shown to drastically attenuate temporal fluctuations, and thus the transfer function of ^{3}H in the spring. The implication of this result is that even relatively large peaks in input ^{3}H concentration may not be observed in the outflow from the system, if a significant lateral inflow of relatively constant concentration is present. It was shown however, that the phase lag is unaltered by this effect, and thus the phase interpretation takes on a greater significance. The travel-time, velocity, dispersivity and volume of the primary karst system were estimated for this application.

An important feature of the results of Chapters 1 and 2 is that different groundwater flow fields produce distinctive frequency response characteristics for solutes within these systems. This would

indicate that the spectral analysis procedure may have a diagnostic potential for helping to evaluate the flow system of a historical water quality 'signal.'

Spatial Variability: In Chapter 2 the effects of a stochastic, nonuniform flow on the depth-averaged equation of solute transport is examined. The velocity field is composed of a mean value and a perturbation caused by the longitudinal variability of aquifer characteristics. In mathematical terms this implies that the coefficients of the transport equation become stochastic processes in the direction of the mean flow. The effect of the stochastic component of the velocity field on the mean solute transport equation is examined by evaluating the additional convective and dispersive flux terms which arise from the perturbation procedure. The significance of a nonuniform velocity field on the average solute behavior can be summarized as follows:

(1) An overall reduction in the mean convective velocity of a solute relative to the mean fluid velocity may result, when flow nonuniformity is significant. The degree of flow nonuniformity is measured by the coefficient of variation of the velocity $\sigma_u/\bar{u}$.

(2) A corresponding increase in the effective dispersion coefficient is observed where $\sigma_u/\bar{u}$ is increased.

(3) The reduction in convective velocity determined by the spectral theory is supported by an elementary Lagrangian calculation of the average travel-time and velocity of particles in a random medium. Both the spectral analysis and lagrangian approaches

indicate that the harmonic mean is the appropriate way to average the velocity along a stream line.

(4) An increase in the dispersion coefficient for stationary non-uniform flows is also shown to occur in a sinusoidally oscillating flow field.

(5) The stochastic theory provides a means of estimating the concentration variance for the mean transport process. The variance in concentration is primarily dependent on the mean gradient ($\partial\bar{c}/\partial x$), but also on $\partial^2\bar{c}/\partial x^2$.

(6) A pulse input solution to the mean solute transport equation demonstrates the retardation and attenuation mechanisms which come into play as $\sigma_u/\bar{u}$ becomes significant. The solution for the spatial distribution of a solute at a fixed point in time clearly illustrates the magnitude of the reduced convective velocity and increased dispersion, even for modest values of $\sigma_u^2/\bar{u}^2$ (=0.3). For a fixed location in space, say at an observation well, it was found that the shape of the solute pulse for nonuniform flow is significantly altered, when compared to the uniform flow case ($\sigma_u/\bar{u} = 0$). This is especially true for the tail of the concentration breakthrough (when 75-95 percent of C* has passed the observation well).

(7) Some of the features of this research were previously suggested by Smith and Schwartz (1980), from results on Monte Carlo experiments. However, field studies have not reported this kind of behavior. This may, however, be due

to the fact that field tests make use of the solute to compute the velocity, and thus the effect demonstrated here would be lost.

(8) Because of the non-Fickian behavior observed during the early stages of solute transport (ie. Gelhar et al., 1979), it is felt that this theory is only applicable at large distances from the source. An exact value for this distance is not precisely known at present, but it is likely to be on the order of a few kilometers. This would indicate that environmental tracers would be the most suitable for applications.

5. RECOMMENDATION FOR FUTURE WORK

During the course of this research it became apparent that treating spatial and temporal variability as separate entities might not be entirely realistic. For example spatial variability of the medium properties will obviously produce temporal variations when the solute is observed at an observation well. Time variations in the source (input) of solute will also be observed at the observation point. To differentiate between these mechanisms, a preliminary study of a space and time spectral representation was made. Although this form of representation is not new (Lumley and Panofsky, 1964), solving differential equations where the variables remain stationary in space and in time proved to be a considerable problem. Although time did not permit a careful analysis of this problem during the course of this study, it is felt that future work in this area may be fruitful.

REFERENCES

Anderson, M. P., 1979, Using models to simulate the movement of contaminants through groundwater flow systems, CRC Critical Reviews in Envir. Control, p. 97-156.

Aris, R., 1956, On the dispersion of a solute in a fluid flowing through a tube, Proc. Royal Soc. (London), Series A, v. 235, p. 943-961.

Bachmat, Y., and Bear, J., 1964, The general equations of hydrodynamic dispersion in a homogeneous, isotropic porous mediums, Jour. Geophy. Res., 69(12), p. 2561-2567.

Baedecker, M. J., and Back, W., 1980, Hydrogeological processes and chemical reactions at a landfill, Ground Water, 17(5), p. 429-437.

Bakr, A. A. M., Gelhar, L. W., Gutjahr, A. L., and MacMillan, J. R., 1978, Stochastic analysis of spatial variability in sub-surface flows, WRR, 14(2), p. 263-271.

Bear, J., 1972, Dynamics of Fluids in Porous Media, New York, Elsevier, 764 pp.

Biggar, J. W., and Nielson, D. R., 1976, Spatial varability of the leaching characteristics of a field soil, WRR, 12(1), p. 78-84.

Boast, C. W., 1973, Modeling the movement of chemicals in soils by water, Soil Sci., 115(3), p. 224-230.

Brunotte, G., Hugon, and Simler, 1971, A study of groundwater pollution by salt, Proc. 5th Int'l Water Poll. Res., p. I-34/1-I-34/13.

Burwell, R. E., Schum, G. E., Saxton, K. E., and Heineman, H. G. 1976, Nitrogen in subsurface discharge from agricultural watersheds, Jour. Envir. Qual., 5(3), p. 325-329.

Buyevich, Yu A., Leonov, A. I., and Safrai, V. M., 1969, Variations in filtration velocity due to random large-scale fluctuations of porosity, Jour. Fluid Mech., 37(2), p. 371-381.

Childs, K. E., Upchurch, S. B., and Ellis, B., 1974, Sampling of variable waste migration patterns, Groundwater 12(6), p. 369-377.

Crosby, III, J. W., Johnstone, D. L., and Fenton, R. L., 1971, Migration of pollutants in a glacial outwash, WRR, 7(1), p. 204-208.

Davison, C. C., and Vonhot, J. A., 1978, Spatial and temporal hydrochemical variations in a semiconfined buried channel aquifer, Groundwater, 16(5), p. 341-351.

de Josselin de Jong, G., 1958, Longitudinal and transverse diffusion in granular deposits, Trans. Amer. Geophy. Union, 39(1), p. 67-74.

de Marsily, G., Ledoux, E., Barbreau, A., and Margat, J., 1977, Nuclear waste disposal: can the geologist guarantee isolation, Science, 97(4303), p. 519-527.

Devitt, D., and Letey, J., 1976, Nitrate nitrogen movement through soil affected by soil profile characteristics, Jour. Envir. Qual., 5(3).

Dooge, J. C. I., 1973, Linear theory of hydrologic systems, Tech. Bul. No. 1468, U. S. Dept. of Agriculture, 327 p.

Duffy, C. J., Gelhar, L. W., and Gross, G. W., 1978, Recharge and groundwater conditions in the western region of the Roswell Basin, New Mexico WRRI, No. 100, 92 pp.

Duffy, C. J., Gelhar, L. W., and Wierenga, P. J., 1981, A stochastic model of irrigation and drainage for estimation of irrigation

efficiency, recharge and aquifer parameters, to be submitted to ASCE Irr. and Drainage Div.

Eldor, M., and Dagan, D., 1972, Solutions of hydrodynamic dispersion in porous media, WRR, 8, p. 1316.

Eriksson, E., 1970, Groundwater time series: an exercise in stochastic hydrology, Nordic Hyd., 1(3), p. 181-205.

Eriksson, E., 1970, Cross-spectrum analysis of groundwater levels in an esker, Nordic Hyd., 4, p. 245-259.

Freeze, R. A., 1975, A stochastic-conceptual analysis of one-dimensional groundwater flow in a nonuniform homogeneous media, WRR, 11(5), p. 725-741.

Freeze, R. A., 1980, A stochastic conceptual analysis of rainfall-runoff processes on a hillslope, WRR, 16(2), p. 391-408.

Geldner, P., 1981, Evaluation of stream aquifer interaction, Geop. Res. Center, Hydrology Res. Program, Rpt. No. H-7, NMIMT, Socorro, 108 pp.

Gelhar, L. W., and Collins, M. A., 1971, General analysis of longitudinal dispersion in nonuniform flow, WRR, 7(6), p. 1511-1521.

Gelhar, L. W., 1974, Stochastic analysis of phreatic aquifers, WRR, 10(3), p. 539-545.

Gelhar, L. W., and Wilson, J. L., 1974, Ground-water quality modeling. Ground water, 12(6), p. 399-408.

Gelhar, L. W., 1976, Stochastic analysis of flow in aquifers, in Advances in Groundwater Hydrology, Proc. Symp. AWRA, September 22-23, 1976, Chicago, Illinois.

Gelhar, L. W., Duffy, C. J., and Gross, G. W., 1979, Stochastic methods and analyzing groundwater recharge, IAHS Pub. No. 128, Proc. of the Canberra Symp., p. 313-321.

Gelhar, L. W., Gutjahr, A. L., and Haff, R. L., 1979, Stochastic analysis of macrodispersion in a stratified aquifer, WRR, 15(6), p. 1387-1397.

Gelhar, L. W., Wierenga, P. J., Duffy, C. J., Rehfeldt, K. R., Senn, R. B., Simonett, M., Yeh, T-C., Gutjahr, A. L., Strong, W. R., and Bustamante, A., 1980, Irrigation return flow studies at San Acacia, New Mexico: Monitoring, modeling and variability: Rpt. No. H-3, Hydrology Res. Program, New Mexico Inst. of Min. and Tech., 133 p.

Gelhar, L. W., Wierenga, P. J., Duffy, C. J., Rehfeldt, K. R., Senn, R. B., Simonett, M., Yeh, T-C, Gutjahr, A. L., Strong, W. R., and Bustamante, A., 1980, Irrigation return flow studies at San Acacia, New Mexico: Monitoring, modeling and variability, Technical Prog. Rpt., Hydrology Program, NMIMT, Socorro, N. M., 195 pp.

Grisak, G. E., Jackson, R. E., and Pickens, J. F., 1978, Monitoring ground water quality: the technical difficulties, AWRA, June, 1978, p. 210-232.

Gunnerson, G. C., 1975, Utilization of data from continuous monitoring networks, Water Quality Parameters, ASTM STP 573, p. 456-486.

Gutjahr, A. L., Gelhar, L. W., Bakr, A. A., and MacMillan, J. R., 1976, Stochastic analysis of spatial variation in subsurface flows, part II, evaluation and applications, WRR, 14(5), p. 953-959.

Harleman, D. R. E., Mehorn, P. F., and Rumer, R. R., 1963, Dispersion-permeability correlation in porous media, Jour. Hyd. Div. ASCE, 89(HY2), p. 67-85.

Harleman, D. E., and Rumer, R. R., 1963, Longitudinal and lateral dispersion in an isotropic porous medium, Jour. Fluid Mech. 16, p. 385-394.

Heller, J. P., 1972, Observations of mixing and diffusion in porous media, in Fundamentals of Transport Phenomena in Porous Media, Proc. 2nd Int. Symp. (IAHR-ISSS), August 7-11, Univ. of Geulph, Ontario, Canada, 1-26.

Hendrick, J., 1973, Techniques for modeling reservoir salinity, Hydrology Papers, Colorado State Univ., 63, 50 pp.

Holley, F. M., 1975, Two-dimensional mass dispersion in rivers: Hydrology Papers, Colorado State Univ. No. 78, 67 pp.

Hoopes, J. A., and Harleman, D. R. F., 1967, Wastewater recharge and discharge in a porous media, ASCE, HYD. DIV., 93(HY5), p. 51-72.

IAEA (International Atomic Energy Agency), 1965, Radioactive waste disposal in the ground, Vienna, Safety Series No. 15, 111 pp.

Jeng, R. I., and Yevjevich, M., 1966, Stochastic properties of lake outflows, Hydrology Papers, Colorado State Univ., No. 14, 21 pp.

Jenkins, G. M., and Watts, D. G., 1968, Spectral Analysis and its Applications, Holden-Day, San Francisco, 525 pp.

Jury, W. A., 1975, Solute travel-time estimates for tile-drained fields: I. Theory, Soil Sci. Soc. Amer. Proc., 39(6), p. 1020-1028.

Kirkham, D., and Affleck, S. B., 1977, Solute travel time to wells, Ground Water, 15(3), p. 231-242.

Kisiel, C. C., 1969, Time series analysis of hydrologic data, in Advances in Hydroscience, V. T. Chow ed., Academic Press, New York, N.Y., 5, p. 1-119.

Kolmogorov, A. N., Uber die analytischen methoden in der Wahrscheinlichkeitsrechnung, 1937, Math., Ann., 104, p. 415-458.

Koopmans, L. H., 1974, The Spectral Analysis of Time Series, Academic Press, 365 pp.

Longmire, P. A., 1981, Geological, geochemical and hydrological criteria for disposal of hazardous wastes in New Mexico, in Environmental Geology and Hydrology in New Mexico, N. M. Geol. Soc. Spec. Pub. No. 10, p. 93-102.

Lumley, J. L., and Panofsky, H. A., 1964, The Structure of Atmospheric Turbulence, New York, John Wiley and Sons, 239 pp.

Marle, C., Simandoux, P., Pacsirzky, J., and Gaulier, C., 1967, Etude du de placement de fluids miscible en mileau poreux stratifie: Revue de l'Institute Francais du Petrole, 22(2), p. 272-294.

Matheron, G., and de Marsily, G., 1980, Is transport in porous media always diffusive? A counter example, WRR, 16(5), p. 901-917.

Mercado, A., 1967, The spreading pattern of injected water in a permeable stratified aquifer, in Artificial Recharge and Management of Aquifers, Symp. of Haifa (IASH), March 19-26, Pub. 72, p. 23-36.

McLin, S. G., 1981, Validity of the generalized lumped parameter hydrosalinity model in predicting irrigation return flow, PhD Dissertation, New Mexico Inst. of Mining and Tech., Socorro, N. M.

Mizell, S. A., 1980, Stochastic analysis of spatial variability in two-dimensional groundwater flow with implications for observation-well-network design, PhD Dissertation, New Mexico Inst. of Mining and Tech., 133 pp.

Molinari, J., Peuadecerf, P., Gaillard, B., and Launay, M., 1977, Essais conjoints en laboratoire et sur le terrain en vue d'une approche simplifiee de la prevision des propagations des substances miscibles dan les auifers reels, in Proc. Symp. Hydrodynamic Diff. and Disp. in Porous Media, IAHR, Pavia Italy, p. 89-102.

Morrison, R. D., and Stearns, R. J., 1980, Statistics for groundwater quality assessment, Public Works, Feb., p. 90.

Muskat, M., 1937, The Flow of Homogeneous Fluids Through Porous Media, McGraw-Hill, New York.

Naff, R. L., 1978, A continuum approach to the study and determination of field longitudinal dispersion coefficients, PhD Dissertation, New Mexico Institute of Mining and Technology, Socorro, New Mexico, 176 pp.

Nelson, R. W., 1978, Evaluating the environmental consequences of groundwater contamination: 1., 2., 3., 4., WRR, 14(3), 409-450.

Nightingale, H., 1970, Statistical evaluation of salinity and nitrate content and trends beneath agricultural areas - Fresno, Calif., Groundwater, 8(1), 22-28.

Nir, A., 1964, On the interpretation of tritium 'age' measurements of groundwater, Jour. Geophy. Res., 69(12), p. 2589-2595.

Notes Et Renseignements Sur L'Eau Souterraine A La Hateur De Strasbourg, 1977, Institut de Mecanique des Fluides, Universite Louis Pasteur.

Orlob, G. T., and Woods, P. C., 1967, Water-quality management in irrigation systems, ASCE, Irr. Drainage Div., 93(IR2), p. 46-66.

Perlemutter, N. M., and Koch, E., 1972, Preliminary hydrogeologic appraisal of nitrate in groundwater and streams, Southern Nassau County, Long Island, N. Y., USGS PP. 800B, B225-B235.

Pickens, J. F., Cherry, J. A., and Gillham, G. W., 1978, Field studies of dispersion in a shallow sandy aquifer, 1978, Proc. Int'l Well Testing Symp., October 19-21, 1977, Lawrence Berkeley Laboratory, 7027, p. 55-62.

Reeves, C. C., Jr., and Miller, W. D., 1978, Nitrate, chloride and dissolved solids, Ogallala aquifer, West Texas, Groundwater, 16(3), p. 167-173.

Robson, S. G., 1978, Application of digital profile modeling techniques to groundwater solute transport at Barstow, Ca., U.S.G.S., WSP 2050, 28 pp.

Rodriguez-Iturbe, I., 1967, The application of cross-spectral analysis to hydrologic time series, Hydrology Papers, Colorado State Univ., No. 24, 46 pp.

Rozkowski, A., 1967, The origin of hydrochemical patterns in Hummocky Morraine, Can. Jour. Earth Sciences, 4, p. 1065-1092.

Saffman, P. G., 1960, A theory of dispersion in porous medium: Jour. Fluid Mech., 6, p. 321-349.

Scheidegger, A. E., 1954, Statistical hydrodynamics in porous media: Jour. Applied Physics, 25(8), p. 994-1001.

Schmidt, K. D., 1977, Water quality variations for pumping wells, Groundwater, 15(2), p. 130-137.

Schotterer, U., Wildberger, A., Siegenthaler, U., Nabholz, W., and Oeschger, H., 1980, Isotope study in the alpine karst region of Rawil, Switzerland, Isotope Hydrology, IAEA, Proc. Symp. Vienna, Vol. I, p. 351-365.

Schwartz, F. W., 1975, On radioactive waste management: an analysis of the parameters controlling subsurface contaminant transfer, Jour. of Hyd., 27, p. 51-71.

Schwartz, F. W., 1977, Macroscopic dispersion in porous media: the controlling factors, WRR, 13(4), p. 743-752.

Simonett, M. J., 1981, Irrigation return flow modeling at San Acacia, New Mexico, M.S. Thesis, New Mexico Inst. of Mining and Tech., Socorro, 112 pp.

Smith, L., and Schwartz, F. W., 1980, Mass transport 1. a stochastic analysis of macrodispersion, WRR, 16(2), p. 303-313.

Sudicky, E. A., and Cherry, J. A., 1979, Field observations of dispersion under natural flow conditions in a sandy aquifer, Water Pollut. Res. Can., 14, p. 1-17.

Taylor, 1954, The dispersion of matter in turbulent flow through a pipe: Proc. Royal Soc. (London), Series A, v. 223, p. 446-468.

Thomman, R. V., 1972, Systems Analysis and Water Quality Management, McGraw-Hill, New York, 286 pp.

Toler, L. G., and Pollock, S. J. 1974, Retention of chloride in the unsaturated zone, Jour. Res. USGS, 2(1), p. 119-123.

van Genuchten, M., Th., and Wierenga, P. J., 1976, Mass transfer studies in sorbing porous media 1. Analytical Solutions, Soil Sci. Soc. of Amer., 40(4), p. 473-480.

Warren, J. E., and Skiba, F. F., 1964, Macroscopic dispersion, Trans. AIME, Soc. Petr. Engrs., v. 321, p. 215-230.

Wastler, T. A., 1969, Spectral analysis application in water pollution control, U. S. Federal Water Pollution Control Administration, 99 pp.

Wierenga, P. J., Duffy, C. J., Kselik, R., Senn, R., and Strong, W., 1979, Impacts of irrigated agriculture on water quality in the Rio Grande below Albuquerque, N. M., Eng. Exp. Sta. Report, New Mexico State Univ., 124 pp.

Wierenga, P. J., Duffy, C. J., Senn, R., and Gelhar, L. W., 1981, Impacts of irrigated agriculture on water quality in the Rio Grande below Albuquerque, N. M., Eng. Exp. Sta. Rpt., New Mexico State Univ.

Wierenga, P. J., van Genuchten, M. Th. and Boyle, F. W., 1975, Transfer of boron and tritiated water through sandstone, Jour. Envir. Qual., 4(1), p. 83-87.

Winograd, I. J., 1974, Radioactive waste storage in the arid zone, EOS, 55(10), p. 884-894.

Yevjevich, V., 1972, Stochastic processes in hydrology, Water Resources Pub., Fort Collins, Colorado, 276 pp.

Young, C. P., Oakes, D. B., and Wilkinson, W. B., 1976, Prediction of future nitrate concentrations in groundwater, Groundwater, 14(6), p. 426-438.

APPENDICES

APPENDIX 1.

EVALUATION OF THE VARIANCE AND COVARIANCE EXPRESSIONS OF CHAPTER 2.

Evaluation of σ_c^2

The steady-state solution to the zero-mean stochastic differential equation (2.21) is given by

$$\phi_{cc}(k) = \phi_{uu}(k)\, g/(\bar{u}^2 k^2 (1 + \alpha^2 k^2)) \quad . \tag{2.27}$$

Integration of (2.27) produces the concentration variance of c'

$$\sigma_c^2 = \int_{-\infty}^{\infty} \phi_{cc}(k)dk = \int_{-\infty}^{\infty} \frac{g^2\, \phi_{uu}(k)}{\bar{u}^2 k^2 (1 + \alpha^2 k^2)}\, dk \quad . \tag{2.28}$$

To remove the singularity at k=0 in (2.28) we assume a particular form for $\phi_{uu}(k)$ after Bakyr et al. (1978)

$$\phi_{uu}(k) = \frac{2}{\pi} \frac{\sigma_u^2\ \ell_x^3\ k^2}{(1 + \ell_x^2\, k^2)^2} \quad . \tag{2.29}$$

Substituting (2.29) into (2.28) yields

$$\sigma_c^2 = \frac{2}{\pi} \int_{-\infty}^{\infty} \frac{\sigma_u^2\ \ell_x^3\ g^2}{\bar{u}^2 (1 + \ell_x^2\, k^2)^2 (1 + \alpha^2 k^2)}\, dk \tag{A.1}$$

which can be written as

$$\sigma_c^2 = \frac{4 g^2 \sigma_u^2 \alpha^3}{\pi\, \bar{u}^2\, \ell_x} \int_0^{\infty} \frac{d\nu}{(1 + \nu^2)(\frac{\alpha^2}{\ell_x^2} + \nu^2)^2} \tag{A.2}$$

where $\nu = \alpha k$.

A standard integral from Gradshteyn and Ryzhik (eq. 3.223-1, p. 289), can be used to evaluate (A.2)

$$\int_0^\infty \frac{x^{\mu-1}}{(\beta+x)(\gamma+x)}\,dx = \frac{\pi}{(\gamma-\beta)}\left[\beta^{\mu-1} - \gamma^{\mu-1}\right]\csc(\mu\pi) \quad . \tag{A.3}$$

Differentiating (A.3) with respect to β yields

$$\int_0^\infty \frac{x^{\mu-1}}{(\beta+x)^2(\gamma+1)}\,dx = -\pi\csc\mu\pi \left\{ \frac{(\gamma-\beta)(\mu-1)\beta^{\mu-2}+(\beta^{\mu-1}-\gamma^{\mu-1})}{(\gamma-\beta)^2} \right\} . \tag{A.4}$$

By another change of variables $u = v^2$ (A.2) can now be expressed as

$$\sigma_c^2 = \frac{2}{\pi}\frac{\sigma_u^2}{\bar{u}^2}\frac{\alpha^3}{\ell_x}\,g^2 \int_0^\infty \frac{u^{-\frac{1}{2}}}{(1+u)\left(\frac{\alpha^2}{\ell_x^2}+u\right)^2}\,du \tag{A.5}$$

The integral (A.4) is equivalent to (A.5) when $\gamma=1$ and $\beta=\alpha^2/\ell_x^2$. Performing the integration produces the following variance expression

$$\sigma_c^2 = \frac{\sigma_u^2\, g^2\, \ell_x^2}{\bar{u}^2}\left[\frac{1 + 2\alpha/\ell_x}{(1 + \alpha/\ell_x)^2}\right] \quad . \tag{2.31}$$

Evaluation of $\overline{u' \frac{\partial c'}{\partial x}}$:

To evaluate this term in the mean equation (2.20) we first expand it into its derivatives

$$\overline{u' \frac{\partial c'}{\partial x}} = \frac{\partial}{\partial x}\overline{u'c'} - \overline{c' \frac{\partial u'}{\partial x}} \tag{A.6}$$

The first term on the right hand side is represented as

$$\overline{u'c'} = \int_{-\infty}^{\infty} \phi_{cu}(k)dk = g\int_{-\infty}^{\infty} \frac{\phi_{uu}(k)}{\bar{u}(\alpha k^2 + ik)}\,dk \tag{A.7}$$

$$= \frac{g}{\bar{u}} \int_{-\infty}^{\infty} \frac{(\alpha k^2 - ik)\ \phi_{uu}(k)}{(\alpha^2 k^4 + k^2)}\ dk$$

The form of $\phi_{uu}(k)$ for this case is again given by (2.29), which upon substitution into (A.7) yields

$$\overline{u'c'} = \frac{4\bar{u}g}{\pi} \frac{\sigma_u^2}{\bar{u}^2} \frac{\ell_x^2}{\alpha} \int_0^{\infty} \frac{\nu^2}{(1+\nu^2)^2 \left[\frac{\ell_x^2}{\alpha^2} + \nu^2\right]}\ d\nu \qquad \text{(A.8)}$$

where $\nu + \ell_x k$. We again use the standard integral given by (A.4) to arrive at the result

$$\overline{u'c'} = \alpha\bar{u}g \frac{\sigma_u^2}{\bar{u}^2} \left[\frac{1}{(1 + \alpha/\ell_x)}\right]^2 \qquad \text{(A.9)}$$

Taking the derivative with respect to x gives

$$\frac{\partial}{\partial x}\overline{u'c'} = -\alpha\bar{u} \frac{\partial^2 \bar{c}}{\partial x^2} \frac{\sigma_u^2}{\bar{u}^2} \left[\frac{1}{(1 + \alpha/\ell_x)}\right]^2 \qquad \text{(A.10)}$$

where g is approximated by

$$g \approx -\partial\bar{c}/\partial x \qquad \text{(A.11)}$$

The second term in (A.6) is evaluated in the same way

$$\overline{c' \frac{\partial u'}{\partial x}} = \int_{-\infty}^{\infty} \phi_{c\dot{u}}(k)\ dk = \frac{-g}{\bar{u}} \int_{-\infty}^{\infty} \frac{\phi_{uu}(k)(1+\alpha ik)}{(1 + \alpha^2 k^2)}\ dk \qquad \text{(A.12)}$$

where $\phi_{c\dot{u}}(k)dk = E(dZ_c \cdot (-ik) dZ_u^*)$

and $dZ_c = dZ_{\dot{u}} \frac{g}{\bar{u}(\alpha k^2 + ik)}$.

Using the change of variable $\nu + \ell_x k$ along with (2.29) produces

$$\overline{c'\frac{\partial u'}{\partial x}} = \frac{-2}{\pi}\cdot g\cdot u\,\frac{\sigma_u^2}{\bar{u}^2}\,\frac{\ell_x^2}{\alpha^2}\int_{-\infty}^{\infty}\frac{\nu^2}{(1+\nu^2)^2\left(\frac{\ell_x^2}{\alpha^2}+\nu^2\right)}\,d\nu \tag{A.13}$$

Again applying (A.4) the resulting form is

$$\overline{c'\frac{\partial u'}{\partial x}} = \bar{u}\,\frac{\partial \bar{c}}{\partial x}\,\frac{\sigma_u^2}{\bar{u}^2}\left[\frac{1}{(1+\alpha/\ell_x)}\right]^2 . \tag{A.14}$$

Thus $u'\frac{\partial c'}{\partial x}$ is given by

$$\overline{u'\frac{\partial c'}{\partial x}} = -D\frac{\partial^2 \bar{c}}{\partial x^2}\,\frac{\sigma_u^2}{\bar{u}^2}\left[\frac{1}{(1+\alpha/\ell_x)}\right]^2 - \bar{u}\frac{\partial \bar{c}}{\partial x}\,\frac{\sigma_u^2}{\bar{u}^2}\left[\frac{1}{1+\alpha/\ell_x}\right]^2 \tag{A.15}$$

Evaluation of $\overline{\alpha u'\frac{\partial^2 c'}{\partial x^2}}$:

The second term on the right hand side of (2.20) can be evaluated by expressing it in this form

$$\overline{\alpha u'\frac{\partial^2 c'}{\partial x^2}} = \alpha\int_{-\infty}^{\infty}\phi_{u\ddot{c}}(k)dk \tag{A.16}$$

where

$$\phi_{u\ddot{c}}(k)dk = E(dZ_u\cdot(-ik)^2 dZ_c^*) = \frac{g(-ik)^2\phi_{uu}(k)}{\bar{u}(\alpha k^2-ik)}\,dk$$

with

$$dZ_c^* = \frac{dZ_u^* g}{\bar{u}(\alpha k^2-ik)} . \tag{A.17}$$

Equation (A.16) can then be written as

$$\overline{\alpha u' \frac{\partial^2 c'}{\partial x^2}} = \frac{-\alpha g}{\bar{u}} \int_{-\infty}^{\infty} \frac{\phi_{uu}(\alpha k^2 + ik)}{(\alpha^2 k^2 + 1)} \, dk \quad . \tag{A.18}$$

If we again let $\phi_{uu}(k)$ be given by 2.29) and using the same procedure as before, the integration produces

$$\overline{\alpha u' \frac{\partial^2 c'}{\partial x^2}} = \bar{u} \frac{\partial \bar{c}}{\partial x} \frac{\sigma_u^2}{\bar{u}^2} \cdot \left[\frac{2\alpha/\ell_x + \alpha^2/\ell_x^2}{(1 + \alpha/\ell_x)^2} \right] \quad . \tag{A.19}$$

The expressions (A.15) and (A.19) will combine to produce the right hand side of (2.20).

APPENDIX 2.

DATA AND RESULTS OF TIME SERIES ANALYSIS

A listing of the time series data, spectral estimates, transfer functions and phase functions are given in this appendix. Confidence intervals on the estimated spectra were calculated with the following expression taken from Jenkins and Watts (see p. 82)

$$\text{Ln } \hat{\phi}_{xx}(f) + \text{Ln } \frac{\nu}{\chi_\nu(1-\alpha/2)} \quad , \text{Ln } \hat{\phi}_{xx}(f) + \text{Ln } \frac{\nu}{\chi_\nu(\alpha/2)}$$

where ν represents the degrees of freedom for a Hamming window, $(1 - \alpha)$ is the confidence level, and χ_ν is the appropriate value of the Chi-squared distribution.

Confidence intervals on the transfer function and phase were determined by using the approximate expressions developed by Jenkins and Watts (p. 434). In order to determine these confidence intervals the square of the coherency function $K^2(f)$ must be estimated from the data. $K^2(f)$ is analogous to the square of the correlation coefficient from linear regression, except $K^2(f)$ applies to correlation between various frequency components of the input and output time series (see Jenkins and Watts for details).

	April	May	June	July	August	Sept.	Oct.
1	16.58	60.47	108.49	140.56	142.24	34.69	27.47
2	12.44	68.31	115.62	124.40	217.36	34.69	23.15
3	14.51	68 11	118.59	108.93	229.03	34.56	22.97
4	239.22	69.68	121.57	102.78	151.79	34.56	22.80
5	128.97	67.18	126.99	104.47	119.99	34.56	22.62
6	89.45	66.96	129.76	120.98	98.49	32.40	20.40
7	74.89	64.48	134.80	112.91	124.90	32.16	20.56
8	64.26	61.82	114.21	109.34	92.62	29.68	18.58
9	60.11	61.58	115.13	139.71	84.00	31.56	20.80
10	59.87	61.38	120.04	144.36	75.81	260.02	20.89
11	80.19	56.15	235.06	109.79	69.37	142.45	21.04
12	63.51	53.21	212.60	95.90	63.25	133.17	19.01
13	57.37	52.22	212.20	84.30	63.25	109.34	18.50
14	53.05	328.97	168.60	76.97	63.03	90.41	17.94
15	45.07	101.24	132.99	321.95	58.96	71.76	17.43
16	45.23	111.63	111.00	317.99	56.69	61.53	22.49
17	39.23	105.50	103.13	211.55	78.96	55.14	14.54
18	35.24	101.82	95.15	144.70	154.52	49.02	14.03
19	35.36	100.43	87.93	116.62	312.18	42.79	11.89
20	33.42	101.24	97.12	103.67	219.23	38.74	12.27
21	29.34	99.50	145.46	107.62	141.87	32.66	16.36
22	25.80	100.03	91.57	101.17	99.50	33.33	239.88
23	20.52	97.95	193.36	96.86	76.97	38.17	165.94
24	19.29	92.56	131.42	92.56	60.78	34.83	89.32
25	94.79	85.47	90.85	87.91	54.93	41.77	69.66
26	94.45	86.62	82.26	79.33	48.95	34.19	61.02
27	196.57	81.74	82.08	72.90	47.17	34.83	51.82
28	85.31	84.99	181.32	65.79	36.59	34.56	46.93
29	64.06	88.41	193.69	61.27	34.69	30.02	44.36
30	59.91	95.56	156.53	58.58	34.69	27.67	37.71
31		100.81		55.85	34.69		37.12

Table A2.1. The time series of the mass flux of total dissolved salts at San Acacia, New Mexico (q·c - Kg/ha/day) for the 1978 irrigation season.

	April	May	June	July	August	Sept.	Oct.
1					1414.99		
2							
3	1170.9						
4							
5							355.23
6							
7							
8					459.09	1055.88	
9				148.90			
10							
11			637.14				
12						487.55	
13							55.34
14		928.41		237.85			
15							
16					1042.69		
17							
18							
19			303.29				
20				535.22			1062.32
21						327.43	
22							297.14
23							
24							
25							
26	1160.48		509.74				
27							
28							
29					559.78		
30							
31							

Table A2.2. The time series of the mass flux of applied irrigation water at San Acacia, N.M. ($q_i c_i$ - Kg/ha/day$^-$) for the 1978 irrigation season.

freq.	$\phi_{m_i m_i}(f)$	$\phi_{m_o m_o}(f)$	$\phi_{m_o m_o}/\phi_{m_i m_i}$	Θ(rads)	$K^2(f)$
.000	2396.78	3428.61	1.431	-0.569	.004
.025	3622.03	2163.06	0.597	0.580	.300
.050	6385.99	1389.69	0.218	0.879	.506
.075	7921.61	1016.96	0.128	1.149	.521
.100	7309.21	820.82	0.112	1.457	.510
.125	8554.70	832.14	0.097	1.782	.320
.150	8903.38	560.70	0.062	1.932	.216
.175	7188.12	565.30	0.079	1.748	.329
.200	7140.12	371.34	0.052	1.956	.153
.225	7970.07	280.34	0.035	2.071	.035
.250	8714.55	221.92	0.025	2.772	.032
.275	8571.94	172.99	0.018	3.071	.013
.300	7969.53	167.03	0.021	4.248	.005
.325	8301.55	146.34	0.018	1.955	.008
.350	6327.81	143.66	0.023	1.067	.026
.375	6918.70	131.13	0.019	2.740	.013
.400	9613.77	145.33	0.015	2.842	.037
.425	8020.89	153.52	0.019	2.564	.049
.450	8505.76	132.01	0.016	2.682	.037
.475	9390.69	153.03	0.016	2.411	.059
.500	9121.48	151.57	0.017	2.459	.079

Table A2.3. Estimates of the spectra, transfer function, phase and coherency squared for the mass flux time series at San Acacia, New Mexico.

	1972	1973	1974	1975	1976
Jan	194.9	174.7	139.3	118.7	233.0
Feb	231.8	208.7	197.6	247.7	184.1
Mar	169.7	279.1	200.2	175.1	234.2
Apr	138.8	157.9	152.8	107.5	186.7
May	24.1	137.9	165.2	95.6	138.5
Jun	165.6	112.3	127.3	76.6	87.5
Jul	131.6	73.7	103.7	34.3	17.0
Aug	100.2	52.5	80.4	56.7	205.9
Sep	157.1	115.9	126.0	125.3	155.6
Oct	190.2	132.9	144.0	147.2	204.4
Nov	120.8	145.9	86.4	153.0	201.3
Dec	51.3	177.9	96.5	84.3	146.9

Table A2.4. The time series of chloride concentration (ppm) in the Rhine River at Strasbourg, France.

	1972	1973	1974	1975	1976
Jan	179.2	100.4	141.0	120.0	140.2
Feb	176.6	83.2	144.0	132.3	145.5
Mar	183.8	101.6	188.0	145.9	166.5
Apr	216.2	163.0	178.4	202.3	174.0
May	210.0	206.7	197.6	177.6	215.0
Jun	204.0	183.2	175.0	130.8	188.4
Jul	189.0	144.0	192.7	109.6	156.2
Aug	166.5	138.0	157.0	80.0	155.0
Sep	148.4	95.2	127.1	79.8	116.3
Oct	123.0	96.0	113.3	96.0	143.0
Nov	128.8	123.0	145.1	123.2	156.0
Dec	162.0	152.0	137.0	134.4	171.4

Table A2.5. The time series of chloride concentration (ppm) in the pumping well at Strasbourg, France.

freq.	$\phi_{c_i c_i}(f)$	$\phi_{c_w c_w}(f)$	$\phi_{c_w c_w}/\phi_{c_i c_i}$	$\Theta(f)$	$K^2(f)$
0.00	354.68	385.29	1.09	0.11	
0.38	576.96	558.22	0.97	0.84	
0.08	1289.46	660.41	0.51	1.31	
0.12	1205.96	384.01	0.32	1.61	
0.15	876.25	251.51	0.29	2.53	
0.19	506.75	187.40	0.37	2.93	
0.23	387.80	75.99	0.20	3.97	
0.27	358.08	62.35	0.17	4.00	
0.31	151.28	48.07	0.32	4.75	
0.35	172.80	27.42	0.16	4.68	
0.38	181.97	19.12	0.11	4.72	
0.42	285.03	36.88	0.13	5.93	
0.46	288.20	31.30	0.14	6.28	
0.50	108.53	20.70	0.19	6.21	

Table A2.6. Estimates of the spectra, transfer function, phase and coherency squared for the chloride time series at Strasbourg, France.

		TIF	Siebenbrunnen
1973	Sep	183	140
	Oct	125	140
	Nov	93	148
	Dec	62	142
1974	Jan	40	141
	Feb	60	137
	Mar	107	141
	Apr	131	143
	May	194	141
	Jun	271	149
	Jul	239	137
	Aug	132	133
	Sep	146	121
	Oct	128	119
	Nov	189	134
	Dec	303	140
1975	Jan	201	128
	Feb	81	133
	Mar	870	129
	Apr	282	131
	May	300	165
	Jun	270	161
	Jul	233	200
	Aug	179	173
	Sep	156	145
	Oct	94	146
	Nov	122	151
	Dec	69	148
1976	Jan	80	147
	Feb	100	135
	Mar	133	141
	Apr	178	133
	May	378	172
	Jun	274	201
	Jul	181	170
	Aug	134	164
	Sep	149	155
	Oct	87	148
	Nov	44	140
	Dec	101	142
1977	Jan	52	146
	Feb	50	142
	Mar	32	129
	Apr	47	132
	May	81	132

Table A2.7. Time series of tritium concentration ^{3}H (in tritium units) of the tritium input function (TIF) and in the Siebenbrunnen spring in the Karst region of Rawil, Switzerland.

		TIF	Siebenbrunnen
	Jun	98	103
	Jul	180	90
	Aug	163	92
	Sep	118	97
	Oct	104	100
	Nov	43	104
	Dec	46	102
1978	Jan	80	108
	Feb	71	109
	Mar	78	114
	Apr	84	101
	May	137	94
	Jun	137	100

Table A2.7. Continued.

freq. (cycles/mo.)	$\phi_{c_i c_i}(f)$	$\phi_{cc}(f)$	$\phi_{cc}/\phi_{c_i c_i}$	$\Theta(f)$	$K^2(f)$
0.00	4729.47	446.56	0.09	0.98	0.27
0.04	5514.17	307.82	0.56	1.22	0.41
0.08	4826.18	128.74	0.03	1.23	0.35
0.13	2131.55	65.94	0.03	1.78	0.09
0.17	800.87	50.62	0.63	2.51	0.18
0.21	1127.34	26.77	0.24	4.18	0.02
0.25	1478.82	12.58	0.01	3.54	0.32
0.29	1648.06	13.32	0.01	4.15	0.19
0.33	1964.15	7.23	0.01	3.78	0.18
0.38	1782.48	11.77	0.01	4.11	0.49
0.42	1318.40	7.69	0.01	4.72	0.43
0.46	1357.63	4.97	0.01	5.55	0.58
0.50	1604.48	4.30	0.01	5.90	0.64

Table A2.8. Estimates of the spectra, transfer function, phase and coherency squared for the tritium time series in the Karst region of Rawil, Switzerland.